



universität  
wien

# MASTERARBEIT / MASTER'S THESIS

Titel der Masterarbeit / Title of the Master's Thesis

„Characterization of the potential metabolite  
binding pocket of RapZ and the interaction of RapZ  
with EI<sup>Ntr</sup> in *Escherichia coli*“

verfasst von / submitted by

Lara Lucija Paporic

angestrebter akademischer Grad / in partial fulfilment of the requirements for the  
degree of

Master of Science (MSc)

Wien, 2021 / Vienna, 2021

Studienkennzahl lt. Studienblatt /  
degree programme code as it appears on  
the student record sheet:

UA 066 830

Studienrichtung lt. Studienblatt /  
degree programme as it appears on  
the student record sheet:

Molekulare Mikrobiologie, Mikrobielle  
Ökologie und Immunbiologie

Betreut von / Supervisor:

Ass.-Prof. Dipl.-Biol. Dr. Boris Görke



# **1. Acknowledgement**

First of all, I would like to thank my supervisor Ass.-Prof. Dr. Boris Görke. Thank you for providing me with such an interesting project and for giving me the opportunity to work in your lab. I am very grateful for the time you invested in this supervision, for your guidance and the encouragement to do better.

A big thank you goes to Muna and Florian. Muna, I am very grateful for your guidance at the beginning of my lab journey and for the time you took to give me advice, even after you left the lab. Thank you for always being patient and making me feel welcome. Without you, the centrifuge would still be blowing plasmids in my sample 😊. Florian, thank you very much for being there for me. You always took the time to answer all my questions and you made this whole experience more fun.

I am also very thankful to Laura, who started this journey together with me and to my colleagues Alexandra, Mandy, Yvonne and Svetlana. Laura, thank you for the good talks about lab and life and for always being there to help. Alexa, I am very grateful for your advice and help around the lab and for the best Christmas cookies ever. Mandy, thank you for taking breaks to drink tea and discuss data with me. Yvonne and Svetlana, it was a pleasure to work with you.

Moreover, I would like to express my thankfulness to Prof. Dr. Karin Schnetz and to Vanessa Bensch from the Department of Biology at the University of Cologne, for providing me with information about photocrosslinking with pBpF and for supplying our laboratory with plasmid pEVOL-pBpF.

Last but not least, a very special thank you goes to my family and friends who were always there to support me. I would especially like to thank my parents Branko and Ursula and my Grandparents Marianne and Walter for their love and support.

# **Table of contents**

1. Acknowledgement.....	3
2. List of abbreviations.....	8
3. Introduction.....	11
3.1 Part I.....	11
3.1.1 Role and synthesis of amino sugars .....	11
3.1.2 Regulation of GlcN6P synthase (GlmS).....	12
3.1.3 Role of the RNA binding protein RapZ .....	12
3.1.4 The GlmY/GlmZ circuit regulates GlmS transcription.....	13
3.1.5 RapZ boosts the activity of RNase E to cleave GlmZ.....	13
3.1.6 Activation of the QseE/QseF Two Component System by RapZ .....	14
3.1.7 GlcN6P availability drives the <i>glmS</i> regulation circuit in <i>E.coli</i> .....	15
3.1.8 Structural features of the metabolite sensing protein RapZ .....	16
3.1.9 Aim.....	17
3.2 Part II.....	18
3.2.1 The two types of phosphotransferase systems.....	18
3.2.2 Features of the Nitrogen related PTS.....	18
3.2.3 Communication between the two PTSs.....	20
3.2.4 Genes encoding the Nitrogen PTS.....	20
3.2.5 Roles of the Nitrogen PTS.....	20
3.2.6 Aim II.....	21
4. Materials and methods.....	22
4.1 Materials.....	22
4.1.1 Media and plates.....	22

4.1.2	<i>Escherichia coli</i> strains.....	23
4.1.3	Plasmids.....	24
4.1.4	Oligonucleotides.....	30
4.2	Methods.....	33
4.2.1	Cultivation of <i>E.coli</i> .....	33
4.2.2	Determination of Optical Density.....	33
4.2.3	Preparation of cryo-cultures.....	33
4.2.4	Preparation of competent cells.....	33
4.2.5	Transformation of cells.....	34
4.2.6	Polymerase chain reaction (PCR).....	35
4.2.7	Analytic PCR.....	36
4.2.8	Preparative PCR for cloning purposes.....	37
4.2.9	Combined Chain Reaction CCR (Bi and Stambrook, 1998).....	38
4.2.10	Agarose gel electrophoresis.....	39
4.2.11	Analytic agarose gel electrophoresis of DNA.....	40
4.2.12	Preparative agarose gel electrophoresis of DNA.....	40
4.2.13	Amplification and purification of plasmids.....	40
4.2.14	Restriction digestion of DNA.....	40
4.2.15	De-phosphorylation of 5'ends of DNA fragments.....	41
4.2.16	Purification of DNA fragments from agarose gels and solutions.....	41
4.2.17	Ligation of DNA fragments.....	41
4.2.18	DNA sequencing (According to Sanger).....	42
4.2.19	General Transduction of genetic markers using phage T4GT7.....	42
4.2.20	Curing strains of the resistance cassette flanked by FRT sites (Datsenko and Wanner, 2000).....	42

4.2.21 Incorporation of pBpF	
(Protocol provided by Prof. Dr. Karin Schnetz.....)	43
4.2.22 Protein purification via StrepTactin affinity chromatography.....	43
4.2.23 Protein purification via Ni <sup>2+</sup> -NTA affinity chromatography.....	44
4.2.24 Dialysis and storage of Strep and His purified proteins.....	45
4.2.25 Determining protein concentration.....	45
4.2.26 UV photo-crosslinking of proteins with incorporated pBpF with their interaction partners (Rust et al., 2014).....	46
4.2.27 Denaturing polyacrylamide gel electrophoresis (SDS-PAGE) (Cleveland et al., 1977).....	46
4.2.28 Western Blotting.....	48
4.2.29 Total RNA extraction.....	49
4.2.30 Denaturing Urea Polyacrylamide Gel Electrophoresis.....	49
4.2.31 Northern Blotting.....	50
4.2.32 Quantitative $\beta$ -galactosidase activity assay (Miller, 1972).....	51
4.2.33 The Bacterial Adenylate Cyclase-based Two-hybrid system (BACTH).....	52
5. Results.....	54
5.1 Part I.....	54
5.1.1 Requirement of the potential ligand binding pocket of RapZ for regulation of <i>glmY</i> and <i>glmS</i> expression.....	54
5.1.2 Self interaction properties of RapZ variants carrying amino acid substitutions in the presumptive GlcN6P binding pocket .....	59
5.1.3 The role of positively charged amino acids in the potential GlcN6P binding pocket.....	62

5.1.4	Requirement of the potential ligand binding pocket of RapZ for controlling GlnY and GlnZ.....	65
5.1.5	Assessing direct interaction of residues composing the putative ligand binding pocket in RapZ with QseE and RNase E using photocrosslinking .....	66
5.1.5.1	Construction of <i>rapZ</i> variants carrying amber stop codons at defined positions.....	69
5.1.5.2	Purification of His <sub>10</sub> -QseE and the Strep-RapZ-pBpF variants for <i>in vitro</i> UV crosslinking experiments.....	72
5.1.5.3	Testing crosslinking of the Strep-RapZ variants with His <sub>10</sub> -QseE.....	76
5.2	Part II.....	88
5.2.1	Interaction of RapZ with PtsP, the first enzyme in the nitrogen phosphotransferase system .....	88
5.2.2	Involvement of the PtsP in <i>glnS</i> transcript regulation.....	91
6.	Discussion.....	95
6.1	Features of the potential ligand binding pocket of RapZ and its involvement in GlcN6P sensing.....	95
6.2	The interaction of RapZ with the PTS <sup>Ntr</sup> .....	104
7.	Supplementary Data.....	108
8.	Abstract.....	112
9.	Zusammenfassung.....	113
10.	References.....	114

## 2. List of abbreviations

%(w/v)	volume percent
%(v/v)	volume percent
°C	degrees Celsius
AA	acrylamide
APS	Ammoniumperoxidedisulfate
Amp	Ampicilline
BACTH	Bacterial Adenylate Cyclase-based Two-hybrid system
BME	β-mercaptoethanol
bp	Base pair
BSA	bovine serum albumin
CCR	Combined Chain Reaction
Cm	chloramphenicol
CTD	C terminal domain
DMSO	Dimethyl sulfoxide
DNA	Deoxyribonucleic acid
dNTP	Deoxynucleoside triphosphate
EMSA	electrophoretic mobility shift assay
g	gram
GlcN	Glucosamine
GlcN6P	glucosamine-6-phosphate
GlcNAc6P	N-acetyl-glucosamine 6-phosphate
h	hour
IPTG	Isopropyl β-D-1-thiogalactopyranoside

Kan	Kanamycin
kDA	kilodalton
L	liter
L-ara	L-arabinose
LB	Luria Bertani / lysogeny broth
M	Molar
mM	millimolar
min	minute
mL	Milliliter
mRNA	Messenger Ribonucleic acid
μg	microgram
μL	microlitre
μM	micromolar
nm	nanomolar
ng	nanogram
NTD	N terminal domain
O/N	Over night
O/D	Over day
PEG	Polyethylene glycol
rpm	Revolutions Per Minute
ODx	Optical density at wavelength x
ONPG	ortho-Nitrophenyl-β-galactoside
PAGE	polyacrylamide gel electrophoresis
pBpF	p-benzoyl-L-phenylalanine

PCR	Polymerase chain reaction
PEP	phosphoenolpyruvate
PTS	Phosphotransferase system
RBS	Ribosome Binding Sites
RNA	Ribonucleic acid
RT	Room temperature
SD	Shine-Delgarno
SDS	sodium dodecyl sulfate
Sec	Second
SPR	Surface Plasmon Resonance
sRNA	Small Ribonucleic acid
TCS	Two Component System
TEMED	Tetramethylethylenediamine
TM	Tryptone media
tRNA	Transfer Ribonucleic acid
U	Unit
UDP-GlcNAc	5'-diphospho-N-acetyl-D-glucosamine
UV	ultraviolet
V	Volt
WT	Wild type
X-Gal	5-bromo-4-chloro-3-indolyl- $\beta$ -D-galactopyranoside

# 3. Introduction

## 3.1 Part I

### 3.1.1 Role and synthesis of amino sugars

Amino sugars are incorporated into several macromolecules of the *E.coli* cell wall and outer membrane (Milewski, 2002). Synthesis of glucosamine-6-phosphate (GlcN6P) is the first step in the amino sugar synthesis and the source of all amino sugar containing components of the cell wall and outer membrane (Khan et al., 2020). GlcN6P is synthesized by the GlcN6P synthase (GlmS) from Fructose-6-phosphate (Fru6P) and L-glutamine (Figure 1). It is then, in a series of reactions, converted into 5'-diphospho-N-acetyl-D-glucosamine (UDP-GlcNAc), which serves as the active form of amino sugar that can be incorporated into macromolecules.

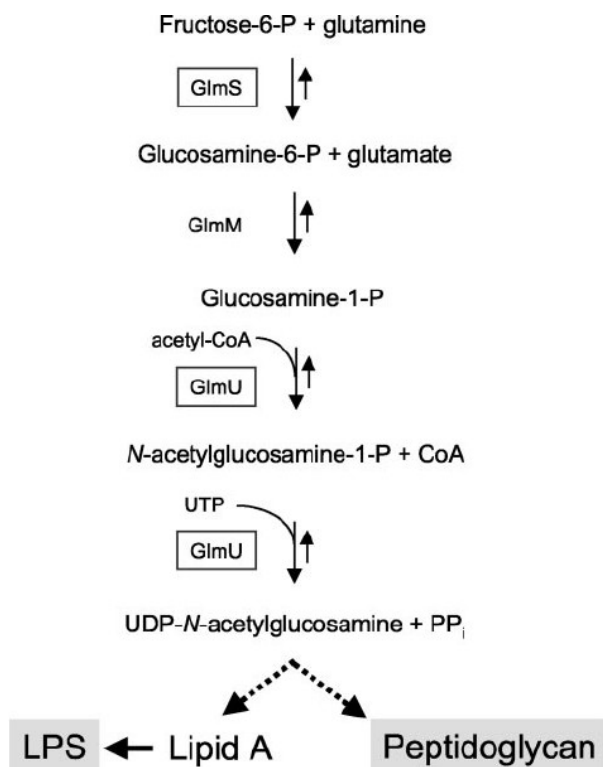


Figure 1. **The UDP-GlcNAc biosynthesis pathway.** UDP-GlcNAc is the active form of amino sugar, which gets incorporated into macromolecules of the cell wall and outer membrane. It gets synthesized from Fructose-6-P in a series of events that includes several enzymes. The first enzyme in this pathway is GlmS, which synthesizes GlcN6P, the first amino sugar of the pathway (Ramos-Aires et al., 2004).

### 3.1.2 Regulation of GlcN6P synthase (GlmS)

The importance of GlmS is demonstrated by the lethality of  $\Delta$ *glmS* cells that grow in an amino sugar depleted environment (Milewski, 2002). However, if present, bacteria can take up amino sugars from the environment, such as Glucosamine (GlcN), and convert them into GlcN6P, independently of GlmS (Khan et al., 2020, Álvarez-Añorve et al., 2016). As it represents the first enzyme in the amino sugar synthesis pathway, GlmS is an important point of metabolic control. In *E.coli* *glmS* is transcribed from the *glmUS* operon which has two promoters that are activated by NagC. However, in the presence of amino sugar GlcNAc6P, the activator is released from the promoter, which results in a 4-fold decrease of expression (Plumbridge et al., 1993).

Even though the mechanisms of regulation vary amongst different species, all of them seem to include some sort of feedback regulation that occurs downstream of transcription. The eukaryotic GlcN6P synthase senses and is inhibited by UDP-GlcNAc (Milewski, 2002). In *Bacillus subtilis*, the *glmS* mRNA contains a riboswitch that is activated for self cleavage in the presence of GlcN6P (Luciano et al., 2009). While those are examples where the enzyme or its transcript are directly inhibited by the metabolites from the pathway, feedback regulation in *E.coli* seems to be more complicated. The enzyme or its transcript don't sense the metabolite by itself, but are regulated by a complex circuit involving small RNAs GlmY and GlmZ, as well as the GlcN6P sensing protein RapZ (Khan et al., 2020).

### 3.1.3 Role of the RNA binding protein RapZ

RapZ (previously known as YhbJ) is a highly conserved protein in both gram positive and gram negative bacteria (Khan et al., 2020). The protein is encoded within the *rpoN* operon that is regulated by a  $\sigma^{70}$  dependent promoter (Studholme and Buck, 2000, Kalamorz et al., 2007, Jones et al., 1994). It has been speculated that the protein has first evolved as a Two-Component System (TCS) regulator and has then taken up different roles in various species (Khan et al., 2020, Luciano et al., 2009, Cui et al., 2018). In *E.coli*, besides controlling the QseEGF TCS, RapZ also acts as a RNA binding protein that is involved in the regulation of cell envelope synthesis. Its target RNAs are two closely related small RNAs, GlmZ and GlmY. By regulating the amounts of those two sRNAs, RapZ indirectly regulates the synthesis of GlmS (Khan et al., 2020, Göpel et al., 2013).

### **3.1.4 The GlmY/GlmZ circuit regulates GlmS transcription**

Small RNAs (sRNAs) are post-transcriptional regulators of protein in bacteria. They regulate gene expression by binding to target mRNAs and promoting their translation or decay. Some of the sRNAs require the help of Hfq for binding to the mRNA (Updegrave et al., 2015). One such example is GlmZ. The sRNA binds to the transcript of the *glmS* gene in an Hfq dependent manner. Basepairing of GlmZ to the GlmS mRNA, releases the Shine-Delgarno (SD) sequestering hairpin and enables ribosome binding (Kalamorz et al., 2007, Rabus et al., 1999). GlmY shares 66% sequence identity and a similar secondary structure with GlmZ (Göpel et al., 2015). Despite that, GlmY is not binding *glmS* mRNA or Hfq (Göpel et al., 2015, Urban and Vogel, 2008). However, both of the sRNAs bind to RapZ. RapZ recruits GlmZ to cleavage by RNase E (Durica-Mitic et al., 2020), while GlmY counters this by sequestering RapZ away from GlmZ (Göpel et al., 2013). In other words, GlmY prevents GlmZ cleavage and enables translation of GlmS.

### **3.1.5 RapZ boosts the activity of RNase E to cleave GlmZ**

The endoribonuclease RNase E plays a crucial role in bacterial gene expression regulation by cleaving RNAs. It can participate in sRNA mediated post-transcriptional gene regulation as well as maturation or decay of transcripts (Bandyra and Luisi, 2018, Vogel and Luisi 2011). The active enzyme is a dimer of dimers that interacts with other proteins to form the degradosome (Miczak et al., 1996, Leroy et al., 2002). In general, there are two distinct ways by which RNase E recognizes its targets. It can either sense a 5'-monophosphate or a specific duplex or single stranded region of the RNA. However, a recent study has demonstrated that RapZ is able to bypass those mechanisms. Namely, the RapZ tetramer directly interacts with the large globular domain of RNaseE, thereby recruiting its target RNA and boosting the catalytic domain of RNase E (Durica-Mitic et al., 2020).

GlmZ seems to be the only target of RapZ. This can be explained by its unique structure. Namely GlmZ consist of three stem-loops and the central one is crucial for RapZ binding and cleavage. Once GlmZ is recruited to RNase E, the sRNA is inactivated by cleavage within its base-pairing region. Despite its homology and ability to bind RapZ, GlmY is not recruited for cleavage, because of differences in the central stem loop (Göpel et al., 2013, Durica-Mitic et al., 2020, Göpel et al., 2016).

Another interesting recent discovery is that the processed version of GlmZ regulates cleavage of full-length GlmZ. Even when RapZ is expressed at very high levels, not all GlmZ is processed. The reason for that is that the processed variant competes with full-length GlmZ for RapZ and thus inhibits GlmZ processing. The role of such a regulatory loop may be to ensure that there is always a basal level of GlmS present in the cell (Durica-Mitic and Görke, 2019).

### **3.1.6 Activation of the QseE/QseF Two Component System by RapZ**

Two component systems (TCS) are common in bacteria. They serve as tools to sense and react to signals from inside the cell, as well as the environment. Such a system usually consists of a histidine kinase and a response regulator. The kinase is often bound to the cytoplasmic membrane and it consists of a sensor complex and a catalytic domain. When the sensor complex senses a specific stimulus, the kinase autophosphorylates itself at a conserved histidine residue, in an ATP dependent manner. This residue is part of the catalytic domain, located at the proteins' C-terminus. The CTD is typically placed in the cytoplasm, allowing it to bring the signal inside of the cell. Next, the phosphoryl group is transferred from the kinase to an aspartate of the response regulator, which results in its activation. Finally the regulator reacts to the received signal, most commonly by acting as a transcription factor (Szurmant et al., 2007, Zschiedrich et al., 2016,).

One example of such a system is the TCS QseE/QseF. In this system QseE acts as the kinase and QseF as the response regulator. Together, they activate the expression of *glmY* and *rpoE* from their  $\sigma^{54}$  dependent promoters (Klein et al., 2016). Recently, it has been shown that this system requires a third component for its function. Namely, protein QseG, which is encoded within the same operon as the other two proteins. QseG is attached to the outer membrane and it interacts with QseE. The interaction takes place within the periplasmic domain of QseE which is located within its sensor complex. QseG is essential for the activity of the system and it has been speculated that it is responsible for signal sensing and transition to QseF. The nature of such a signal, however, has yet to be revealed (Göpel and Görke, 2018). A novel study has shown that RapZ can interact with both QseE and QseF and can stimulate phosphorylation and therefore activation of the system. This activation is abolished when GlcN6P is bound to RapZ, which makes GlcN6P depletion the first known stimuli of this system (Khan et al., 2020).

### 3.1.7 GlcN6P availability drives the *glmS* regulation circuit in *E.coli*

The binding of sRNAs to RapZ is GlcN6P dependent. Namely, the metabolite counters GlmY binding to RapZ. Upon GlcN6P depletion, RapZ is free to bind GlmY, which results in stable complexes and an increase in GlmY stability. In addition, when GlcN6P amounts are limited, RapZ interacts with and activates the QseE/QseF TCS. This results in the activation of GlmY transcription. Together, the increase in GlmY stability and the activation of its transcription, result in high GlmY levels upon GlcN6P starvation. The accumulated GlmY binds to RapZ, sequestering it away from GlmZ (Figure 2) (Khan et al., 2020). Under those conditions, GlmZ is free to upregulate translation of *glmS*, which results in GlcN6P synthesis (Kalamorz et al., 2007). The accumulated metabolite then releases RapZ from the complex with GlmY and the RNA gets quickly degraded (Khan et al., 2020). RapZ is now free to bind GlmZ and recruit it to RNase E. RNase E cleaves GlmZ, therefore inhibiting *glmS* translation (Durica-Mitic et al., 2020). The cleaved variant of GlmZ binds to RapZ, inhibiting cleavage of full-length GlmZ. This allows for a basal expression of *glmS*, even under GlcN6P sufficiency (Durica-Mitic and Görke, 2019). In order to limit *glmY* expression under GlcN6P starvation, the cells employ another feedback loop. Namely, both sRNAs are counteracting TCS binding and activation by RapZ. Therefore, the system can activate *glmY* expression only when there are enough RapZ molecules that are not in complex with RNA (Khan et al., 2020).

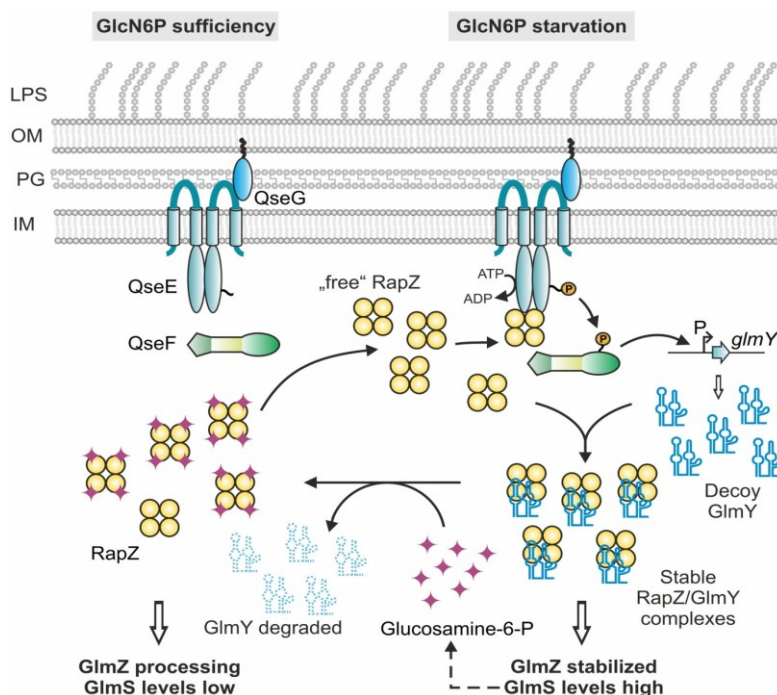


Figure 2. **The GlcN6P sensing and regulation circuit of RapZ.** Upon GlcN6P depletion conditions, RapZ interacts with the QseE/QseF TCS and activates *glmY* expression. This results in high levels of GlmY sRNA, which is bound and stabilized by RapZ. In this way GlmY sequesters RapZ away from GlmZ, which enables GlmZ sRNA to bind to the *glmS* mRNA and activate translation of *glmS*. When the GlmS protein is produced, it synthesizes GlcN6P, and its levels rise in the cell. RapZ senses higher levels of the metabolite and releases GlmY, which then gets quickly degraded. RapZ is now free to bind GlmZ and recruit it to RNase E for cleavage. This results in low translation of *glmS*, GlcN6P levels decrease and the cycle continues (Khan et al., 2020).

### 3.1.8 Structural features of the metabolite sensing protein RapZ

In 2017 a study revealed the crystal structure of RapZ, which together with genetic and biochemical data provided new insights in the role and function of the protein. RapZ has shown to be a tetramer that consists of a dimer of dimers. The RapZ monomer consists of a C-terminal domain (CTD) and an N-terminal domain (NTD). The tetramer has a mass of 119,9 kDa and there are three different interaction surfaces within it: The NTD:NTD, The CTD:CTD and the NTD:CTD interaction surface (Figure 3A). The C-terminus alone was shown to be sufficient for RNA binding. In addition, software predictions, genetic experiments (Göpel et al., 2013), as well as structure analysis (Gonzalez et al., 2017), suggest that different residues of the CTD could be involved in RNA binding. Those experiments indicate a putative RNA binding domain in the 19 terminal residues of RapZ (aa266-283), which is rich in lysinines and arginines. When a quadruple mutation, comprised of Lys270, Lys281, Arg282 and Lys283, was introduced, RapZ abolished its RNA binding ability. In addition, arginine 196 and lysines 251 and 281 were also predicted to play a role in RNA binding (Göpel et al., 2013, Gonzalez et al., 2017). While the CTD alone seems to be enough for RNA binding, interaction with RNase E requires both domains. It has also been suggested that the correct oligomerization of the protein is a prerequisite for its function. The RNA binding affinity of the tetramer is somewhat lower as compared to the CTD alone, suggesting that the N-terminus could have an autoinhibitory role.

Beside that, the NTD shares similarities with eukaryotic and archaeal kinases and reveals a walker A and walker B motif. Interestingly, the crystal structure of the CTD defined a pocket that could accommodate a non-protein ligand. The pocket is composed of the following amino acids: H190, T248, G249, H252 and R253 (Figure

3B). According to the authors of this study, the pocket could bind the phosphate moiety of a ligand (Gonzalez et al., 2017).

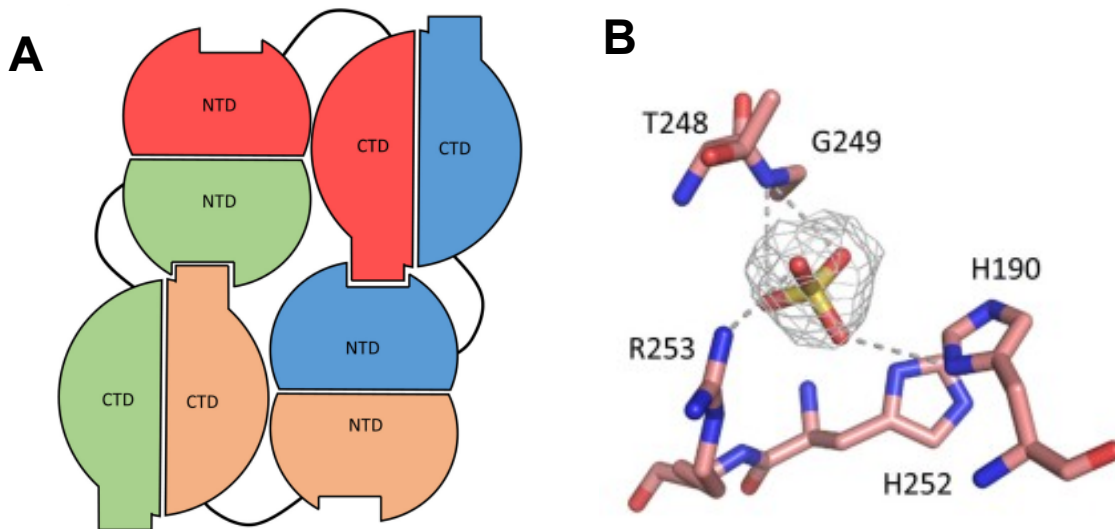


Figure 3 **Structural features of the metabolite sensing protein RapZ.** **A** RapZ consists of a dimer of dimers and it has three distinct interaction surfaces within its tetrameric structure: The NTD:NTD, The CTD:CTD and the NTD:CTD interaction surface. **B** The potential ligand binding pocket of RapZ, consists of six amino acid residue: H190, C247, T248, G249, H252 and R253. Five out of the six amino acids are marked in the figure. The figures have been taken from a study that revealed the crystal structure of RapZ (Gonzalez et al., 2017).

### 3.1.9 Aim

The aim of this part of the study is to investigate the potential ligand binding pocket of RapZ. To this end, the 5 amino acids from the pocket and C247, that is close by, were mutated to alanine, or in the case of G249 to tryptophan. The 6 different variants of RapZ were then tested for different features. Since RapZ senses GlcN6P, but it is not yet known how, it is tempting to speculate that it binds to this pocket. The pocket is also located in the C terminus of the protein and overlaps with the presumptive RNA binding domain.

If the pocket is involved in GlcN6P sensing or RNA binding, the mutants might have an impact on *glmY* and/or *glmS* expression. To test this, reporter gene assays were performed. In addition, northern blots were used to monitor accumulation of GlmY and GlmZ directly. To exclude that the observed results are due to a loss of RapZ

oligomerization or interaction with other proteins, bacterial two hybrid experiments were performed. To this end, it was investigated if the RapZ variants obtain self interaction, both within the full length protein and the isolated CTD. In a further part of the thesis, it was checked whether the amino acids from the pocket are in direct contact with the TCS, RNase E or itself. To test this, a photocrosslinking approach was used.

## **3.2 Part II**

### **3.2.1 The two types of phosphotransferase systems**

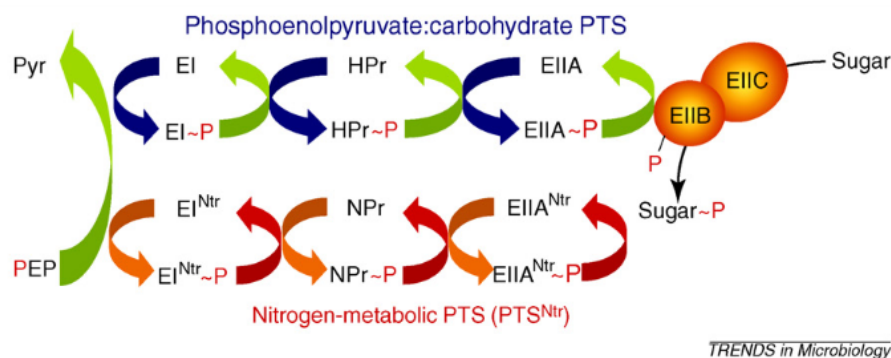
Phosphotransferase system (PTS) is a term that describes a group of proteins that take phosphate moieties from phosphoenolpyruvate (PEP) and transfer it amongst each other in a cascade. There are two general types of PTSs in Proteobacteria: The sugar PTS and the nitrogen PTS (PTS<sup>Ntr</sup>) (Fig. 5). The sugar PTS is a well studied system that is present amongst both Gram-positive and Gram-negative bacteria. Its role is to catalyze transport and phosphorylation of carbohydrates into the cell, as well as regulation of proteins and genes in response to carbon availability. The system consists of 3 enzymes: enzyme I (EI), histidine protein (HPr) and enzyme II (EII). The phosphate cascade goes from EI to HPr, which are both cytoplasmic proteins and then ends at the membrane-bound transporter EII. EII then allows for sugar uptake (Deutscher et al., 2014, Postma et al., 1993).

### **3.2.2 Features of the Nitrogen related PTS**

The nitrogen PTS (PTS<sup>Ntr</sup>), is a phosphotransferase system present only in Gram-negative bacteria. It is highly conserved in all proteobacteria, with the exception of the  $\epsilon$ -subdivision. Similar to the sugar PTS, the nitrogen PTS also consists of three proteins. EI<sup>Ntr</sup>, also known as PtsP, is the first enzyme in the cascade and it corresponds to EI in the sugar PTS (Pflüger-Grau and Görke, 2010). The two EI proteins are homologous, with an exception for one domain. Namely, PtsP carries a GAF signaling domain. GAF domains contribute to signal sensing and are known to bind a broad variety of ligands (Pflüger-Grau and Görke, 2010). It has been suggested that the GAF domain of PtsP senses the glutamine/ $\alpha$ -ketoglutarate ratio.

Cells that have sufficient nitrogen, convert  $\alpha$ -ketoglutarate to glutamine and hence the ratio indicates nitrogen abundance in the cell (Yoo et al., 2016, Goodwin and Gage, 2014, Lee et al., 2013).

The next enzyme in the cascade is NPr, that is similar to HPr of the sugar PTS. It has been shown recently, that phosphatase sixA can impact the phosphorylation state of the nitrogen PTS by dephosphorylation of Npr (Schulte et al., 2020, Schulte and Goulian 2018). Npr interacts with  $EIIA^{Ntr}$ , also known as PtsN, and phosphorylates it. PtsN is homologous with the A domain of the sugar PTS enzyme II. However, while the EIIA of the sugar PTS participates in mannitol transport, the nitrogen EIIA lacks such an ability. It is therefore speculated that the Nitrogen PTS system exclusively serves as a regulator and has no role in transport (Pflüger-Grau and Görke, 2010, Powell et al., 1995).



*TRENDS in Microbiology*

**Figure 4 Two Types of Phosphotransferase Systems in Proteobacteria.** The sugar PTS consists of enzymes EI, HPr and EII and it plays a role in carbohydrate transport and regulation. The nitrogen PTS, on the other hand consists of protein  $EI^{Ntr}$  (PtsP) which is homologous to EI, NPr (PtsO) which corresponds to the HPr enzyme of the sugar PTS, and  $EIIA^{Ntr}$  (PtsN) that is homologous to the EIIA subunit of EII. Since  $EIIA^{Ntr}$  lacks the ability to transport sugars, the role of the nitrogen PTS is thought to be strictly regulatory. In both system, the first enzyme, EI or  $EI^{Ntr}$  take a phosphoryl group of phosphoenolpyruvate (PEP) and transfer it to HPr or NPr. Lastly, HPr or NPr phosphorylate the last enzyme in the cascade, which is EII or  $EIIA^{Ntr}$ . The figure is taken from a review (Pflüger-Grau and Görke, 2010).

### 3.2.3 Communication between the two PTSs

Despite the differences in their function, it has been shown that the sugar and the nitrogen PTS communicate via exchange of phosphoryl groups. Namely, PtsN is able to exchange phosphoryl groups with both NPr and HPr (Zimmer et al., 2008, Powell et al., 1995) and NPr can be phosphorylated by both EI and PtsP. PtsP, on the other hand, can only phosphorylate Npr, but not HPr (Pflüger-Grau and Görke, 2010, Rabus et al., 1999, Lüttmann et al., 2015).

### 3.2.4 Genes encoding the Nitrogen PTS

The organization of genes encoding the Nitrogen PTS, varies amongst different subdivisions of proteobacteria. In most species, including *E.coli ptsO*, encoding NPr and *ptsN*, encoding PtsN are found within the *rpoN* operon (Pflüger-Grau and Görke, 2010, Jones et al., 1994), while PtsP is transcribed from *ptsP* that is located elsewhere in the genome (Pflüger-Grau and Görke, 2010, Reizer et al., 1996). In *E.coli* the operon containing *ptsO* and *ptsN* also comprises the genes *rpoN*, *hpf* and *rapZ* and they are all transcribed from a single promoter (Pflüger-Grau and Görke, 2010, Jones et al., 1994). However, different species contain different genes in the *rpoN* operon. Judging by the function of the proteins encoded in this operon, it has been speculated that the Nitrogen PTS has roles in nitrogen utilization, carbon catabolite repression and cell envelope homeostasis (Pflüger-Grau and Görke, 2010).

### 3.2.5 Roles of the Nitrogen PTS

Because two of its proteins are encoded in the *rpoN* operon, it was believed that the Nitrogen PTS is involved in the regulation of nitrogen metabolism and hence its name. However, the involvement of this PTS in nitrogen metabolism has shown to be somewhat weak and indirect (Reaves and Rabinowitz, 2011). Thus, it's not likely that this is its main role. The PTS<sup>Ntr</sup> has also been shown to affect the metabolism of other nutrients (Velázquez et al., 2007, Segura and Espin, 1998, Noguez et al., 2008) and in some pathogens it plays a role in interaction with the host cell (Edelstein et al., 1999, Higa and Edelstein, 2001, Tan et al., 1999). However, what seems to be a more prominent role of this phosphotransferase system is the regulation of potassium homeostasis. Namely, PtsN has been shown to regulate both a high and a low affinity K<sup>+</sup> transporter (Pflüger-Grau and Görke, 2010, Lee et al., 2007, Lüttmann et al.,

2009, Mörk-Mörkenstein et al., 2017). According to some studies, the phosphorylation state of PTS<sup>Ntr</sup> is controlled by nitrogen and carbohydrate. This suggests that the nitrogen PTS regulates uptake of K<sup>+</sup>, depending on the metabolic state of the cell (Lee et al., 2013, Mörk-Mörkenstein et al., 2017, Lüttmann et al., 2015). In addition, dephosphorylated PtsN was speculated to reduce potassium efflux by blocking YcgO, a protein that triggers potassium limitation in a  $\Delta ptsN$  strain (Sharma et al., 2016). The regulation of potassium levels in the cell could also explain the indirect involvement of PTS<sup>Ntr</sup> in many unrelated pathways. In addition, the system has also been associated with cell wall stress. Namely, previous studies have shown that the lethality of the  $\sigma^E$  deletion can be suppressed by PtsN overexpression (Hayden and Ades, 2008). Next, *sixA*, which encodes a protein that dephosphorylates Npr (Schulte et al., 2020, Schulte and Goulian 2018), is encoded within the  $\sigma^E$  regulon (Rezuchova et al., 2003) and NPr inhibits LPS synthesis (Kim et al., 2011, Lüttmann et al., 2012). Lastly, it was shown that PtsN can activate the PhoR/PhoB TCS (Lüttmann et al., 2012), a system involved in the regulation of phosphate starvation (Hsieh and Wanner, 2010).

So far, the system has been shown to have a direct role in potassium and phosphate regulation. However, it can not be excluded that it has additional direct targets that have yet to be revealed (Pflüger-Grau and Görke, 2010). It is tempting to speculate that the system is somehow interconnected with other genes in the *rpoN* operon. In agreement with this hypothesis, a study showed that PtsN might be regulating activity of the GlmS protein (Yoo et al., 2016). Translation of the *glmS* transcript, on the other hand is regulated by RapZ, that is also part of the *rpoN* operon (Khan et al., 2020, Jones et al., 1994).

### 3.2.6 Aim

The aim of this part of the thesis is to investigate the relationship between RapZ and the nitrogen PTS. Previously, preliminary data suggested that there might be an interaction between RapZ and PtsP (Khan, 2019). To test this, bacterial two hybrid experiments were performed. In addition, it was tested whether PtsP influences *glmS* expression on a post-transcriptional level. To this end, quantitative  $\beta$ -galactosidase activity assays were performed, as well as Northern blotting to monitor cleavage of GlmZ.

## 4. Materials and Methods

### 4.1 Materials

#### 4.1.1 Media and plates

Cultures were growing in either LB or Tryptone media that was supplemented with appropriate antibiotics or inducers, depending on the strain and plasmids. The plates consisted of LB, solidified with 15 g/L agar. For purposes of phenotypic selection, when using strain BTH101, X-Gal was added to LB plates, while strain RH785 was growing on MacConkey agar (Roth and Difco). For strains carrying a deletion in the *glmS* gene, LB was supplemented with Glucosamine (GlcN).

Table 1 Composition of media

LB	Tryptone Media
5 g/L NaCl (Roth)	5 g/L NaCl (Roth)
10 g/L Trypton (Roth)	10 g/L Trypton (Roth)
5 g/L Yeast Extract (Roth)	

Table 2 Antibiotics and Supplements

Antibiotic/Supplement	Stock	Final concentration	Sterilization
Ampicillin	50 mg/mL in 70% ethanol	100 µg/mL	Filtration
Chloramphenicol	15 mg/mL in 70% ethanol	15 µg/mL	Filtration
Kanamycin	30 mg/mL in H <sub>2</sub> O	30 µg/mL	Filtration
Tetracycline	12,5 mg/mL in 70% ethanol	12,5 µg/mL	Filtration
IPTG	1 M in H <sub>2</sub> O	1 mM	Filtration
L-arabinose	1 M in H <sub>2</sub> O	10 mM	Filtration
Glucosamine	20% (w/v)	0,2%	Filtration
pBpF	200 mM in 1 M NaOH	200 µM	/
X-Gal	40 mg/ml in Dimethylformamide	40 µg/ml	Filtration

#### 4.1.2 *Escherichia coli* strains

Table 3 List of Strains used in this work

Name	Genotype	Reference
<b>XL1 Blue</b>	<i>recA1, endA1, gyrA96, thi-1, hsdR17, relA1, supE44, lac, F[proAB lac<sup>q</sup> lacZDM15 Tn10]</i>	(Bullock et al., 1987)
<b>BTH101</b>	<i>F-, cya-99, araD139, galE15, galK16, rpsL1 (strp<sup>R</sup>), hsdR2, mcrA1, mcrB1</i>	(Karimova et al., 1998)
<b>IBPC750</b>	<i>thi1 argG6 argE3 his4 mtl1 xyl5 rpsLΔlacX74 mlc1 ΔglmS::tc</i>	(Plumbridge and Vimr, 1999)
<b>JW2797</b>	<i>F-, Δ(araD-araB)567, ΔlacZ4787(::rrnB-3), LAM-, ΔptsP753::kan, rph-1, Δ(rhaD-rhaB)568, hsdR514</i>	(Baba et al., 2006)
<b>RH785</b>	MG1655 Δ <i>cyaA</i>	(Abel et al., 2011)
<b>R1279</b>	CSH50 Δ( <i>pho-bgl</i> )201 Δ( <i>lac-pro</i> ) <i>ara thi</i>	(Schnetzer et al., 1996)
<b>Z8</b>	R1279 λ <i>attB</i> ::[ <i>aadA, glmS'-lacZ</i> ], <i>strp<sup>R</sup></i> , <i>F'(lac<sup>q</sup>)</i>	(Kalamorz et al., 2007)
<b>Z28</b>	R1279 Δ <i>rapZ</i> λ <i>attB</i> ::[ <i>aadA, glmS'-lacZ</i> ], <i>strp<sup>R</sup></i> , <i>F'(lac<sup>q</sup>)</i>	(Kalamorz et al., 2007)
<b>Z197</b>	R1279 λ <i>attB</i> ::[ <i>aadA, glmY'-lacZ</i> ]	(Reichenbach et al., 2009)
<b>Z225</b>	R1279 Δ <i>rapZ</i> λ <i>attB</i> ::[ <i>glmY-5'-lacZ (glmY-5' (-238 to +22))</i> ]	(Khan et al., 2020)
<b>Z37</b>	R1279 Δ <i>rapZ</i>	(Kalamorz et al., 2007)
<b>Z1126</b>	R1279 Δ <i>glmS</i> :: <i>tet</i> λ <i>attB</i> ::[ <i>aadA, glmS'-lacZ</i> ], <i>strp<sup>R</sup></i> , <i>F'(lac<sup>q</sup>)</i>	(Khan et al., 2020)
<b>Z1226</b>	R1279 λ <i>attB</i> ::[ <i>aadA, glmS'-lacZ</i> ], <i>strp<sup>R</sup></i> , <i>F'(lac<sup>q</sup>)</i> Δ <i>ptsP</i> :: <i>kan</i>	T4GT7 (JW2797) → Z8, This work
<b>Z1227</b>	R1279 λ <i>attB</i> ::[ <i>aadA, glmS'-lacZ</i> ], <i>strp<sup>R</sup></i> , <i>F'(lac<sup>q</sup>)</i> Δ <i>ptsP</i>	Z1226 cured from <i>kan</i> , This work
<b>Z1228</b>	R1279 λ <i>attB</i> ::[ <i>aadA, glmS'-lacZ</i> ], <i>strp<sup>R</sup></i> , <i>F'(lac<sup>q</sup>)</i> Δ <i>glmS</i> :: <i>tet</i> Δ <i>ptsP</i>	T4GT7 (IBPC750) → Z1227, This work

### 4.1.3 Plasmids

Table 4 List of Plasmids used in this work

Name	Relevant structure	Reference
<b>pBAD33</b>	<i>P<sub>Ara</sub></i> , MCS 2, <i>cat</i> , <i>ori</i> p15A	(Guzman et al., 1995)
<b>pBGG61</b>	<i>rapZ</i> under <i>P<sub>Ara</sub></i> control in pBAD33	(Göpel et al. 2013)
<b>pBGG164</b>	<i>strep-rapZ</i> under <i>P<sub>tac</sub></i> control, <i>lacI<sup>q</sup></i> , <i>bla</i> , <i>ori</i> ColEI	(Lüttmann et al. 2012)
<b>pBGG220</b>	<i>qseE'</i> (aa196-475)- <i>His<sub>10</sub></i> , under <i>P<sub>tac</sub></i> control, <i>lacI<sup>q</sup></i> , <i>bla</i> , <i>ori</i> ColEI	(Khan et al., 2020)
<b>pBGG237</b>	<i>strep-tag</i> under <i>P<sub>tac</sub></i> control, <i>lacI<sup>q</sup></i> , <i>bla</i> , <i>ori</i> ColEI	(Lüttmann et al. 2012)
<b>pBGG261</b>	encodes T25-PtsN fusion in pKT25	(Lüttmann et al. 2009)
<b>pBGG348</b>	encodes T25-RapZ in pKT25	(Göpel et al. 2013)
<b>pBGG349</b>	encodes T18-RapZ in pUT18C	(Göpel et al. 2013)
<b>pBGG457</b>	encodes T25-RapZ-R253A in pKT25	(Khan, 2019)
<b>pBGG461</b>	as pBGG61, but <i>rapZ</i> -R253A	(Khan, 2019)
<b>pEVOL-pBpF</b>	tRNA synthetase/tRNA pair for the <i>in vivo</i> incorporation of a photocrosslinker, p-benzoyl-l-phenylalanine into proteins in <i>E.coli</i> in response to the amber codon, TAG	(Chin et al. 2002)
<b>pKES170</b>	<i>bla</i> , <i>lacI<sup>q</sup></i> , <i>P<sub>tac</sub></i> (with two operators), SD T7 <i>gene 10</i> , NdeI, XbaI, 10×His-tag, pBR322- <i>ori</i> . Vector for overproduction of proteins with C-terminal His-tag	(Lüttmann et al. 2009)
<b>pKESK23</b>	<i>lacI<sup>q</sup></i> , <i>P<sub>tac</sub>::MCS</i> , <i>neo</i> , <i>attP</i> , <i>aadA</i> , <i>ori</i> p15A	(Lüttmann et al. 2012)
<b>pKT25</b>	<i>P<sub>lac</sub>::cyaA</i> [1-224] (T25), MCS, <i>neo</i> , <i>ori</i> p15A	(Karimova et al. 1998)
<b>pKT25-ZIP</b>	encodes T25-GCN4 leucine zipper fusion in pKT25	(Karimova et al. 1998)
<b>pMK15</b>	encodes T25-PtsP-H356E in pKT25	Khan and Görke; unpublished

<b>pMK16</b>	encodes T18-PtsP-H356E in pUT18C	Khan and Görke; unpublished
<b>pMK17</b>	encodes T25-PtsP-H356D in pKT25	Khan and Görke; unpublished
<b>pMK18</b>	encodes T18-PtsP-H356D in pUT18C	Khan and Görke; unpublished
<b>pMK21</b>	encodes T18-RapZ-H190A in pUT18C	(Khan, 2019)
<b>pMK22</b>	encodes T18-RapZ-T248A in pUT18C	(Khan, 2019)
<b>pMK23</b>	encodes T18-RapZ-G249W in pUT18C	(Khan, 2019)
<b>pMK24</b>	encodes T18-RapZ-H252A in pUT18C	(Khan, 2019)
<b>pMK25</b>	encodes T18-RapZ-R253A in pUT18C	(Khan, 2019)
<b>pMK31</b>	encodes RapZ in pKESK23	This work; Subcloned from pBGG61 into pKESK23 via Xbal/EcoRI
<b>pMK32</b>	encodes RapZ-H190A in pKESK23	This work; Subcloned from pSD107 into pKESK23 via Xbal/EcoRI
<b>pMK33</b>	encodes RapZ-T248A in pKESK23	This work; Subcloned from pSD108 into pKESK23 via Xbal/EcoRI
<b>pMK34</b>	encodes RapZ-G249W in pKESK23	This work; Subcloned from pSD109 into pKESK23 via Xbal and EcoRI
<b>pMK35</b>	encodes RapZ-H252A in pKESK23	This work; Subcloned from pSD110 into pKESK23 via Xbal/EcoRI
<b>pMK36</b>	encodes RapZ-C247A in pKESK23	This work; Subcloned from pSD130 into pKESK23 via Xbal/EcoRI
<b>pMK37</b>	encodes RapZ-R253 in pKESK23	This work; Subcloned from pBGG461 into pKESK23 via Xbal/EcoRI
<b>pMK38</b>	encodes PtsP in pKESK23	This work; Amplified from

		pSB4 with primers BG1893/BG1894 and cloned into pKESK23 via Xbal/EcoRI
<b>pMK39</b>	encodes PtsP-H356A in pKESK23	This work; Amplified from pSB5 with primers BG1893/BG1894 and cloned into pKESK23 via Xbal/EcoRI
<b>pMK40</b>	encodes T25-RapZ-H190A CTD (153-284aa) in pKT25	This work; Amplified from pSD107 with primers BG1223/BG639 and cloned into pKT25 via Xbal/KpnI
<b>pMK41</b>	encodes T25-RapZ-T248A CTD (153-284aa) in pKT25	This work; Amplified from pSD108 with primers BG1223/BG639 and cloned into pKT25 via Xbal/KpnI
<b>pMK42</b>	encodes RapZ-G249W CTD (153-284aa) in pKT25	This work; Amplified from pSD109 with primers BG1223/BG639 and cloned into pKT25 via Xbal/KpnI
<b>pMK43</b>	encodes T25-RapZ-H252A CTD (153-284aa) in pKT25	This work; Amplified from pSD110 with primers BG1223/BG639 and cloned into pKT25 via Xbal/KpnI
<b>pMK44</b>	encodes T18-RapZ-H190A CTD (153-284aa) in pUT18C	This work; Amplified from pSD107 with primers BG1223/BG639 and cloned into pUT18C via Xbal/KpnI
<b>pMK45</b>	encodes T18-RapZ-T248A CTD (153-284aa) in pUT18C	This work; Amplified from pSD108 with primers BG1223/BG639 and cloned into pUT18C via Xbal/KpnI
<b>pMK46</b>	encodes T18-RapZ-G249W CTD (153-284aa) in pUT18C	This work; Amplified from pSD109 with primers

		BG1223/BG639 and cloned into pUT18C via Xbal/KpnI
<b>pMK47</b>	encodes T18-RapZ-H252A CTD (153-284aa) in pUT18C	This work; Amplified from pSD110 with primers BG1223/BG639 and cloned into pUT18C via Xbal/KpnI
<b>pMK48</b>	encodes T18-RapZ-R253A CTD (153-284aa) in pUT18C	This work; Amplified from pBGG461 with primers BG1223/BG639 and cloned into pUT18C via Xbal/KpnI
<b>pMK49</b>	encodes RapZ- H190D in pKESK23	This work; Amplified with CCR from pBGG348 with BG1049/397 and CCR primer BG1935; cloned into pKESK23 via Xbal/SacI-HF
<b>pMK50</b>	encodes RapZ- R253K in pKESK23	This work; Amplified with CCR from pBGG348 with BG1049/397 and CCR primer BG1934; cloned into pKESK23 via Xbal/SacI-HF
<b>pMK51</b>	encodes T25-RapZ- H190D in pKT25	This work; Amplified with CCR from pBGG348 with BG637/639 and CCR primer BG1935; cloned into pKT25 via Xbal/KpnI
<b>pMK52</b>	encodes T25-RapZ- R253K in pKT25	This work; Amplified with CCR from pBGG348 with BG637/639 and CCR primer BG1934; cloned into pKT25 via Xbal/KpnI
<b>pMK53</b>	encodes T18-RapZ- H190D in pUT18C	This work; Amplified with CCR from pBGG348 with BG637/639 and CCR primer

		BG1935; cloned into pUT18C via XbaI/KpnI
<b>pMK54</b>	encodes T18-RapZ- R253K in pUT18C	This work; Amplified with CCR from pBGG348 with BG637/639 and CCR primer BG1934; cloned into pUT18C via XbaI/KpnI
<b>pMK55</b>	encodes Strep-RapZ with H190 replaced with stop codon TAG in pBGG237	This work; Amplified with CCR from pBGG348 with BG1015/397 and CCR primer BG2019; cloned into pBGG237 via XbaI/NheI
<b>pMK56</b>	encodes Strep-RapZ with C247 replaced with stop codon TAG in pBGG237	This work; Amplified with CCR from pBGG348 with BG1015/397 and CCR primer BG2020; cloned into pBGG237 via XbaI/NheI
<b>pMK57</b>	encodes Strep-RapZ with T248 replaced with stop codon TAG in pBGG237	This work; Amplified with CCR from pBGG348 with BG1015/397 and CCR primer BG2021; cloned into pBGG237 via XbaI/NheI
<b>pMK58</b>	encodes Strep-RapZ with G249 replaced with stop codon TAG in pBGG237	This work; Amplified with CCR from pBGG348 with BG1015/397 and CCR primer BG2022; cloned into pBGG237 via XbaI/NheI
<b>pMK59</b>	encodes Strep-RapZ with H252 replaced with stop codon TAG in pBGG237	This work; Amplified with CCR from pBGG348 with BG1015/397 and CCR primer BG2023; cloned into pBGG237 via XbaI/NheI
<b>pMK60</b>	encodes Strep-RapZ with R253	This work; Amplified with

	replaced with stop codon TAG in pBGG237	CCR from pBGG348 with BG1015/397 and CCR primer BG2024; cloned into pBGG237 via XbaI/NheI
<b>pMK61</b>	encodes Strep-RapZ with D182 replaced with stop codon TAG in pBGG237	This work; Amplified with CCR from pBGG348 with BG1015/397 and CCR primer BG2034; cloned into pBGG237 via XbaI/NheI
<b>pMM20</b>	encodes T25-PtsP in pKT25	Mörk-Mörkenstein and Görke; unpublished
<b>pMM21</b>	encodes T25-PtsP-H356A in pKT25	Mörk-Mörkenstein and Görke; unpublished
<b>pSB2</b>	encodes T18-PtsO in pUT18C	Bajad and Görke; unpublished
<b>pSB4</b>	encodes T18-PtsP in pUT18C	Bajad and Görke; unpublished
<b>pSB5</b>	encodes T18-PtsP- H356A in pUT18C	Bajad and Görke; unpublished
<b>pSB6</b>	encodes T25-PtsO in pKT25	Bajad and Görke; unpublished
<b>pSD10</b>	encodes T25-RapZ (aa 153-284) fusion in pKT25	(Gonzalez et al. 2017)
<b>pSD12</b>	encodes T18-RapZ (aa 153-284) fusion in pUT18C	(Gonzalez et al. 2017)
<b>pSD59</b>	encodes T25-RapZ(153-284aa) - R253 in pKT25	Durica-Mitic and Görke; unpublished
<b>pSD107</b>	As pBGG61, but <i>rapZ</i> -H190A	(Khan, 2019)
<b>pSD108</b>	As pBGG61, but <i>rapZ</i> -T248A	(Khan, 2019)
<b>pSD109</b>	As pBGG61, but <i>rapZ</i> -G249A	(Khan, 2019)
<b>pSD110</b>	As pBGG61, but <i>rapZ</i> -H252A	(Khan, 2019)
<b>pSD121</b>	encodes T25-RapZ-H190A in pKT25	(Khan, 2019)

<b>pSD122</b>	encodes T25-RapZ-T248A in pKT25	(Khan, 2019)
<b>pSD123</b>	encodes T25-RapZ-G249W in pKT25	(Khan, 2019)
<b>pSD124</b>	encodes T25-RapZ-H252A in pKT25	(Khan, 2019)
<b>pSD130</b>	As pBGG61, but <i>rapZ</i> -C247A	Durica-Mitic and Görke; unpublished
<b>pSD139</b>	encodes T25-RapZ-C247A in pKT25	Durica-Mitic and Görke; unpublished
<b>pSD155</b>	encodes T18-RapZ-C247A in pUT18C	Durica-Mitic and Görke; unpublished
<b>pSD179</b>	encodes T25-RapZ (153-284 aa) - C247A in pKT25	Durica-Mitic and Görke; unpublished
<b>pSD180</b>	encodes T18-RapZ (153-284 aa) - C247A in pUT18C	Durica-Mitic and Görke; unpublished
<b>pUT18C</b>	<i>P<sub>lac</sub>::cyaA</i> [225-399] (T18), MCS, <i>bla</i> , <i>ori</i> ColEI	(Karimova et al. 1998)
<b>pUT18C-ZIP</b>	encodes T18-GCN4 leucine zipper fusion in pUT18C	(Karimova et al. 1998)
<b>pYG46</b>	encodes T18-PtsN fusion in pUT18C	(Göpel et al. 2013)

#### 4.1.4 Oligonucleotides

Table 5 List of oligonucleotides used in this work

Name	Description/Sequence
<b>BG397</b>	Reverse primer for amplification of <i>rapZ</i> and cloning into pKESK23; <u>PstI</u> ; <i>rapZ</i> +833 to +855 TGGCTGCAGTCTAGATTATCATGGTTTACGTTTTTCCAGCG
<b>BG409</b>	Forward sequencing primer for pKES170-derivates; TM=70°C CGCGTTGGCCGATTCATTAATGC
<b>BG410</b>	Reverse sequencing primer for pKES170-derivates; TM=70°C CCATCGGCGCTACGGCGTTTC
<b>BG531</b>	Forward sequencing primer for <i>ptsP</i> ; <i>ptsP</i> +650 to +670 AGAAGCGGCAAACGAGTTTC
<b>BG637</b>	Forward primer, XbaI, TM=66°C; <i>rapZ</i> +1 to +22,

	GCGTCTAGAGATGGTACTGATGATCGTCAGCG
<b>BG639</b>	Reverse primer for creating N-terminal truncation of RapZ (153-284aa); ;KpnI;TM=66°C; rapZ +475 to +457 CGCGGTACCTCATGGTTTACGTTTTTCCAGCG
<b>BG647</b>	Reverse sequencing primer for pKT25; TM 64° GGGGATGTGCTGCAAGGCG
<b>BG1015</b>	Forward primer, NheI, TM=66°; rapZ +1 to +22 GGCTGCTAGCATGGTACTGATGATCGTCAGCG
<b>BG1049</b>	Forward primer for amplification of rapZ and cloning into pKESK23 with rapZ SD;Sacl;TM=66°C; rapZ -17 to +22 GGCGAGCTCGTGAGGAGAAACAGTACATGGTACTGATGATCGTCAGCG
<b>BG1223</b>	Forward primer for creating N-terminal truncation of RapZ (153-284aa); ;XbaI;TM=66°C; rapZ +457 to +475 GCGTCTAGAGCTGGGTAAACGTGAACGCG
<b>BG1419</b>	Forward sequencing primer for pUT18C; TM=72°C GAAGTTCTCGCCGGATGTACTGG
<b>BG1420</b>	Reverse sequencing primer for pUT18C; TM=72°C AGCGGGTGTGGCGGGTGTGG
<b>BG1645</b>	Forward sequencing primer for pKT25; TM 62°C. GCCATTATGCCGCATCTGTC
<b>BG1893</b>	Forward primer for cloning ptsP with strong Bacillus subtilis sacB RBS into vector pKESK23; EcoRI; TM = 62°C. ptsP +1 to +18 AAACAGAATTCAAAGGAGACATGACATATGCTCACTCGCCTGCGC
<b>BG1894</b>	Reverse primer for BG1893, i.e. for cloning ptsP with strong Bacillus subtilis sacB RBS into vector pKESK23; XbaI; TM = 64°C. ptsP +2247 to +2227 GGCTCTAGACTATAACCCTCCGCGAATCAG
<b>BG1934</b>	Phosphorylated mutagenesis primer to mutate R253K (CGT → AAA) in rapZ; TM= 46°C + 46°C; rapZ +744 to +775 Exchanged residues marked in red [P]-CGGCGGGAAGCACAAATCGGTGTATATTGCAAG
<b>BG1935</b>	Phosphorylated mutagenesis primer to mutate H190D (CAC → GAC) in rapZ; TM= 46°C + 46°C; rapZ +555 to +583 Exchanged residues marked in red

	[P]-CTTGCCGAACCCG <b>G</b> ACTGGGATCCGAAAC
<b>BG1951</b>	Reverse sequencing primer for pKESK23 constructs; TM= 64 °C GGTGATATGGGGCAAATGGTG
<b>BG2019</b>	Phosphorylated mutagenesis primer to exchange H190 to an amber stop codon (TAG) in <i>rapZ</i> ; TM = 60°C + 60°C; <i>rapZ</i> +550 to +589 Exchanged residues marked in <b>red</b> . [P]-CGCTTCTTGCCGAACCCG <b>TAG</b> TGGGATCCGAAACTGCGTC
<b>BG2020</b>	Phosphorylated mutagenesis primer to exchange C247 to an amber stop codon (TAG) in <i>rapZ</i> ; TM = 58°C + 60°C; <i>rapZ</i> +721 to +758 Exchanged residues marked in <b>red</b> . [P]-TTGACGGTCGCCATTGGTT <b>AG</b> ACCGGCGGGAAGCACCG
<b>BG2021</b>	Phosphorylated mutagenesis primer to exchange T248 to an amber stop codon (TAG) in <i>rapZ</i> ; TM = 60°C + 58°C; <i>rapZ</i> +723 to +761 Exchanged residues marked in <b>red</b> . [P]-GACGGTCGCCATTGGTTGT <b>AG</b> GGCGGGAAGCACCGTTC
<b>BG2022</b>	Phosphorylated mutagenesis primer to exchange G249 to an amber stop codon (TAG) in <i>rapZ</i> ; TM = 60°C + 60°C; <i>rapZ</i> +726 to +765 Exchanged residues marked in <b>red</b> . [P]-GGTCGCCATTGGTTGTACCT <b>AG</b> GGGAAGCACCGTTCGGTG
<b>BG2023</b>	Phosphorylated mutagenesis primer to exchange H252 to an amber stop codon (TAG) in <i>rapZ</i> ; TM = 60°C + 58°C; <i>rapZ</i> +736 to +776 Exchanged residues marked in <b>red</b> . [P]-GGTTGTACCGGCGGGAAG <b>TAG</b> CGTTCGGTGTATATTGCAGA
<b>BG2024</b>	Phosphorylated mutagenesis primer to exchange R253 to an amber stop codon (TAG) in <i>rapZ</i> ; TM = 60°C + 60°C; <i>rapZ</i> +739 to +780 Exchanged residues marked in <b>red</b> . [P]-TGTACCGGCGGGAAGCACT <b>AG</b> TCCGGTGTATATTGCAGAGCAA
<b>BG2034</b>	Phosphorylated mutagenesis primer to exchange D182 to an amber stop codon (TAG) in <i>rapZ</i> ; TM = 58°C + 58°C; <i>rapZ</i> +523 to +564 Exchanged residues marked in <b>red</b> . [P]- ATCGATGCAGATTACGTCTTT <b>AG</b> GTGCGCTTCTTGCCGAAC

## 4.2 Methods

### 4.2.1 Cultivation of *E.coli*

The cryo culture of the strain in use was streaked out on a plate and incubated O/N at 37°C. A single colony from the plate was inoculated in 5 mL LB for growth over night. The pre-culture grew at 37°C while shaking at 165 rpm.

### 4.2.2 Determination of Optical Density

Measuring optical density of bacterial cultures at a wavelength of 600 nm was used to estimate the concentration of cells in the media and determine their growth stage. 1 mL of the culture was transferred in a cuvette and OD<sub>600</sub> was determined in a spectrophotometer (Ibra S22, Biachrome). If the density was above a value of 1, the culture was diluted in LB and remeasured.

### 4.2.3 Preparation of cryo-cultures

For long term storage, strains and transformants were frozen at -80°C. Therefore, 1 mL of an overnight culture was mixed with 80 µL of DMSO, incubated on ice and transferred to the -80°C freezer.

### 4.2.4 Preparation of competent cells

Competent cells were prepared using two different methods, depending on the strain. For most strains the CaCl<sub>2</sub> method was used, while strain RH785 was made competent using the PEG method.

#### CaCl<sub>2</sub> method (Lederberg and Cohen, 1974)

O/N cultures were inoculated in 25 mL LB to an OD<sub>600</sub>=0,1 and they grew at 37°C, 165 rpm until an OD<sub>600</sub>=0,3-0,4. From this point on, the cells were kept on ice. The cultures were centrifuged at 3900 rpm, 4°C for 15 min (Eppendorf Centrifuge 5810 R, rotor S-4-104). The supernatant was removed and the pellet was resuspended in 10 mL 1 mM CaCl<sub>2</sub>. The cells were incubated on ice for 20 min and the previous centrifugation step was repeated. The supernatant was removed and the pellet resuspended in 1 mL CaCl<sub>2</sub>.

### PEG method (Chung et al., 1989)

O/N cultures were inoculated in 50 mL LB to an  $OD_{600}=0,1$  and they grew at  $37^{\circ}\text{C}$ , 165 rpm until an  $OD_{600}=0,5$ . The cells were incubated on ice for 10 min and pelleted for 10 min, at 3900 rpm and  $4^{\circ}\text{C}$  (Eppendorf Centrifuge 5810 R, rotor S-4-104). The pellets were resuspended in 2 mL cold TSS and incubated on ice for 30 min.

Table 6 Composition of TSS Buffer

TSS	
Stock Solutions	Working solution
	10% (w/v) PEG (MW3350), weighed in
1 M $\text{MgCl}_2$ , weighed in, autoclaved	10 mM $\text{MgCl}_2$
1 M $\text{MgSO}_4$ , weighed in, autoclaved	10 mM $\text{MgSO}_4$
2xLB, weighed in, set to pH 6,1, autoclaved	Diluted in 1xLB pH 6,1
	ddH <sub>2</sub> O to 50 mL, filter sterilized

### **4.2.5 Transformation of cells**

The cells were transformed in two different ways, depending on the method that was used to make them competent.

#### Transformation of $\text{CaCl}_2$ -competent cells (Lederberg and Cohen, 1974)

100  $\mu\text{L}$  of competent cells were added to 10-100 ng of plasmid and incubated on ice for 20 min. The cells were heat shocked at  $42^{\circ}\text{C}$  for 2,5 min and cooled down on ice for 10-15 min. 1 mL of LB was added to the cells and they were incubated at  $37^{\circ}\text{C}$  for 45 min. 100  $\mu\text{L}$  of cells were then plated on a fresh LB plate containing appropriate antibiotics. The remaining 900  $\mu\text{L}$  were then pelleted, resuspended in  $\sim 50$   $\mu\text{L}$  of the supernatant and plated. The plates were incubated at  $37^{\circ}\text{C}$  O/N. If bacterial two hybrid experiments were performed subsequently, the transformants grew at  $28^{\circ}\text{C}$  for 2 days.

### Transformation of PEG-competent cells (Chung et al., 1989)

10-100 ng of plasmid was mixed with 20  $\mu$ L of 5xKCM and 79  $\mu$ L of sterile ddH<sub>2</sub>O. The tubes were cooled down on ice and 100  $\mu$ L of competent cells were added. The cells were incubated on ice for 20 min and heat shocked at 37°C for 2 min. They were cooled down on ice, 1 mL LB was added and they were incubated at 37°C for 40 min. After that the cells were pelleted, resuspended in ~50  $\mu$ L of supernatant and plated. The cells grew for 2 days at 28°C.

Table 7 Composition of 5xKCM buffer

5xKCM	
Stock Solution	Working Solution
3 M KCl, weighed in, autoclaved	500 mM KCl
1 M MgCl <sub>2</sub> , weighed in, autoclaved	250 mM MgCl <sub>2</sub>
1 M CaCl <sub>2</sub> , weighed in, autoclaved	150 mM CaCl <sub>2</sub>

### **4.2.6 Polymerase chain reaction (PCR)**

PCRs were performed for DNA amplification purposes *in vitro*. A thermostable DNA polymerase was used to amplify the DNA. In case of analytic PCR, NEB-Taq polymerase was used, while PhuS was used for preparative PCRs. Alongside the polymerase, a PCR mix contained DNA, appropriate primers, dNTPs and a buffer containing Mg<sup>2+</sup> ions. The reaction tube was then placed in a Thermocycler (SensoQuest labcycler) where it underwent cycles of temperature changes. The incubation at different temperatures, allowed the DNA to denature, the primers to anneal and the polymerase to elongate the fragment. Denaturation was carried out at 94 or 98,5°C and elongation at 68 or 72°C depending on the polymerase. Annealing was performed at a temperature 5°C lower than the primers' melting temperature. To see if the amplification was successful, the entire reaction, or a sample of it were loaded on an agarose gel and checked via gel electrophoresis.

Table 8 PCR program NEB-Taq polymerase

PCR Program		
	94°C, 5 min	Initial denaturation
30 x	94°C, 45 sec	Denaturation
	Tm(primers)-5°C, 45 sec	Annealing
	68°C, 1 min/1000bp	Elongation
	68°C, 10 min	Final elongation
	4°C, ∞	Cooling

Table 9 PCR program PhuS polymerase

PCR Program		
	98,5°C, 5 min	Initial denaturation
30 x	98,5°C, 25 sec	Denaturation
	Tm(primers)-5°C, 45 sec	Annealing
	72°C, 1 min/1000bp	Elongation
	72°C, 2 min	Final elongation
	4°C, ∞	Cooling

#### 4.2.7 Analytic PCR

PCR is a convenient method to check whether a bacterial culture or colony contains a specific feature. To check if bacteria in a colony have a certain plasmid, a gene from the plasmid was amplified with primers annealing to the backbone, surrounding the place where the gene was incorporated. Alternatively to prove the presence or absence of a gene in the genome, two reactions were set up. One reaction contained primers that anneal inside of the gene, while the other had flanking primers that anneal both inside and outside of the gene. The reactions were set up in 12,5 or 25 µL. In case of a colony PCR, the colony was diluted in 100 µL of LB, and 0,5 or 1 µL of the suspension were added to the reaction. Taq polymerase was used to amplify the DNA.

Table 10 Composition of a PCR reaction used for checking features of a bacterial culture or colony

Component	Stock Solution	Final concentration
10xThermoPol Buffer	10x	1x
dNTPs	2 mM	0,2 mM
Forward Primer	5 pmol/ $\mu$ L	0,4 pmol/ $\mu$ l
Reverse Primer	5 pmol/ $\mu$ L	0,4 pmol/ $\mu$ l
Taq polymerase	5 U/ $\mu$ L	0,625 U per 25 $\mu$ l
DNA	1 colony in 100 $\mu$ L LB/ liquid culture	1 $\mu$ L per 25 $\mu$ l
ddH <sub>2</sub> O		To 12,5/25 $\mu$ L

#### 4.2.8 Preparative PCR for cloning purposes

For cloning purposes, a DNA fragment was amplified from a suitable template, cut and ligated into a new vector. The fragment was amplified via PCR, using primers that anneal to the beginning and end of the gene but also contain restriction sites and other features like Ribosome Binding Sites (RBS), if necessary. The PCR reaction for cloning was set up in 50  $\mu$ L and PfuS polymerase was used to amplify the fragment. PfuS polymerase has a proof-reading activity which, compared to the Taq polymerase, reduces the likelihood of mutations in the amplified product.

Table 11 Composition of a cloning PCR reaction

Component	Stock Solution	Final concentration
Buffer Hf (NEB)	5x	1x
dNTPs	2 mM	0,2 mM
Forward Primer	5 pmol/ $\mu$ L	0,4 pmol/ $\mu$ l
Reverse Primer	5 pmol/ $\mu$ L	0,4 pmol/ $\mu$ l
PfuS polymerase		1 $\mu$ L per 50 $\mu$ l
DNA (plasmid)	~ 100 ng/ $\mu$ l	~ 2 ng/ $\mu$ l
ddH <sub>2</sub> O		To 50 $\mu$ L

#### 4.2.9 Site directed mutagenesis by Combined Chain Reaction CCR (Bi and Stambrook, 1998)

CCR was used to introduce site specific single mutations into a gene. The reaction was set up similarly to a standard PCR, but it contained an additional primer that was 5'-phosphorylated and annealed to a sequence containing the nucleotides to be exchanged. Those nucleotides were replaced with the desired bases in the primer. The elongation was performed by Pfu polymerase. A thermo stable ampligase was used to incorporate the additional primer into the fragment during the 5'→3' extension.

Table 12 Composition of a CCR reaction

Component	Stock Solution	Final concentration
CCR buffer (10x)	10x	1x
dNTPs	2 mM	0,5 mM
Forward Primer	5 pmol/μL	0,2 pmol/μl
Reverse Primer	5 pmol/μL	0,2 pmol/μl
Mutagenesis Primer	5 pmol/μL	0,8 pmol/μl
BSA	10 mg/mL	0,2 mg/mL
Pfu polymerase	2,5 U/μl	5 U per 50 μl
Ampligase	5 U/μl	10 U per 50 μl
DNA (plasmid)	~ 100 ng/μl	~ 2 ng/μl
ddH <sub>2</sub> O		To 50 μl

Table 13 CCR program

CCR Program		
34 x	95°C, 5 min	Initial denaturation
	95°C, 45 sec	Denaturation
	Tm(primers)-5°C, 45 sec	Annealing
	65°C, 2.5min per 1000bp	Elongation
	65°C, 5 min	Final elongation
	4°C, ∞	Cooling

Table 14 Composition of the 10x CCR buffer

10x CCR Buffer (prepared by Dr. Muna Khan)	
200 mM Tris-HCl (pH 8,5)	
30 mM MgCl <sub>2</sub>	
500 mM KCl	
5 mM NAD <sup>+</sup>	

#### 4.2.10 Agarose gel electrophoresis of DNA

To separate DNA fragments by size, a DNA agarose gel electrophoresis was performed. A 1% agarose gel was prepared in 60 mL 1xTAE. The agarose was dissolved in the buffer by heating for 1-2 min in the microwave. The solution was then cooled to ~60°C and 3 µL of ethidium bromide solution were added. Next, the solution was poured into a tray and a 10 or 14 well comb was placed in it. The gel polymerized for 20 min. Samples were mixed with 10x DNA loading dye and loaded on the polymerized gel, next to 3 µL of 2-log DNA ladder (NEB #N3200). Electrophoresis was carried out in 1xTAE buffer.

Table 15 Concentration of Ethidium Bromide

Ethidium Bromide	
Stock Solution	Final Concentration
10 mg/µL	0,5 µg/µL

Table 16 Composition of buffers used for agarose gel electrophoresis of DNA

50xTAE (1L)	10x DNA loading dye	
	Stock Solutions	Working Solution
242 g Tris, weighed in		
57,1 ml acetic acid (glacial)	1 M Tris-HCl, weighed in, set to pH 8, autoclaved	0,25% (w/v) bromophenol blue, weighed in
18,61 g EDTA, weighed in	500 mM EDTA, weighed in, set to pH 8, autoclaved	10 mM Tris-HCl (pH 8,0)
autoclaved		1 mM EDTA (pH 8,0)
		30% (w/v) glycerol

#### **4.2.11 Analytic agarose gel electrophoresis of DNA**

In order to check whether a DNA method, such as PCR or restriction digestion, has worked, an analytic agarose electrophoresis was carried out. To this end, Agarose standard (Roth) was used and only a fraction of the PCR or restriction reaction was loaded on the gel, saving the remaining volume for further use. The samples were prepared in a way that 6,5  $\mu\text{L}$  of the reaction was mixed with 1  $\mu\text{L}$  of 10x DNA loading dye and filled up with ddH<sub>2</sub>O to a volume of 10  $\mu\text{L}$ . All 10  $\mu\text{L}$  were loaded on the agarose gel, as well as 3  $\mu\text{L}$  of DNA ladder. Electrophoresis was carried out for 20 min at 135V. Lastly, the gel was then visualized in a BioRad GelDoc system.

#### **4.2.12 Preparative agarose gel electrophoresis of DNA**

In cases where the desired DNA fragment was mixed with other fragments of a similar size, a preparative agarose gel electrophoresis was carried out. The aim of this method was to separate the fragments, so that specific ones can be cut out of the gel and purified. To this end, Universal agarose (VWR Life Science) was used, as it enables a better separation and is suitable for preparative purposes and the entire sample was loaded on the gel. 10x DNA loading dye was added to the sample to a final concentration of 1x and the sample was distributed amongst several lanes of the gel, loading a maximum of 20  $\mu\text{L}$  to each lane. 3  $\mu\text{L}$  of DNA ladder were loaded and electrophoresis was carried out for 35 min at 100V. Next, the desired fragments were cut out of the gel, on a UV trans-illuminator (360 nm).

#### **4.2.13 Amplification and purification of plasmids**

XL1-blue carrying the plasmid of interest was inoculated in 5 mL LB with the appropriate antibiotic and was growing O/N. The "NucleoSpin® Plasmid" kit was used for extracting the plasmid from the culture by following the protocol provided by the manufacturer. The plasmid was eluted in MiliQ water and stored at -20°C.

#### **4.2.14 Restriction digestion of DNA**

When cutting DNA with restriction enzymes, 2  $\mu\text{g}$  of DNA was added to a 60  $\mu\text{L}$  reaction. The reaction also contained 10-20 units of restriction enzyme and the corresponding buffer. The restriction was carried out for 2 hours at 37°C. Cutting DNA with two restriction enzymes, results in additional, unwanted fragments, next to the desired one. If those fragments are small enough (10-20 bp), they can be

removed during DNA purification, using the “NucleoSpin® Gel and PCR Clean-up” kit. However if the unwanted fragments are of considerable size, the restriction reaction needs to be loaded on a preparative agarose gel, the fragments separated via electrophoresis and the desired fragment cut out of the gel. The DNA is then extracted from the gel using the “NucleoSpin® Gel and PCR Clean-up” kit.

Table 17 Restriction enzymes used in this work

Restriction Enzyme	Concentration	Buffer	Supplier
EcoRI-HF	20 U/μL	CutSmart buffer	NEB
KpnI-HF	20 U/μL	CutSmart buffer	NEB
NheI-HF	20 U/μL	CutSmart buffer	NEB
SacI-HF	20 U/μL	CutSmart buffer	NEB
XbaI	20 U/μL	CutSmart buffer	NEB

#### 4.2.15 De-phosphorylation of 5'ends of DNA fragments

To prevent self-ligation of the empty vector, the vector was treated with alkaline phosphatase prior to ligation. 1 μL of FastAP alkaline phosphatase was added to 60 μL of the cut and cleaned DNA, together with the corresponding buffer. The reaction was carried out O/N at 37°C. The enzyme was inactivated by 5 min incubation at 75°C.

#### 4.2.16 Purification of DNA fragments from agarose gels and solutions

For extracting DNA out of gels and solutions, the “NucleoSpin® Gel and PCR Clean-up” kit was used. The procedure was done according to the provided protocol. The DNA was eluted in 30-60 μL MiliQ water and stored at -20°C until further use.

#### 4.2.17 Ligation of DNA fragments

Prior to ligation, the vector and the fragment were cut with the same restriction enzymes and purified. The vector was then treated with alkaline phosphatase. The ligation was performed in a 20 μL reaction and 50-100 ng vector was used. The amount of the insert was 3 times the molarity of the vector. 2,5 U of T4-DNA ligase was added to the reaction as well as the 10xligase buffer to an end volume of 1x. The reaction was incubated at RT for 2 hours. The entire volume was then used to transform competent XL1-blue cells.

#### **4.2.18 DNA sequencing (according to Sanger)**

To determine the sequence of a DNA fragment on a plasmid, 1 µg of plasmid was mixed with 3 µL of primer (5 pmol/µL) and filled up to a volume of 15 µL with sterile milliQ water. When sequencing a PCR product, 18 ng/100 bp were used. The sequencing samples were then sent to MicroSynth for sequencing. Once the results were received, they were analyzed using the Vector NTI software.

#### **4.2.19 General Transduction of genetic markers using phage T4GT7**

In order to move gene deletions tagged with an antibiotic resistance marker between strains, general transductions with phage T4GT7 were performed. For purposes of this work, already existing phage lysates were used, that were constructed earlier by colleagues and kept in the laboratory stock. The recipient strain grew O/N in 5 mL LB. 100 µL of four dilutions of the desired phage lysate were prepared ( $10^{-1}$ ,  $10^{-2}$ ,  $10^{-3}$  and  $10^{-4}$ ) and 500 µL of the O/N cultures were added to each dilution. After 20 min of incubation at RT, 100 µL were plated on one selective plate and 300 µL on another one. The plates were incubated for 2 days at 37°C until colonies appeared. To get rid of the phage, the colonies were streaked out on a fresh plate and grew O/N at 37°C. This was repeated 3 times.

#### **4.2.20 Curing strains of resistance cassettes flanked by FRT sites (Datsenko and Wanner, 2000)**

In order to cure newly constructed strains of the resistance marker, the FLP-FRT recombination system was used. Namely, the resistance cassette that was moved by transduction is located in between two flippase recognition target (FRT) sites. When expressed from a plasmid, the flippase recombination enzyme (FLP) cleaves the FRT sites, thereby enabling recombination of these sites and removal of the cassette. In this study, the strains were cured with plasmid pCP20, which is arabinose inducible and has a temperature sensitive origin of replication. To this end, the strain to be cured was transformed with pCP20 and grown O/N at 28°C. The next day, a colony was inoculated in 3 mL LB, supplemented with 0,2% arabinose at 37°C for several hours. Afterwards, 3 µL of culture were plated on a LB agar plate and incubated O/N at 42°C. This procedure was repeated 3 times.

#### **4.2.21 Incorporation of pBpF (Protocol provided by Prof. Dr. Karin Schnetz)**

Strain Z37 was double transformed with a plasmid carrying *strep-rapZ* containing an amber stop codon at the desired position (plasmids pMK55-61) and pEVOL-pBpF. The transformants were plated on LB-agar plates and grew for 2 days at 28°C. The colonies were inoculated in Tryptone media (TM; 5 g/L NaCl, 10 g/L Tryptone), supplemented with 15 µg/mL cloramphenicol, 100 µg/mL ampicilin and grew O/N at 37°C. When growing big cultures for protein purification, 2 mL of the O/N cultures were inoculated in 50 mL of the same media and were grown O/N at 37°C. The next day the cultures were inoculated to an OD<sub>600</sub>=0,1 in 25 mL or 250 mL of TM, supplemented with 15 µg/mL cloramphenicol, 100 µg/mL ampicilin and 10 mM L-arabinose, for either the incorporation test or protein purification. The cultures grew at 37°C for 5 h and then an analytic sample for SDS-page was harvested. Subsequently, they were induced with 1 mM IPTG and 200 µM pBpF and then grew for another 3 hours at 28°C, after which another analytic sample for SDS-page was taken. When growing cultures for protein purification, the cultures were pelleted for 20 min at 4°C and 5000 rpm (Sorvall RC 6+ Cntrifuge, rotor F12-6x500). The pellets were washed with 20 mL buffer W and pelleted again for 20 min at 4°C and 3900 rpm (Eppendorf Centrifuge 5810 R, rotor S-4-104). The pellets were stored at -20°C until purification. As a control, a culture with WT *rapZ* on plasmid was grown in parallel, as well as cultures that were not supplemented with pBpF.

#### **4.2.22 Protein purification via StrepTactin affinity chromatography**

The frozen pellets were thawed on ice and resuspended in 5 mL buffer W. The cells were then lysed using a one shot cell disruptor (Constant Systems) at 2 kbar. This was followed by two centrifugation steps, first at 4000 rpm and 4°C for 20 min (Eppendorf Centrifuge 5810 R, rotor S-4-104) and then 18000 rpm, 4°C for 60 min (Sorvall RC 6+ Cntrifuge, rotor F21S-8x50).. The lysate was loaded onto a Strep-Tactin sepharose column that was previously equilibrated with 2x 2,5 mL buffer W. A sample of the clear lysate and flow through was taken for SDS-PAGE. Once the sample completely run through the column, 4x 2,5 mL buffer W was loaded and a sample of each washing step was collected. The protein was eluted in 3 elution steps, using 300 µL buffer E, all of which was collected.

Table 18 Composition of buffers used for Strep-

Buffer W		Buffer E (prepared by Dr. Muna Khan)
Stock Solution	Working Solution	100 mM Tris-HCl pH 8
	100 mM Tris, weighed in	150 mM NaCl
	150 mM NaCl, weighed in	1 mM EDTA
500 mM EDTA, weighed in, set to pH 8, autoclaved	1 mM EDTA	2,5 mM D-desthiobiotin
	Adjusted to pH 8; autoclaved	

#### 4.2.23 Protein purification via Ni<sup>2+</sup>-NTA affinity chromatography

An overnight culture of BL21, transformed with a plasmid expressing His tagged QseE, grew in 10 mL LB+amp. An over day culture was inoculated in 250 mL LB+amp and grew at 37°C, 165 rpm, until OD<sub>600</sub>=0,5-0,8. An analytic sample for SDS-page was harvested and the culture was induced with 1 mM IPTG. It then grew for another hour. A second analytic sample for SDS-page was collected and the culture was centrifuged at 5000 rpm, 4°C for 20 min (Sorvall RC 6+ Cntrifuge, rotor F12-6x500). The cells were washed with 25 mL 1xZAP buffer and pelleted at 3900 rpm, 4 °C for 20 min (Eppendorf Centrifuge 5810 R, rotor S-4-104).

The frozen pellet was thawed on ice and resuspended in 5 mL of 1xZAP. The cells were then lysed using a one shot cell disruptor (Constant Systems) at 2 kbar. This was followed by two centrifugation steps, first at 4000 rpm and 4°C for 20 min and then 1800 rpm, 4°C for 60 min. The lysate was loaded onto a column, containing 750 µL Ni-NTA matrix that was previously equilibrated with 2 times 2,5 mL 1xZAP. A sample of the clear lysate and flow through was taken for SDS-PAGE. Once the sample completely run through, the matrix was washed with 10 mL of imidazole buffer containing increasing concentration of imidazole (5,10,25,50 and 80 mM). A sample of each washing step was collected. The protein was eluted using 3 mL of 125, 250 and 500 mM imidazole solution, all of which was collected.

Table 19 Composition of buffers used for His-purification

10x ZAP (everything weighed in)	Imidazole Stock Solution	Imidazole Working Solutions
500 mM Tris/HCl, weighed in, set to pH 7,5	500 mM Imidazole, weighed in	The Imidazole Stock solution was diluted to 50 mL of 5, 10, 25, 50, 80, 125 and 250 mM in 1xZAP
2 M NaCl, weighed in	1x ZAP to 500 mL	
Autoclaved	Autoclaved	

#### 4.2.24 Dialysis and storage of Strep and His purified proteins

The second elution fraction of the strep purified proteins was dialyzed in dialysis buffer I. For the second elution fraction of the His purified protein, 1 mL was also dialyzed in dialysis buffer I and the other 2 mL were frozen at -80°C, later thawed and dialyzed in dialysis buffer II. The proteins were dialyzed for 48 hours and the buffer was exchanged once in between. They were then shock frozen in liquid nitrogen and stored at -80 °C.

Table 20 Composition of buffers used for dialysis

10x Stock I (everything weighed in)	Dialysis Buffer I	10x Stock II (everything weighed in)	Dialysis Buffer II
0,5 M Tris/HCl pH 7,6	500 mL of 10x stock (1x)	0,5 M Tris/HCl pH 7,6	500 mL of 10x stock (1x)
2 M KCl	25 mL of 1M MnCl <sub>2</sub> (5 mM)	500 mM KCl	290 mL 86% glycerol (5%)
100 mM MgCl <sub>2</sub>	290 mL 86% glycerol (5%)	10 mM MgCl <sub>2</sub>	Cold MiliQ to 5L
MiliQ to 1L, autoclaved	Cold MiliQ to 5L	MiliQ to 1L, autoclaved	

#### 4.2.25 Determining protein concentration

Protein concentration was determined with the Pierce™ BCA Protein Assay Kit. Equal amounts of protein (according to the assay) were then loaded on a SDS gel. The bands were compared with each other and with a band of BSA of known

concentration. Since contaminant protein were co-purified with the proteins of interest, this method allowed for a more precise evaluation of the concentration of proteins of interest.

#### **4.2.26 UV photo-crosslinking of proteins with incorporated pBpF with their interaction partners (Rust et al., 2014)**

1 µg of each protein of a reaction was diluted in CL buffer to a volume of 50 µL. The reactions were pipetted into a 96-well plate, which was placed on ice and irradiated for 30 min using a 365 nm UV lamp. The reaction was quenched by adding 12,5 µL of 5x Laemmli buffer. 20 µL of each reaction was loaded on a 10% SDS gel. For Western Blotting, 15 µL of each reaction was loaded.

Table 21 Composition of buffers used for cross-linking

CL Buffer I	CL Buffer II	CL Buffer III
2 mL of 10xStock I (Table 20)	2 mL of 10xStock I (Table 20)	2 mL of 10xStock II (Table 20)
0,1 mL of 1M MnCl <sub>2</sub> (Table 18) (5 mM)	0,1 mL of 1M MnCl <sub>2</sub> (Table 18) (5 mM)	ddH <sub>2</sub> O to 20 mL
ddH <sub>2</sub> O to 20 mL	20 µL of 100 mM ATP	
	ddH <sub>2</sub> O to 20 mL	

#### **4.2.27 Denaturing polyacrylamide gel electrophoresis (SDS-PAGE) (Cleveland et al., 1977)**

Depending on the experiment, 10, 12,5 or 15% polyacrylamide separating gels were used, while the stacking gel always contained 5% polyacrylamide. When using cell lysates, the volume corresponding to 1 OD<sub>600</sub> was pelleted and resuspended in 200 µL of 1xLaemmli buffer. The tubes were incubated for 5-10 minutes at 65°C and placed on ice. 10 µL of the samples was then loaded on the gel, next to 3 µL of unstained, denatured protein molecular weight marker (Product #26612, Thermo Scientific). Purified proteins were mixed with 5xLaemmli to a final concentration of 1x and 20 µL of the sample was loaded. Gel electrophoresis was performed in 1x SDS Running buffer at 75 V in a BioRad electrophoresis chamber, until the samples reached the separating gel. Next, the voltage was increased to 120V. The

electrophoresis was stopped when the dye run out of the gel. The gels were then stained with fresh coomassie solution for 2 h or with already used coomassie solution O/N and destained with destaining solution for 2x 40 min. Imaging was performed using the ChemiDoc™ MP imaging system (BioRad).

Table 22 Composition of buffers used for SDS-PAGE

Separating gel (8 mL)				Stacking gel (5 mL)	
AA Percentage	10%	12,5%	15%	AA Percentage	5%
40% AA/bis 29:1	2 mL	2,5 mL	3 mL	40% AA/bis 29:1	625 µL
1,5 M Tris/HCl pH 8,8	2 mL			1 M Tris/HCl pH 6,8	600 µL
10% SDS	80 µL			10% SDS	50 µL
ddH <sub>2</sub> O	3,83 mL	3,33 mL	2,83 mL	ddH <sub>2</sub> O	3,67 mL
10% APS	80 µL			10% APS	50 µL
TEMED	8 µL			TEMED	5 µL
<b>Running Buffer</b>	<b>1x SDS gel loading dye (Laemmli Buffer)</b>			<b>Coomassie Staining Solution</b>	<b>Detaining Solution</b>
25 mM Tris	62,5 mM Tris/HCl pH 6,8			40% (v/v) Ethanol	40% (v/v) Ethanol
184 mM Glycine	5% (v/v) β-mercaptoethanol			10% (v/v) Acetic Acid	10% (v/v) Acetic Acid
0,1% SDS	2% (w/v) SDS			0,4% (w/v) Coomassie Brilliant blue R-250	
	0,05% (w/v) bromophenol blue				
	10% (v/v) glycerol				

#### 4.2.28 Western Blotting

15 µL of sample was loaded on a 10% denaturing polyacrylamide gel, next to 3 µL of prestained, denatured protein molecular weight marker (Product #26612, Thermo Scientific) and run as described before (see SDS-PAGE). Prior to blotting, a PVDF membrane (GE healthcare) was shortly dipped in methanol and then incubated for 5 minutes in transfer buffer. 6 Whatman paper as well as the gel were shortly dipped into Transfer buffer. 3 of the 6 Whatman paper were placed on the blotter (Peqlab) and the membrane was put on top of them. The gel was placed on the membrane and was covered with 3 additional Whatman paper. The proteins were then transferred from the gel to the membrane, using a semi dry blotting apparatus at 120 V for 1 hour. The membrane was first incubated in Blotto for 3 hours and then in the anti-Strep or anti-His antibody O/N. The anti-Strep antibody was diluted 1:15000 and the anti-His 1:20000 in 1xTBS + tween 20 (1:1000) + 3% BSA or anti-His. The next day, it was washed 3x 30 minutes in Blotto and then incubated for 1 hour in 15 µL of 1:100000 diluted Promega Anti-Rabbit antibody coupled with alkaline phosphatase. The membrane was washed for 3x20 min in blotto and incubated for 5 min in the dark with 1 mL 2x diluted CDP\* in Buffer III. The blots were imaged using ChemiDoc™ MP imaging system (BioRad).

Table 23 Composition of buffers used for western

Transfer-buffer 1L	Blotto 500 mL
3 g Tris, weighed in	50 mL 10x TBS
14,4 g Glycin, weighed in	15 g Milkpowder, weighed in
150 mL Methanol	500 µL Tween 20
ddH <sub>2</sub> O to 1L, autoclaved	
10x TBS	Buffer III
30 g Tris, weighed in	0,1 M Tris, weighed in
45 g NaCl, weighed in	0,1 M NaCl, weighed in
ddH <sub>2</sub> O to 1L, set to pH 7,6, autoclaved	ddH <sub>2</sub> O to 0,5 L, set to pH 9,5, autoclaved

#### 4.2.29 Total RNA extraction

RNA was extracted from cultures that grew to a specific OD or time point. 2 mL of the culture were harvested and centrifuged for 2 minutes at 11 000 rpm and 4°C. The pellets were then frozen in liquid nitrogen and stored at -80 °C until further use. For RNA extraction, the ReliaPrep™ RNA Miniprep kit was used. The pellets were thawed on ice and resuspended in 100 µL TE buffer with 400 µg/mL lysozyme, following 5 min incubation at RT. During the incubation, the samples were vortexed every 2 min. Next, 350 µL of BL-TG buffer supplemented with BME, was added and the solution was vortexed. Prior to loading on a column, 250 µL of 96% ethanol was added. The column was placed in a collection tube and centrifuged at 14 000 rpm for 45 s. The column was washed with 500 µL of the RNA wash solution and centrifugation was repeated. This was followed by a wash with 200 µL of Column wash solution and another centrifugation step, this time for 30 s at 14 000 rpm. The last two washes were performed with first 500, and then 300 µL of RNA wash, followed by a 45 s or 2 min centrifugation step at 14 000 rpm. Finally, the RNA was eluted in 50 µL nuclease free water, by two 1 min centrifugation steps at 14 000 rpm.

Table 24 Composition of buffers used for RNA extraction

1x TE-buffer + lysozyme		BL-TG buffer + BME
Stock Solutions	Working Solution	BL buffer provided in the kit
1 M Tris-HCl, weighed in, set to pH 8, autoclaved	Tris/HCl, pH8 stock diluted to 10 mM	1-thioglycerol (10 µl/ml)
500 mM EDTA, weighed in, set to pH 8, autoclaved	EDTA, pH8 stock diluted to 1 mM	β-mercaptoethanol (10 µl/ml)
	400 µg/ml lysozyme, weighed in	

#### 4.2.30 Denaturing Urea Polyacrylamide Gel Electrophoresis

8% polyacrylamide gels were casted and pre-run for 15 min in 0,5xTBE at 100V. The samples were mixed with 2xRNA loading dye and denatured for 15 min at 65°C. This was followed by 5 min incubation on ice and a short spin. The gel pockets were cleaned from urea and 10 µL sample was loaded on the gel while the gel was running.

Table 25 Composition of buffers used for urea gel electrophoresis

Denaturing Urea Gel (8% AA) 15 mL	10x TBE	2x RNA loading dye
6,3 g Urea	890 mM Tris	95% Formamide
3 mL 40% AA/bis 29:1	890 mM Boric Acid	0,025% SDS
1,5 mL 10xTBE	20 mM EDTA	0,025% bromophenol blue
5,25 ddH <sub>2</sub> O	To pH 8	0,025% Xylene cyanol FF
150 µL 10% APS		0,5 mM EDTA
3 µL TEMED		

#### 4.2.31 Northern Blotting

Three Whatman paper were placed on a semi dry blotter (Peqlab) and a nylon transfer membrane (GE healthcare) was put on top. The urea gel was put on the membrane and covered with additional 3 Whatman paper. All 6 Whatman paper, the membrane as well as the gel were dipped in 0,5xTBE buffer prior to the assembly. The transfer was performed for 1 hour at 120mA. After blotting, the RNA was crosslinked to the membrane by exposure to UV (254 nm) for 2-3 minutes and incubated in Pre-hybridization solution for 30 min at 68°C in a hybridization chamber. 0,5 µL of the DIG-labeled RNA probe was diluted in 500 µL pre-hybridization solution and added to the membrane. For hybridization, the membrane was incubated O/N at 68°C, rotating. The blots were washed by shaking 2x5 min in Wash-buffer I and incubation for 2x15 min in the hybridization chamber at 68°C in Wash-buffer II. They were then incubated for 30 min in Buffer II, after which, 1:10000 Anti-DIG Antibody conjugated with alkaline phosphatase, was added. This was followed by 3 incubation steps for 10 min in Buffer I and 10 min in Buffer II. The membrane was then incubated for 5 min in the dark with 280 µL 4x diluted CDP\* in Buffer III. The blots were imaged using ChemiDoc™ MP imaging system (BioRad).

Table 26 Composition of buffers used for northern

Pre-hybridization Solution (200 mL)	Wash-buffer I	5x Buffer I
100 mL Formamide	2x SSC	0,75 M NaCl
50 mL 20xSSC	0,1% SDS	0,5 M Malic Acid
40 mL 10% Blocking reagent		To pH 7,5
2 mL 10% N-laurylsarcosine		
0,4 mL 10% SDS	Wash-buffer II	Buffer II
	0,1x SSC	1x Buffer I
	1% SDS	1% Blocking reagent
20xSSC	Blocking Solution	Buffer III
3 M NaCl	10% Blocking reagent	0,1 M NaCl
0,3 M Sodium Citrate	1xBuffer I	0,1 M Tris
To pH 7		To pH 9,5

#### 4.2.32 Quantitative $\beta$ -galactosidase activity assay (Miller, 1972)

Cultures were growing to certain time points or optical densities at which a 1 mL sample was harvested and frozen at  $-20^{\circ}\text{C}$  until the assay was performed. The samples were thawed and resuspended in 1 mL Z-buffer. From that, 3 different solutions in Z-buffer were prepared, depending on the expected activity. 20  $\mu\text{L}$  of 0,1% SDS and 40  $\mu\text{L}$  Chloroform were added to the tubes, which were then vortexed for 15 seconds. The tubes were incubated at  $28^{\circ}\text{C}$  for 5 min and the reaction was started by adding 200  $\mu\text{L}$  ONPG solution. The reaction was going on for at least 30 min and was stopped with 500  $\mu\text{L}$  1M  $\text{Na}_2\text{CO}_3$  when a visible yellow color was developed. The samples were centrifuged at 13 000 rpm for 10 min and transferred into cuvettes to determine  $\text{OD}_{420}$ . The  $\beta$ -galactosidase activity was calculated in Miller units using the following formula:  $1 \text{ Miller unit} = \frac{\text{OD}_{420} \times V \times 1000}{t \times \text{OD}_{600}}$ , where  $t$ =reaction time [min],  $V$ =dilution factor,  $\text{OD}_{600}$ = optical density of cultures upon harvesting.

Table 27 Composition of Z-buffer and ONPG

Z-buffer	ONPG
60 mM Na <sub>2</sub> HPO <sub>4</sub>	60 mM Na <sub>2</sub> HPO <sub>4</sub>
40 mM NaH <sub>2</sub> PO <sub>4</sub>	40 mM NaH <sub>2</sub> PO <sub>4</sub>
10 mM KCl	4 mg/mL ONPG
1 mM MgSO <sub>4</sub>	

#### 4.2.33 The Bacterial Adenylate Cyclase-based Two-hybrid system (BACTH)

Adenylate cyclase (CyaA) is an enzyme that synthesizes cAMP. cAMP binds to the catabolite activator protein (CAP) and the cAMP/CAP complex acts as a pleiotropic regulator of gene transcription in *E.coli*. Amongst other genes, this complex activates expression of the *lac* operon, which enables the bacteria to utilize lactose and which makes them easily distinguishable on indicator or selective media. In *Bordetella pertussis* the catalytic domain of CyaA is composed of two complementary fragments T25 and T18, which are not active when physically separated, but their fusion results in cAMP synthesis. The bacterial adenylate cyclase-based two-hybrid system takes advantage of the nature of the CyaA of *Bordetella pertussis*, in order to detect and characterize protein-protein interaction *in vivo* in *E.coli* (Karimova et al., 1998). To detect interaction between two proteins, one of them needs to be fused to the T18 and the other to the T25 fragment of the *Bordetella pertussis* CyaA and the fusions need to be co-expressed in an *E.coli* strain lacking endogenous adenylate cyclase activity (strain BTH101 or RH785). This is achieved by using two plasmids with the corresponding fusions (derivatives of vectors pKT25 and pUT18C). The bacteria are co-transformed with the two plasmids and plated on indicator media (X-Gal or MacConkey plates) in order to detect the resulting phenotype. Interaction of the proteins of interest and thereby fusion of T18 and T25 fragments, can be quantified by measuring  $\beta$ -galactosidase enzymatic activity. The expression of the gene encoding  $\beta$ -galactosidase is positively regulated by cAMP/CAP and therefore the activity of the enzyme correlates with cAMP levels.

## **5. Results**

### **5.1 Part I**

The focus of the first part of this thesis was to investigate the potential ligand binding pocket of RapZ. Since the mechanism by which RapZ binds GlcN6P is not known, it was speculated that this pocket might play a role in the sensing of the metabolite. GlcN6P availability impacts *glmS* and *glmY* expression, as well as the stability of sRNAs GlmY and GlmZ. Therefore, in this thesis it was tested if changes in the pocket impact expression of *glmY* and *glmS* and whether there are changes in the accumulation of GlmY and GlmZ. In addition, it was investigated whether RapZ variants, carrying mutations in the potential binding pocket, can self interact. Lastly, a photo-crosslinking approach was used to determine whether the amino acids surrounding the pocket are located within the interaction surface of RapZ and QseE.

#### **5.1.1 Requirement of the potential ligand binding pocket of RapZ for regulation of *glmY* and *glmS* expression**

Regulation of *glmS* and *glmY* expression depends on GlcN6P availability, which is sensed by RapZ. Since it is hypothesized that the potential ligand binding pocket of RapZ binds GlcN6P, it was tested whether amino acid exchanges in the pocket could have an impact on *glmY* and *glmS* expression. In the case that amino acid exchanges in the pocket selectively impair GlcN6P binding and no other activity, it would be expected that RapZ acts as if there are GlcN6P depletion conditions. In the latter case, expression of, both *glmS* as well as *glmY* expression should be increased as compared to WT RapZ.

For the purpose of this experiment, 6 plasmids (pMK32-pMK37) were constructed, expressing various mutant *rapZ* genes from the IPTG inducible  $P_{tac}$  promoter. Each plasmid encodes for a RapZ variant carrying a particular single amino acid substitution in the presumptive GlcN6P-binding pocket. To test whether these substitutions influence expression of *glmY* or *glmS*, reporter gene assays were performed. The plasmids were used to complement a strain lacking endogenous *rapZ* and carrying either a *glmY'*- or a *glmS'-lacZ* fusion in the ectopic  $\lambda attB$  site on the chromosome.  $\beta$ -Galactosidase activity assays were performed to measure

expression of *glmY* or *glmS*. Each experiment was performed 3 times using two independent transformations. Averages and standard deviations were calculated and are shown in the graphs. For comparison, the  $\Delta rapZ$  strain carrying the empty expression vector (pKESK23) or the plasmid encoding *wild-type rapZ* (pMK31), were also employed. Additionally, the *wild-type* strain carrying endogenous *rapZ* was also tested.

In the experiments in which *glmS* expression was tested using a reporter gene fusion, the region -311 to +129 relative to the first nucleotide of the *glmS* gene was fused to *lacZ* (Kalamorz et al., 2007). This region includes a few nucleotides of the *glmU* gene, the *glmU-glmS* intergenic region (IGS) including the GImZ base-pairing site as well as a few nucleotides of the *glmS* 5' end. The fusion was expressed from the weak constitutive promoter driving expression of the upstream located *aadA* resistance gene (Kalamorz et al., 2007) and therefore independent of the cognate *glmUS* promoter. In this way it was possible to study post-transcriptional regulation of the *glmS* transcript, independently of transcription regulation. From each O/N culture, two 10 mL cultures were inoculated to  $OD_{600}=0,1$  and 1 mM IPTG was added to one of the two cultures. The cultures grew to exponential phase and were harvested at  $OD_{600}=0,5-0,8$ . As expected, only low activities were measured in the *wild-type* strain and in the  $\Delta rapZ$  mutant complemented with *wild-type rapZ* on a plasmid (Fig. 5A). In contrast, the  $\Delta rapZ$  mutant carrying the empty vector showed much higher activities. This is explained by the absence of RapZ, leaving GImZ un-cleaved and thereby active to upregulate translation of the *glmS'-lacZ* fusion by base-pairing. Interestingly, the RapZ variants carrying the T248A and H252A substitutions were still able to downregulate *glmS* expression, but all the other mutants were not capable to complement the  $\Delta rapZ$  mutation (Fig. 5A). This result indicates that residues H190, C247, G249 and R253 are essential for the regulation of *glmS* expression by RapZ. Since *rapZ* was expressed under the control of an IPTG inducible promoter, it was expected that the addition of 1 mM IPTG would increase RapZ amounts in the cell and therefore impact on the expression of *glmS*. However, addition of IPTG did not change the outcome of the experiment. Complementation could be observed in case of RapZ-T248A and RapZ-H252A, whereas the remaining variants were inactive, regardless of presence or absence of IPTG. To confirm these results, accumulation

of the GImS protein was monitored directly through analysis of total protein extracts by SDS-PAGE and Coomassie blue staining. The results are in perfect agreement with the data obtained in the  $\beta$ -galactosidase activity assays (Fig. 5B). Presence of wild-type RapZ or the variants with the T248A and H252A substitutions led to no visible GImS band in the gel. In all other cases, strong accumulation of GImS could be observed. These data show that 4 out of 6 residues in the presumptive GlcN6P binding pocket are required for repression of *glmS* expression and GImS synthesis by RapZ.

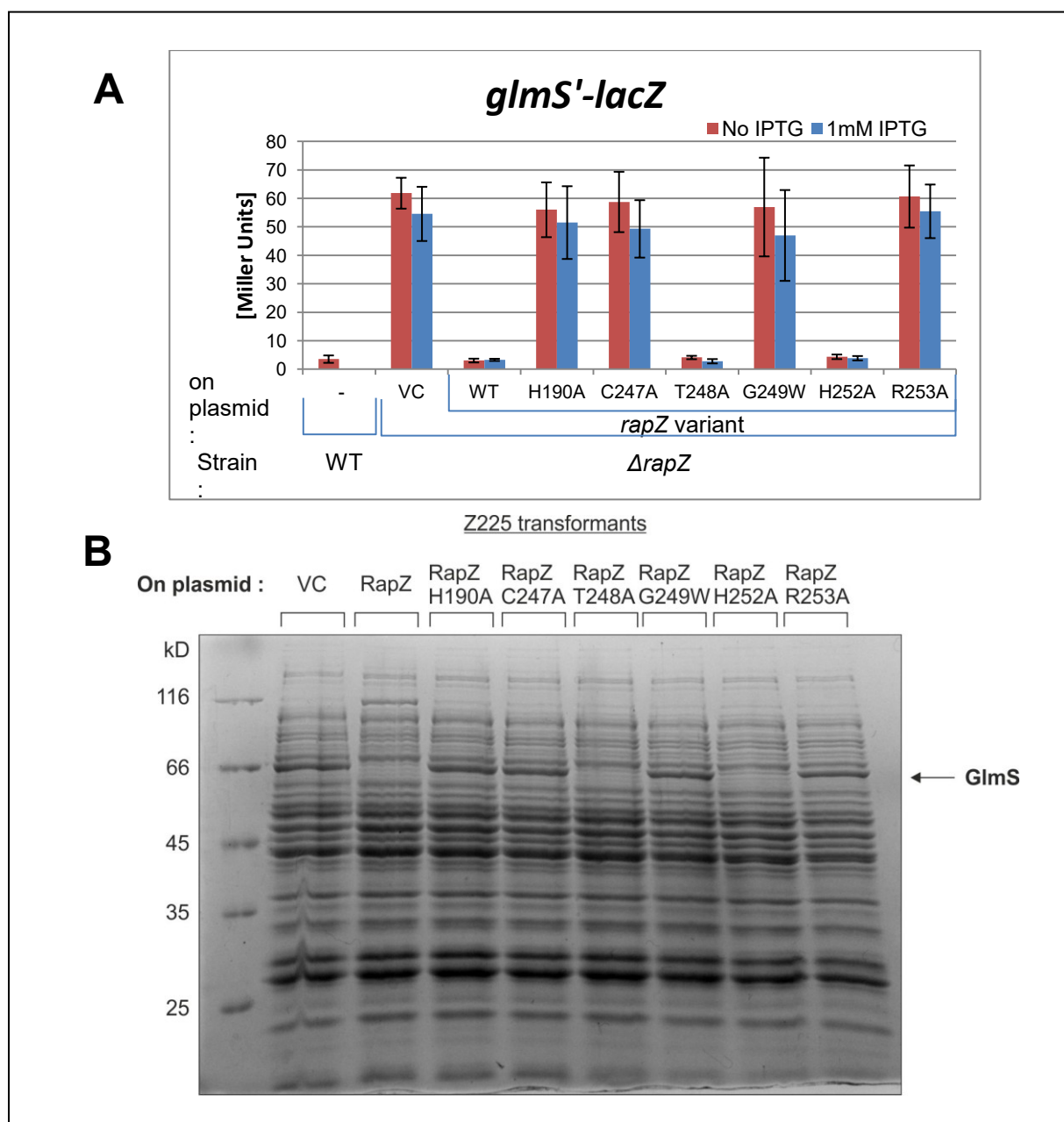


Figure 5. **Impact of substitutions in the presumptive GlcN6P binding pocket in RapZ on *glmS* expression.** **A**  $\beta$ -Galactosidase activity measured in strains carrying the *glmS'-lacZ* fusion under a constitutive promoter. The fusion was present in the chromosomes of strains Z8 (*wild-type*) and Z28 ( $\Delta rapZ$ ), while the RapZ variants carrying different mutations in the ligand binding pocket were produced from plasmids pMK32-37. The empty expression vector (pKESK23) and the plasmid encoding *wild-type rapZ* (pMK31), were assessed for comparison. From each O/N culture two cultures were inoculated in 10 mL LB+kan to OD<sub>600</sub>=0,1 and one of the two was induced with 1 mM IPTG. They grew at 37°, 165 rpm and were harvested in exponential growth phase (OD<sub>600</sub>=0,5-0,8). The shown values are the means, calculated from 3 independent measurements. The error bars indicate the standard deviation between different measurements. **B** SDS-PAGE analysis of total protein extracts of strain Z225 carrying the plasmids described in A. The cultures were induced with 1 mM IPTG at OD<sub>600</sub>=0,1 and harvested in exponential growth phase (OD<sub>600</sub>=0,5-0,8). The SDS-PAA gel was stained with Coomassie brilliant blue. The arrow indicates the band for the GlmS protein.

Next, the effects of the RapZ variants on expression of *glmY* were investigated. In this case, a reporter fusion was used consisting of the region -238 to +22 of *glmY* fused to *lacZ*. This region contains both the  $\sigma^{70}$ - and  $\sigma^{54}$ -dependent promoters including the QseF binding sites required for transcription initiation by  $\sigma^{54}$ . The experiments were performed similarly to the *glmS* reporter gene measurements discussed before, but additional samples were collected in the exponential growth phase as well as after 4 h (OD<sub>600</sub>=2-3) and 6 h (OD<sub>600</sub>=3-4) of growth. As expected, *glmY* expression was decreased in the  $\Delta rapZ$  mutant carrying the empty vector control, as compared to the strains containing *rapZ*, either endogenously or produced from a plasmid (Fig. 6). This result reflects previous findings that activity of QseE/QseF controlling *glmY* transcription is stimulated by interaction with RapZ. This occurs in particular under GlcN6P depletion conditions, but even under normal growth conditions a fraction of RapZ may remain GlcN6P-free and is thereby capable to activate QseE/QseF (Khan et al., 2020). In the exponential growth phase, none of the mutants was able to complement the  $\Delta rapZ$  mutation and to activate *glmY* transcription (Fig. 6A). In contrast, following 4 or 6 hours of growth, the RapZ-H190A and -T248A variants were able to complement partially, in case their synthesis was induced with IPTG (Figs. 6B and 6C). These data unexpectedly revealed that the tested residues are all required for proper activation of *glmY* expression by RapZ.

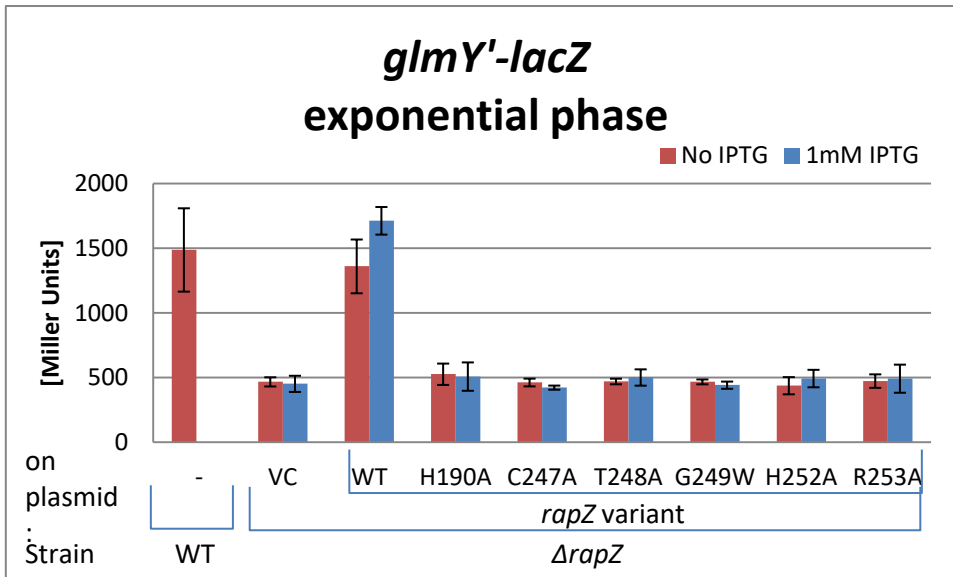
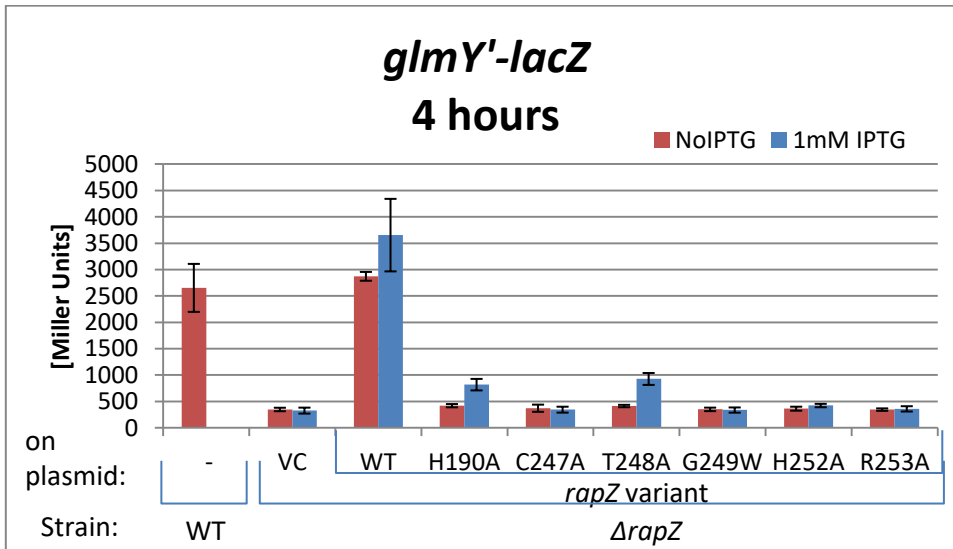
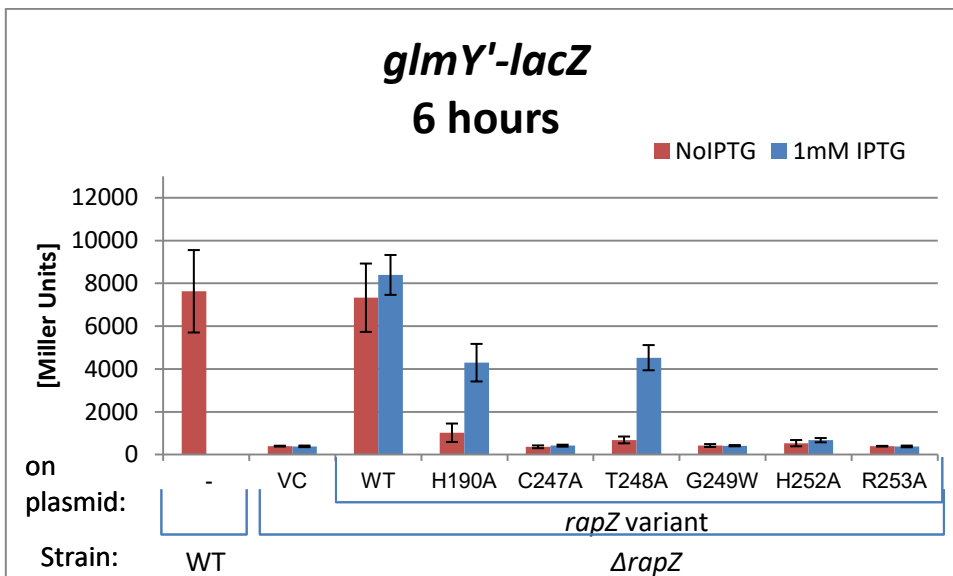
**A****B****C**

Figure 6. . **Impact of substitutions in the presumptive GlcN6P binding pocket in RapZ on *glmY* expression.**  $\beta$ -Galactosidase activity measured in strains carrying the *glmY*-*lacZ* fusion under the native promoters. The fusion was present in the chromosomes of strains Z197 (*wild-type*) and Z225 ( $\Delta rapZ$ ), while the RapZ variants carrying different mutations in the ligand binding pocket were produced from plasmids pMK32-37. The empty expression vector (pKESK23) and the plasmid encoding *wild-type rapZ* (pMK31), were assessed for comparison. From each O/N culture two cultures were inoculated in 10 mL LB+kan to  $OD_{600}=0,1$  and one of the two was induced with 1 mM IPTG. They grew at 37°, 165 rpm and were harvested in exponential growth phase ( $OD_{600}=0,5-0,8$ ) (A), after 4 hours of growth (B) and after 6 hour of growth (C) . The shown values are the means, calculated from 3 independent measurements. The error bars indicate the standard deviation between different measurements.

### 5.1.2 Self interaction properties of RapZ variants carrying amino acid substitutions in the presumptive GlcN6P binding pocket

The amino acid substitutions introduced to RapZ, could have an impact on the protein structure and interaction properties. This could then influence the expression patterns of *glmY* or *glmS*, as well as the RNA binding properties of the protein. For example, if a RapZ variant is no longer able to self-interact, it is no longer active since the tetrameric form of RapZ is required for its function (Gonzalez et al., 2017). To assess whether the inability to complement a chromosomal  $\Delta rapZ$  deletion as observed in the previous experiments (Figs. 5 and 6) is due to a loss of self-interaction of the corresponding RapZ variants, bacterial two hybrid experiments were performed. In the following experiment, it was tested whether the various RapZ variants are still able to self-oligomerize when carrying amino acid substitutions in the potential GlcN6P binding pocket. To this end, the experiments were performed in strain RH785 ( $\Delta cyaA$ ). The strain was co-transformed with two plasmids, via PEG transformation. One of them encoded a particular RapZ variant fused to the T25 domain of adenylate cyclase, while the other plasmid encoded the same variant fused to the T18 domain. For comparison, a transformant carrying the plasmids encoding *wt-rapZ* fused to the T18- and T25-domains of the adenylate cyclase, respectively, was included. In addition, strain was also co-transformed with two plasmids encoding the yeast GCN4 leucine zipper fused to the T25- and T18-domains. Dimerization of the latter fusion proteins is monitored as positive control in the BACTH assay. A transformant carrying the empty plasmids pUT18C and pKT25

encoding the unfused T18- and T25-domains, served as negative control. Colonies were inoculated in 10 mL LB+amp+kan+IPTG, respectively, and the cultures grew for 16-17h at 28°C, 165 rpm to an OD<sub>600</sub>~3. Subsequently, the  $\beta$ -galactosidase activities were determined.

As expected, only low activities were detectable in case of the negative control. In contrast, the positive control monitoring GCN4 leucine zipper dimerization, generated high  $\beta$ -galactosidase activities (Fig. 7A, columns 2). Similar high activities were detected for the various RapZ variants indicating their unrestricted self-oligomerization (Fig. 7A). This result indicates that the amino acids of the putative ligand pocket are not essential for self-interaction of full length RapZ. However, previous results have shown that both, the RapZ-NTD as well as the CTD can dimerize on their own (Gonzalez et al., 2017). Therefore, self-interaction of the NTD could mask possible dimerization defects of the CTD. To account for this possibility, the separated CTDs of the various RapZ variants were tested for self-interaction by BACTH (Fig. 7B). In this case, an impaired dimerization of the RapZ-CTD was observed, when containing the amino acid substitution H252A. The corresponding transformant produced three-fold lower values as compared to the strain producing the WT-RapZ-CTDs fused to the T18- and T25-domains of adenylate cyclase, respectively (Fig. 7B, cf. columns 3 and 8). However, the deviations between individual measurements performed in Fig. 7B were quite high. Nonetheless, in each individual measurement, the activities measured for self-oligomerization of RapZ-CTD-H252A were 2-6 fold lower as compared to the corresponding WT constructs. Altogether, these experiments show that both full-length RapZ as well as RapZ-CTD can self-interact regardless of the amino acid substitutions introduced in the potential substrate binding pocket. An exception is RapZ carrying the H252A substitution, since this exchange impairs CTD dimerization.

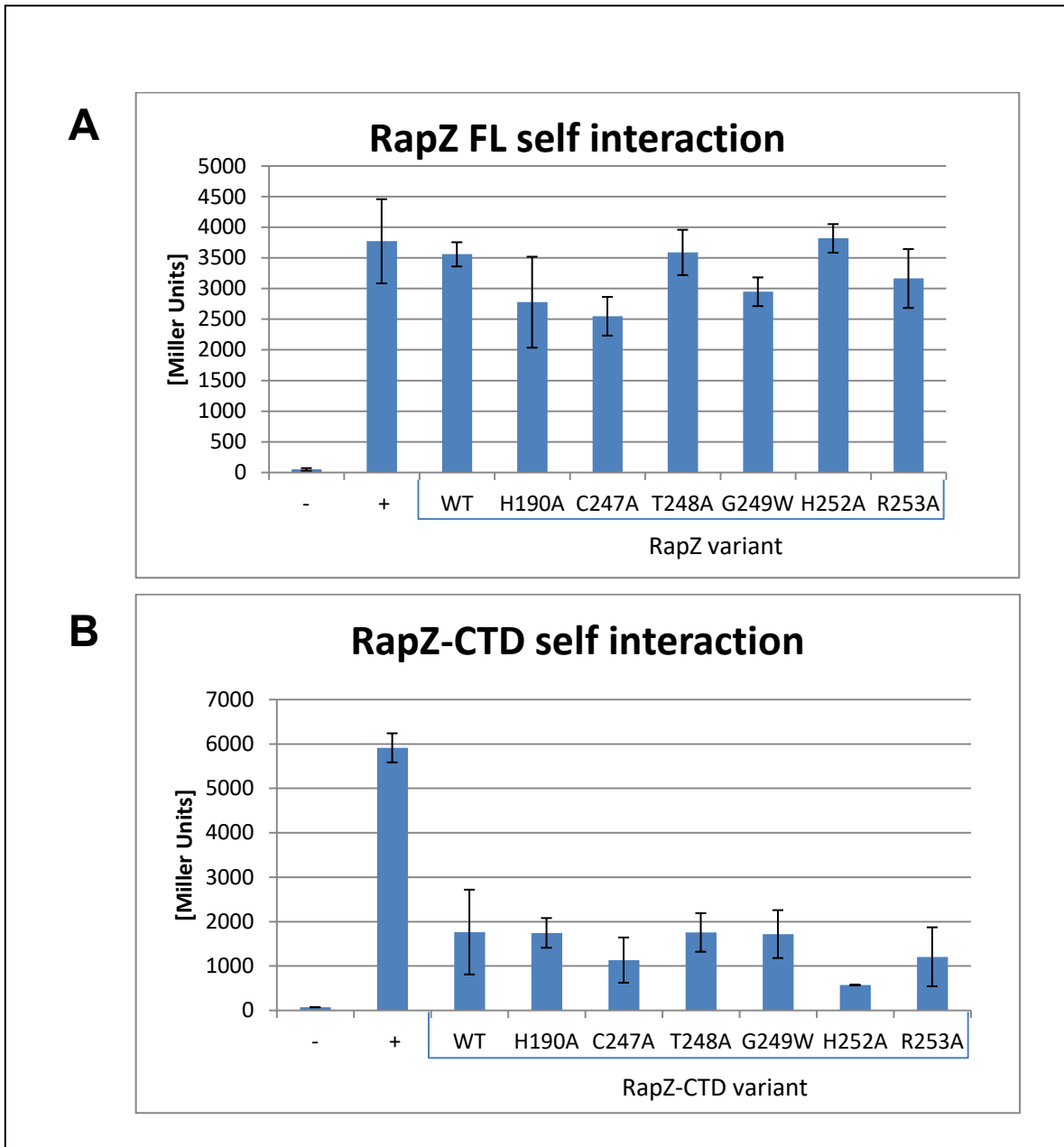


Figure 7. **Self-interaction of RapZ carrying amino acid substitutions in the presumptive GlcN6P binding.** **A**  $\beta$ -Galactosidase activity, measured as part of the BACTH assay that was performed in strain RH785. The strain was transformed with plasmids encoding full-length RapZ variants fused to the T18 (plasmids pMK21-25 and pSD155) and T25 (plasmids pBGG457, pSD121-124 and 139) domain of adenylate cyclase. For comparison the experiment was performed in RH785 transformed with plasmids encoding T18- and T25-WT-RapZ fusions (plasmids pBGG348 and pBGG349). **B**  $\beta$ -Galactosidase activity, measured as part of the BACTH assay that was performed in strain RH785. The strain was transformed with plasmids encoding RapZ-CTD variants fused to the T18 (plasmids pMK44-48 and pSD180) and T25 (plasmids pMK40-43, pSD59 and 179) domain of adenylate cyclase. For comparison the experiment was performed in RH785 transformed with plasmids encoding T18-

and T25-WT-RapZ-CTD fusions (plasmids pSD10 and 12).

Colonies were inoculated in 10 mL LB+amp+kan, induced with 1 mM IPTG and the cultures grew for 16-17h at 28°C, 165 rpm to an OD<sub>600</sub>~3. In both graphs “+” stands for the strain transformed with plasmids pUT18C-ZIP and pKT25-ZIP, which encode the T25- and T18-GCN4 leucine zipper fusions, while “-” represents RH785 transformed with plasmids where nothing is fused to the T18 and T25 domain of adenylate cyclase (pKT25 and pUT18C). The shown values are the means, calculated from 3 independent measurements. The error bars indicate the standard deviation between different measurements.

### **5.1.3 The role of positively charged amino acids in the potential GlcN6P binding pocket**

Three of the six amino acids comprising the putative metabolite binding pocket of RapZ, carry a positive charge. In the previous experiments, all of those three amino acids (H190, H252 and R253) were substituted with a neutrally charged alanine. Replacement of R253 with an Ala residue abolished the ability of RapZ to activate *glmY* expression, whereas the H190A variant retained residual activity (Fig. 6). To see whether the positive charges of these two residues play a role in the activation of *glmY* expression, H190 was substituted with a negatively charged aspartic acid, whereas R253 was substituted with a positively charged lysine residue. A complementation experiment was performed, in which *glmY* expression was assessed in the same way as described in chapter 5.1.1. It was already observed before that RapZ-H190A can partially complement in respect to activation of *glmY* expression (Fig. 6B and C). However, when the positively charged histidine was replaced with a negatively charged aspartic acid, this complementation was almost lost (Fig. 9). This implies that the positive charge of this amino acid could be important for the activation of the QseE/QseF TCS and thereby *glmY* expression. Introduction of a negatively charged Asp residue could abolish interaction of RapZ with QseE/QseF by electrostatic repulsion. In contrast, expression of *glmY* is lost in case of both RapZ-R253 variants, regardless whether substituted with a neutral alanine or a positively charged lysine residue (Fig. 6 and 9). Thus, a positively charge at position 253 per se is not sufficient for RapZ activity. This suggests that the loss of activity as observed for RapZ-R253A is not simply due to the change of the charge. To see whether the charges of the amino acids surrounding the potential ligand binding pocket in RapZ are important for self-interaction, a BACTH experiment was

performed. The experiment was performed as described in chapter 5.1.2. All tested variants were able to self-interact (Fig. 8). These results show that the positive charge of amino acid H190 in RapZ is important for the activation of *glmY* expression through interaction with the QseE/QseF TCS. In contrast, a positive charge at position 253 is not sufficient to retain RapZ activity. An Arg residue at this position is specifically required for the latter process.

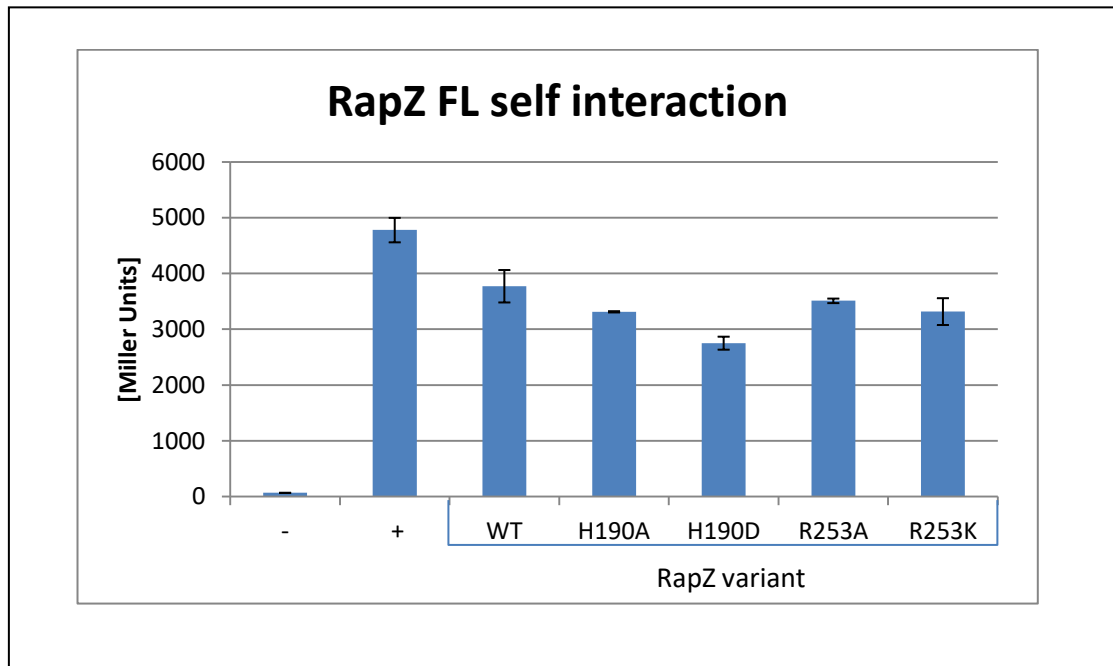


Figure 8. **Impact of the positive charges at positions H190 and R253 for self-interaction of full-length RapZ.**

$\beta$ -Galactosidase activity, measured as part of the BACTH assay that was performed in strain RH785. The strain was transformed with plasmids encoding full-length RapZ variants fused to the T18 (plasmids pMK 21,25,53 and 54) and T25 (plasmids pBGG457, pMK51 and 52 and pSD121) domain of adenylate cyclase. For comparison the experiment was performed in RH785 transformed with plasmids encoding T18- and T25-WT-RapZ fusions (plasmids pBGG348 and 349). Colonies were inoculated in 10 mL LB+amp+kan, induced with 1 mM IPTG and the cultures grew for 16-17h at 28°C, 165 rpm to an  $OD_{600} \sim 3$ . “+” stands for the strain transformed with plasmids pUT18C-ZIP and pKT25-ZIP, which encode the T25- and T18-GCN4 leucine zipper fusions, while “-” represents RH785 transformed with plasmids where nothing is fused to the T18 and T25 domain of adenylate cyclase (pKT25 and pUT18C). The shown values are the means, calculated from 3 independent measurements. The error bars indicate the standard deviation between different measurements.

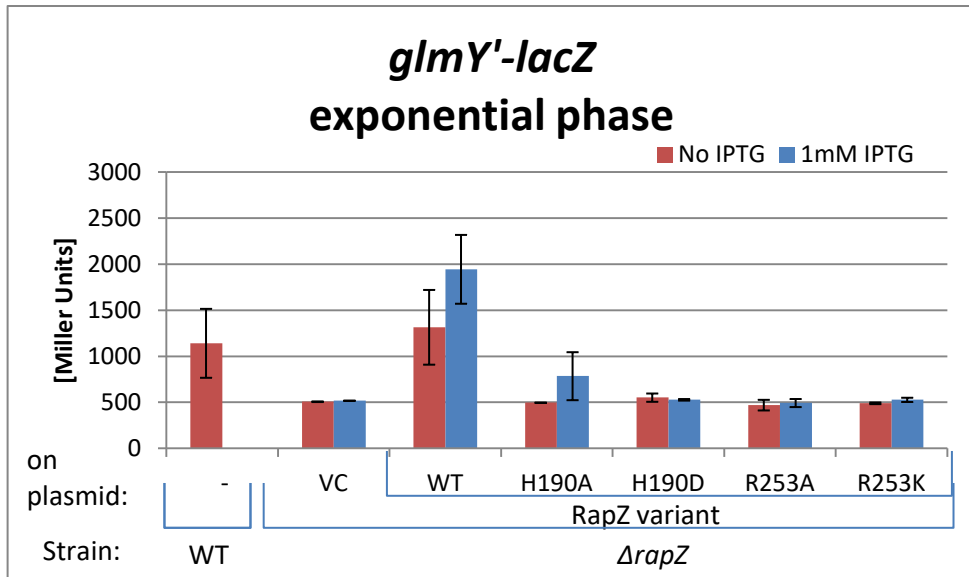
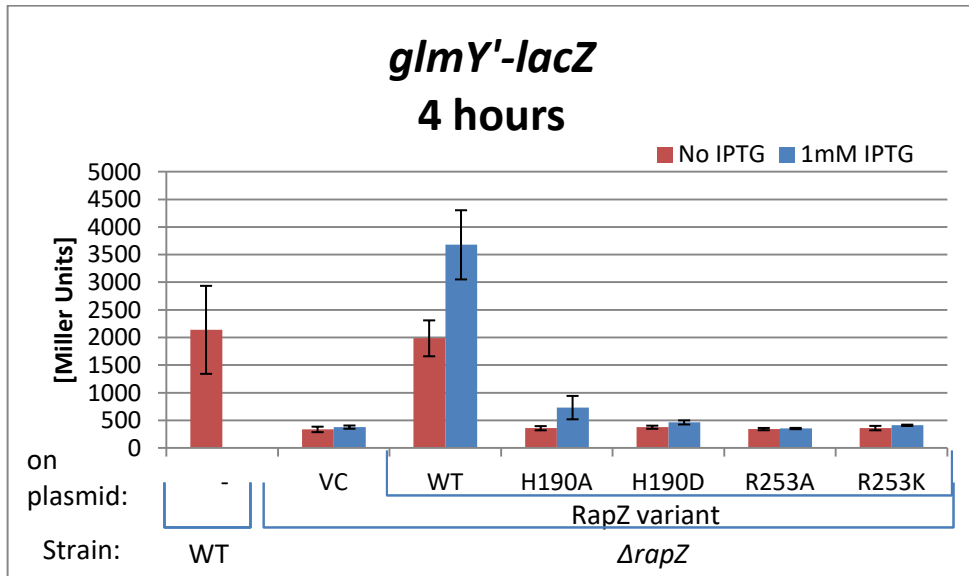
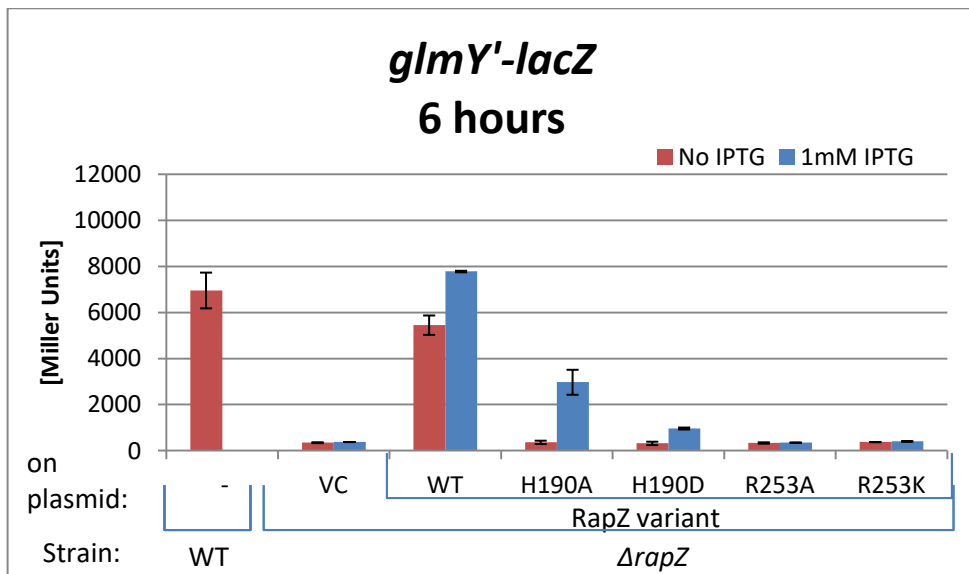
**A****B****C**

Figure 9. **Impact of the positive charge in amino acid residues H190 and R253 of RapZ on *glmY* expression.**  $\beta$ -Galactosidase activity measured in strains carrying the *glmY*-*lacZ* fusion under the native promoters. The fusion was present in the chromosomes of strains Z197 (*wild-type*) and Z225 ( $\Delta$ *rapZ*), while the RapZ variants carrying different mutations in the ligand binding pocket were produced from plasmids (pMK32, pMK37, pMK49, pMK50). The empty expression vector (pKESK23) and the plasmid encoding *wild-type rapZ* (pMK31), were assessed for comparison. From each O/N culture two cultures were inoculated in 10 mL LB+kan to  $OD_{600}=0,1$  and one of the two was induced with 1 mM IPTG. They grew at 37°, 165 rpm and were harvested in exponential growth phase ( $OD_{600}=0,5-0,8$ ) (A), after 4 hours of growth (B) and after 6 hour of growth (C) . The shown values are the means, calculated from 2 independent measurements. The error bars indicate the standard deviation between different measurements.

#### 5.1.4 Requirement of the potential ligand binding pocket of RapZ for controlling GlmY and GlmZ

So far it was suggested that 4 out of 6 residues in the presumptive GlcN6P binding pocket of RapZ are required for repression of *glmS* expression and GlmS synthesis and that all of them are required for proper activation of *glmY* expression. In order to investigate this further, it was tested wheter RapZ variants that carry substitutions of those residues are still able to control the levels of GlmY and GlmZ *in vivo*. To this end, Northern blotting experiments were performed. Since WT-RapZ decreases GlmZ levels by recruiting it to RNase E (Durica-Mitic et al., 2020), higher levels of full-length GlmZ were expected for the variants wich lost the ability to bind GlmZ or recruit it to RNase E. On the other hand, in depletion conditions, RapZ increases levels of GlmY on two levels. Firstly, by activating *glmY* transcription and secondly by stabilizing the sRNA via binding (Khan et al., 2020).. Therefore, this experiment shows the results of the combined effect that RapZ has on GlmY levels.

To investigate this idea, accumulation of GlmY and GlmZ was monitored *in vivo* in a  $\Delta$ *rapZ* strain, which was complemented with plasmids triggering production of the various RapZ variants with substitutions in the potential ligand binding pocket. For this purpose, samples were used that were harvested from the same cultures tested before in chapter 5.1.1 (Fig. 5). Total RNA was extracted from cultures and Northern blotting was performed. To this end, 2.3  $\mu$ g of each extracted RNA was separated on a denaturing urea gel. The gel was then blotted and hybridized with probes specific for either GlmZ or GlmY. Subsequently, the membranes were stripped and re-probed

with a probe for 5S to obtain loading controls. It was shown before that none of the RapZ variants can activate *glmY* expression to the extent as observed for WT-RapZ (Fig. 6). Therefore, it was unsurprising that GlmY levels appeared to be lower in the transformants synthesizing the various RapZ variants as compared to WT-RapZ (Fig. 10A). However, this observation must be treated with caution as high GlmY levels were sometimes even observed in the un-complemented strain or in the empty vector control (Fig. 10A, right panel, lanes 1-3). These inconsistencies might be blotting artifacts or caused by loading differences.

In the case of GlmZ, none of the RapZ variants was able to trigger its cleavage as efficiently as observed for WT RapZ (Fig. 10B). However, differences regarding the steady state level of unprocessed GlmZ became detectable between individual RapZ variants. The amount of full-length GlmZ appeared to be decreased in case of RapZ-T248A and RapZ-H252A when compared with the non-complemented strain or the other RapZ variants (Fig. 10B). In addition, a very faint band representing cleaved GlmZ could be detected in the blots. This result is very similar to observations made previously for RapZ variants that lack RNA-binding activity but retain the ability to interact with RNase E (Durica-Mitic et al., 2020, RNA). These latter variants still trigger processing of GlmZ by RNase E, but are not capable to stabilize the cleaved variant of GlmZ through binding, resulting in its rapid degradation. Consequently, it is reasonable to assume that the RapZ-T248A and RapZ-H252A variants can still recruit RNase E to activate cleavage of GlmZ via protein-protein interaction, but are affected in RNA-binding and lack the ability to stabilize processed GlmZ.

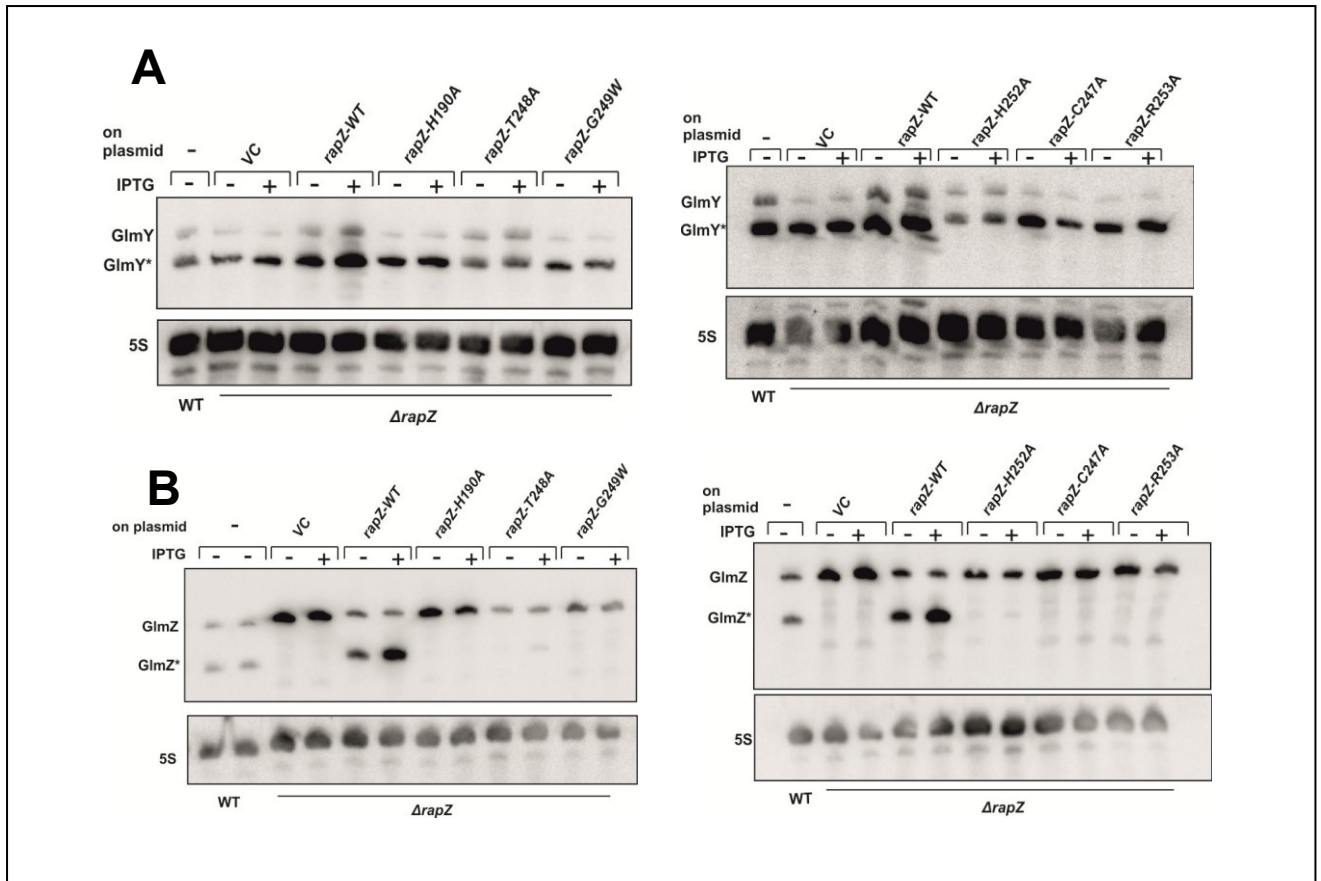


Figure 10. **Accumulation of GlmY and GlmZ in response to RapZ variants carrying substitutions in the presumptive GlcN6P binding pocket**. Northern blots of total RNA isolated from strain Z28 with different RapZ variants encoded from plasmids pMK32-37. The empty expression vector (pKESK23) and the plasmid encoding *wild-type rapZ* (pMK31), were assessed for comparison, as well as the *wild-type* strain Z8, carrying endogenous *rapZ* (marked as – on the blots). The cultures were harvested in exponential growth phase ( $OD_{600}=0,5-0,8$ ) and 2.3  $\mu\text{g}$  of RNA was separated on a 8% urea gel. In picture **A** the signals indicate GlmY, while in picture **B** the blots were hybridized with a probe against GlmZ. The membranes were stripped and re probed for 5S as an internal control. In picture **B**, there was overflow from the first into the second lane in the left blot.

### 5.1.5 Assessing direct interaction of residues composing the putative ligand binding pocket in RapZ with QseE and RNase E using photocrosslinking

In a previous experiment it was shown that RapZ loses its ability to activate *glmY* expression (Fig. 6), when residues comprising the potential ligand binding pocket are substituted with another amino acid. The previous experiments have shown that RapZ loses its ability to activate *glmY* expression (Fig. 6), when residues comprising the potential ligand binding pocket are substituted with another amino acid. Substitution of residues C247, G249, H252 and R253 abolished the ability of RapZ to activate *glmY* expression, whereas substitution of H190 and T248 decreased this

response. One possible explanation for this result is that residues from the pocket are in direct contact with the QseE/QseF TCS. However, previous experiments have shown that substitution of these residues in RapZ has no major impact on its interaction with QseE or QseF as measured by BACTH (Khan, 2019, doctoral thesis). Thus, it is possible that corresponding RapZ variants are still capable to bind QseE/QseF (i.e. substitution of only one residue is not sufficient to abrogate binding), but lack the ability to activate the TCS. To investigate whether residues of the putative ligand binding pocket are indeed contacting the TCS, a photocrosslinking approach was used. In addition, it was previously shown that the C-terminal region of RapZ is also involved in interaction with RNase E. Even though the CTD alone is not able to interact with RNase E, when in the tetrameric form, RapZ interacts with the endoribonuclease via multiple residues from both the NTD and CTD (Durica-Mitic et al., 2020). Therefore in this experiment it was also tested whether the residues of the presumptive GlcN6P binding pocket are contacting RNase E.

A photocrosslinking approach was chosen to determine, whether the amino acids located in the presumptive GlcN6P binding pocket of RapZ, are also in vicinity to the interaction surfaces used by QseE and RNase E to bind RapZ. For this purpose, the non-canonical photocrosslinkable amino acid p-benzoyl-L-phenylalanine (pBpF) was incorporated, replacing the natural amino acids at the corresponding positions in the pocket, respectively. To accomplish such a site-specific incorporation, the nucleotides coding for the respective amino acid were mutated to an amber stop codon (TAG). This stop codon is recognized by an orthogonal tRNA (o-tRNA), which is aminoacylated with pBpF by a corresponding cognate orthogonal aminoacyl-tRNA synthetase (o-aaRS) (Fig. 11B). To achieve incorporation of pBpF into RapZ, a two-plasmid system was used. One of the plasmids, pEVOL-pBpF, encodes the o-tRNA and two copies of the o-aaRS under the arabinose inducible  $P_{BAD}$  promoter and it carries a chloramphenicol resistance marker. *strep-rapZ* with the amber stop codon was expressed from the IPTG inducible  $P_{tac}$  promoter on the other plasmid (pMK55-pMK60 and pMK61), which contained an ampicillin resistance marker (Fig. 11A).

Once pBpF was incorporated into the potential ligand binding pocket, the corresponding Strep-tagged RapZ variant was purified via StrepTactin affinity chromatography, subsequently mixed with purified His<sub>10</sub>-tagged QseE or RNase E

and UV-crosslinked at a wavelength of 365 nm. Afterwards, SDS-PAGE and Western blotting were performed to determine whether higher molecular weight complexes are formed after crosslinking. Importantly, the formed crosslinks are not resolved by denaturing SDS gel electrophoresis and their maintenance would indicate that the amino acid replaced with pBpF is in direct contact with QseE. In other words, a stable crosslink would only form if pBpF is incorporated within the interaction surface used by RapZ to contact QseE (Rust et al., 2014). Residue D182 in RapZ was previously shown to participate in dimerization of the RapZ-CTD and substitution of this residue with Ala abolishes self-interaction (Gonzalez et al., 20217). Therefore, a RapZ variant incorporating pBpF at this position was included as a control. Photocrosslinking should allow for detection of higher RapZ oligomers in this case, providing a positive control.

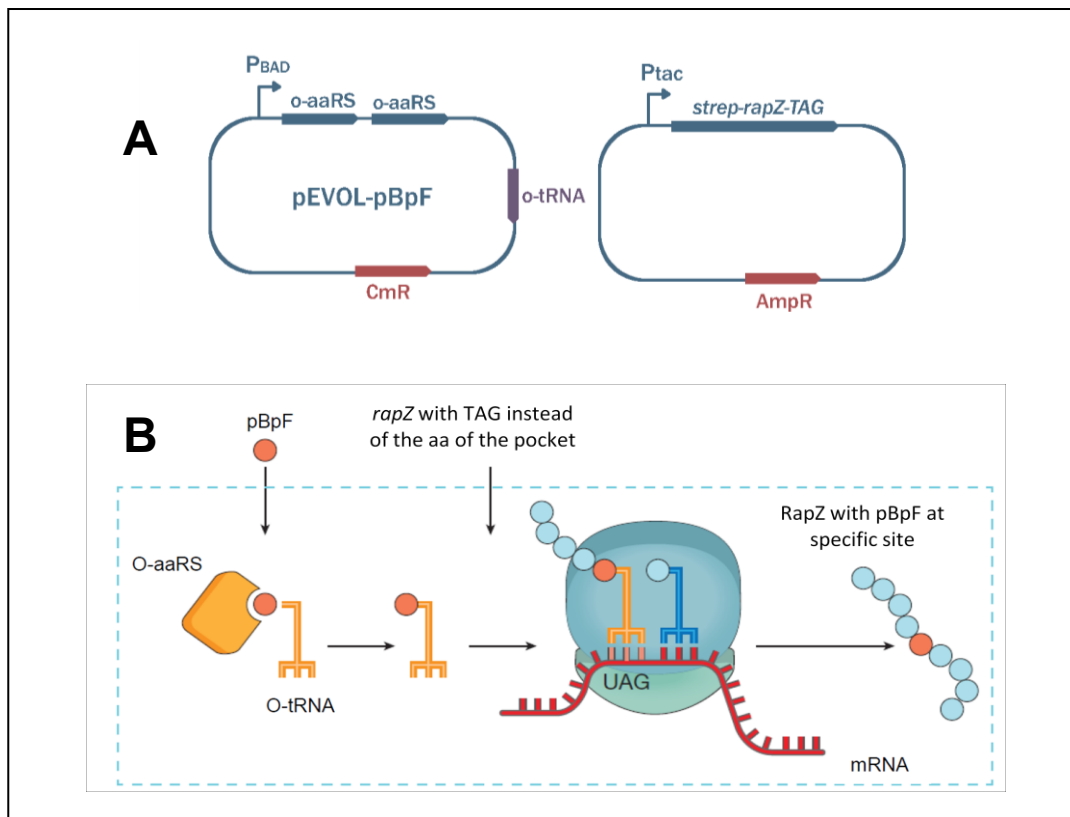


Figure 11. **Incorporation of the non-canonical amino acid pBpF into RapZ.** **A.** The two-plasmid system used to achieve incorporation of pBpF into RapZ. One of the two plasmids, pEVOL-pBpF encodes for an orthogonal tRNA (o-tRNA), which recognizes the amber stop codon and two copies of the cognate orthogonal aminoacyl-tRNA synthetase (o-aaRS), which aminoacylates the o-tRNA with pBpF. The plasmid carries a chloramphenicol resistance marker. The other plasmid (pMK55-pMK60 and pMK61) encodes Strep-RapZ that carries an amber stop codon and an ampicillin resistance marker. **B.** O-aaRS stands for orthogonal aminoacyl-tRNA synthetase and O-tRNA for orthogonal

tRNA. The O-aaRS loads the crosslinkable pBpF onto the O-tRNA. O-tRNA recognizes the amber stop codon in the *rapZ* mRNA and pBpF becomes incorporated at the desired site. The image was adopted from a review and modified (Chin, 2017).

#### **5.1.5.1 Construction of *rapZ* variants carrying amber stop codons at defined positions**

In first step in this experiment, site directed mutagenesis was used to replace the codons of interest with amber stop codons, respectively. For this purpose, combined chain reactions were performed, which incorporated 5'-phosphorylated oligonucleotides carrying the desired exchanges during a PCR reaction into the *rapZ* gene, respectively. To this end, *rapZ* was amplified with the external primers BG1015/BG397 using plasmid pBGG348 as template. In addition, a 5'-phosphorylated mutagenesis primer carrying the desired mutation (oligonucleotides BG2019-BG2024 and BG2034) was added to the PCR reactions, respectively. The resulting PCR fragments comprising *rapZ* with the desired stop codon was then cloned into plasmid pBGG237 by using the XbaI/NheI restriction sites. This latter construction fused the *rapZ* alleles in frame with the sequence encoding the Strep-tag, allowing for a later purification of the resulting Strep-RapZ proteins via StrepTactin affinity chromatography. Correct incorporation of the amber stop codons at the level of the DNA was verified through DNA sequencing. To test whether presence of the stop codons also results in synthesis of accordingly truncated RapZ variants, strain Z37 ( $\Delta rapZ$ ) was transformed with the constructed plasmids (pMK55-pMK61), respectively. A strain lacking endogenous RapZ was used to avoid later co-purification of *wild-type* RapZ through oligomerization with the constructed RapZ variants. To this end, O/N cultures were inoculated in 10 mL LB+amp to OD<sub>600</sub>=0,1 and grown to the exponential phase at 37°C. Subsequently, the cultures were induced with 1 mM IPTG and a first series of samples was harvested at this time. Following an additional hour of growth, a second series of samples was harvested. The samples were mixed with 1x Laemmli buffer and denatured for 5 min at 65°C. 10 µL of each sample were separated by SDS-PAGE using a 15% polyacrylamide gel (Fig. 12). Indeed, in presence of IPTG synthesis of truncated RapZ variants was observed, as reflected by accumulation of strong protein bands in the range of 20-30 kDa. The theoretical molecular weights of the various RapZ variants (including their Strep-tag) proteins were calculated using the VectorNTI software (Table 28) and

compared with the apparent molecular weights of these proteins as deduced from their migration velocity in the SDS-gel. In all cases, the theoretical and apparent molecular weights were in agreement, indicating that translation stops at the incorporated stop codons, as expected

Table 28 Predicted molecular mass of truncated RapZ proteins, calculated with VectorNTI

Strep-RapZ:	WT	D182 <sub>amber</sub>	H190 <sub>amber</sub>	C247 <sub>amber</sub>	T248 <sub>amber</sub>	G249 <sub>amber</sub>	H252 <sub>amber</sub>	R253 <sub>amber</sub>
kDa	33,8	21,8	22,8	29,5	29,6	29,6	29,9	30

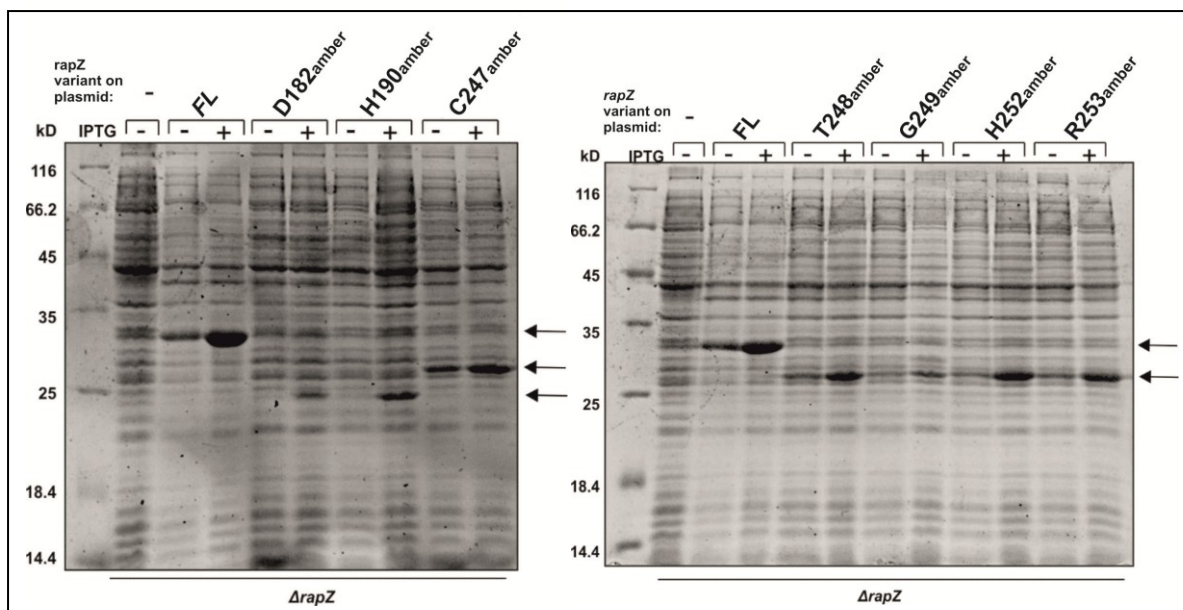


Figure 12. **Verification of synthesis of truncated RapZ variants as a consequence of introduction of stop codons at various positions.** Cell lysates of strain Z37 transformed with plasmids pMK55-pMK61, respectively, separated on 15% polyacrylamide SDS-PAGE gels. The O/N cultures were inoculated to  $OD_{600}=0,1$  in 10 mL LB+amp. They grew at 37°C, 165 rpm until the exponential growth phase ( $OD_{600}=0,5-0,8$ ), when a sample was harvested and 1 mM IPTG was added. They grew for 1 more hour, when another sample was harvested. For comparison, Z37 transformed with pMK31 (marked as FL on the picture) that encodes WT-RapZ, and the empty vector pBGG237 were tested. The arrows indicate the band for the full length and truncated RapZ proteins.

In the next step, it was tested whether cells would incorporate pBpF during *rapZ* translation at the amber stop codons that were introduced before by site-directed mutagenesis. For this purpose, strain Z37 was doubly transformed with plasmid pEVOL-pBpF and the newly constructed plasmids (pMK55-pMK61) carrying the various *strep-rapZ* mutants (Supplementary table 1). Plasmid pEVOL-pBpF encodes for both, the O-tRNA that recognizes the amber stop codon and the O-aaRS that

aminoacylates O-tRNA with pBpF. In order to incorporate pBpF into RapZ, three sets of cultures were inoculated from the O/N cultures in 25 mL tryptone media supplemented with amp, cm and L-arabinose for induction of O-aaRS synthesis. Tryptone media was used in order to minimize the abundance of other amino acids and ensure the uptake of pBpF. The cultures grew at 37°C under 165 rpm agitation until they reached the exponential growth phase ( $OD_{600}=0,5-0,8$ ). At this time, a first series of analytic samples was harvested and one set of cultures was supplemented with 1 mM IPTG and 200  $\mu$ M pBpF, another with 1 mM IPTG and 200  $\mu$ M pBpF and the last one with only 1 mM IPTG. Subsequently, growth was continued for additional 3 h at 28°C, to ensure incorporation of pBpF at the stop codon and finally a second set of analytic samples was harvested. The samples were mixed with 1x Laemmli buffer, denatured for 5 min at 65°C and separated by SDS-PAGE on a 15% polyacrylamide gel. The SDS gel was analyzed by Coomassie blue staining. Indeed, protein bands corresponding to full-length RapZ accumulated exclusively in those cultures that were grown in presence of both IPTG and pBpF (Fig. 13). When pBpF was omitted (but IPTG included), only the corresponding shorter RapZ variants became visible whose translation was stopped at the premature stop codons (Fig. 13). No additional protein bands differing from the vector control were observable in the absence of both, pBpF as well as IPTG. These results prove that cells incorporated pBpF correctly at the positions of the premature amber stop codons in *rapZ*. Presence of pBpF enabled the ribosome to continue translation, regardless of the stop codon, and accordingly full length RapZ variants were obtained.

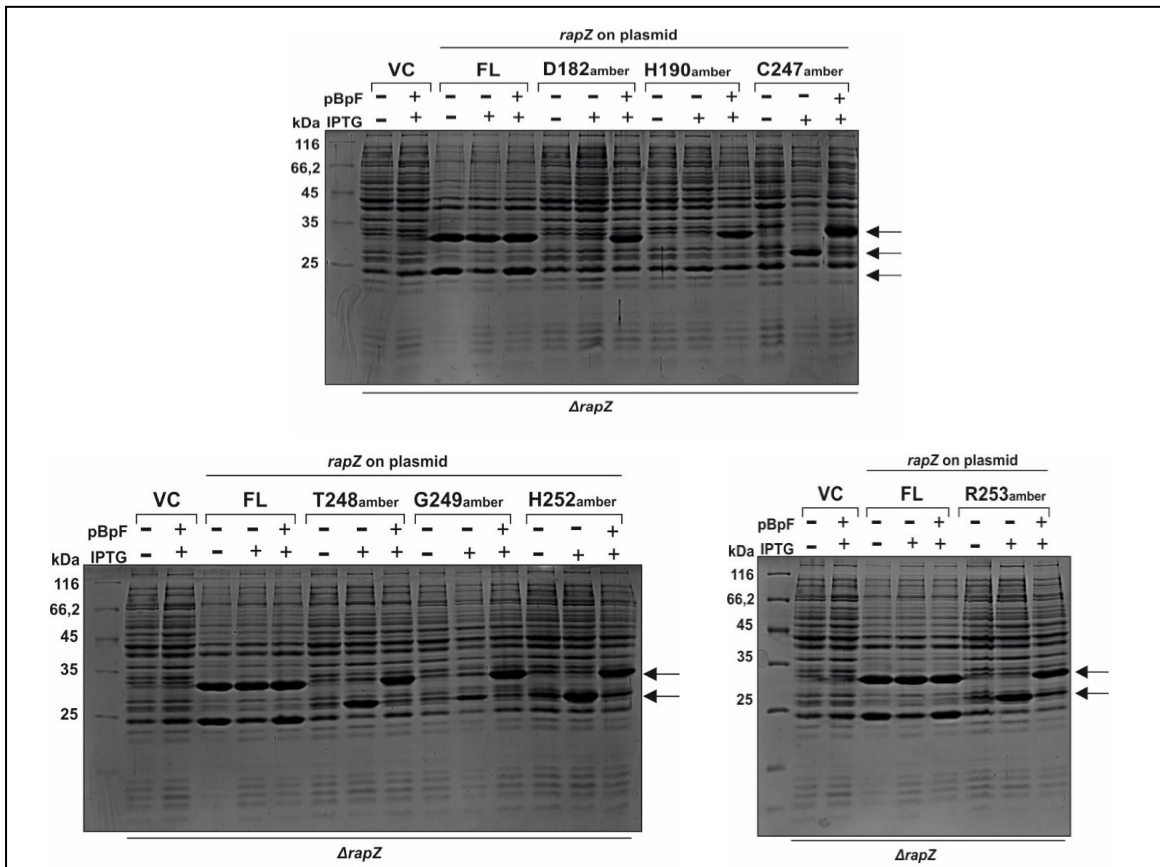


Figure 13. . **Test of pBpF incorporation at premature amber stop codons during translation of *rapZ*.** Cell lysates of strain Z37 double-transformed with one of the plasmids pMK55-61 and pEVOL-pBpF were separated on 15% polyacrylamide SDS-PAGE gels. The O/N cultures were inoculated in 25 mL TM/amp/cm/L-ara to  $OD_{600}=0,1$  and grew at 37°C until the exponential growth phase ( $OD_{600}=0,5-0,8$ ). The cultures were induced with either 1 mM IPTG alone or 1 mM IPTG and 200  $\mu$ M pBpF and they grew for 3h at 28°C. . For comparison, Z37 double-transformed with pEVOL-pBpF and pMK31 that encodes WT-RapZ (marked as FL on the picture), and pEVOL-pBpF and empty vector pBGG237 were tested. The arrows indicate the band for the full length and truncated RapZ proteins.

### 5.1.5.2. Purification of His<sub>10</sub>-QseE and the Strep-RapZ-pBpF variants for *in vitro* UV crosslinking experiments.

Once incorporation of pBpF at the desired positions in RapZ had been verified (see chapter before), purification of larger quantities of these proteins was required to carry out the planned UV crosslinking experiments. To this end, 250 mL cultures were grown and incorporation of pBpF into Strep-RapZ was achieved as explained before (see 5.1.5.2.). Once again, analytic samples were harvested before and after addition of IPTG and pBpF, to verify overproduction of the full-length proteins in the latter cases. Indeed, analysis of the cell extracts by SDS-PAGE/Coomassie blue staining confirmed accumulation of full-length Strep-RapZ exclusively in the cells treated with IPTG and pBpF (Fig. 14).

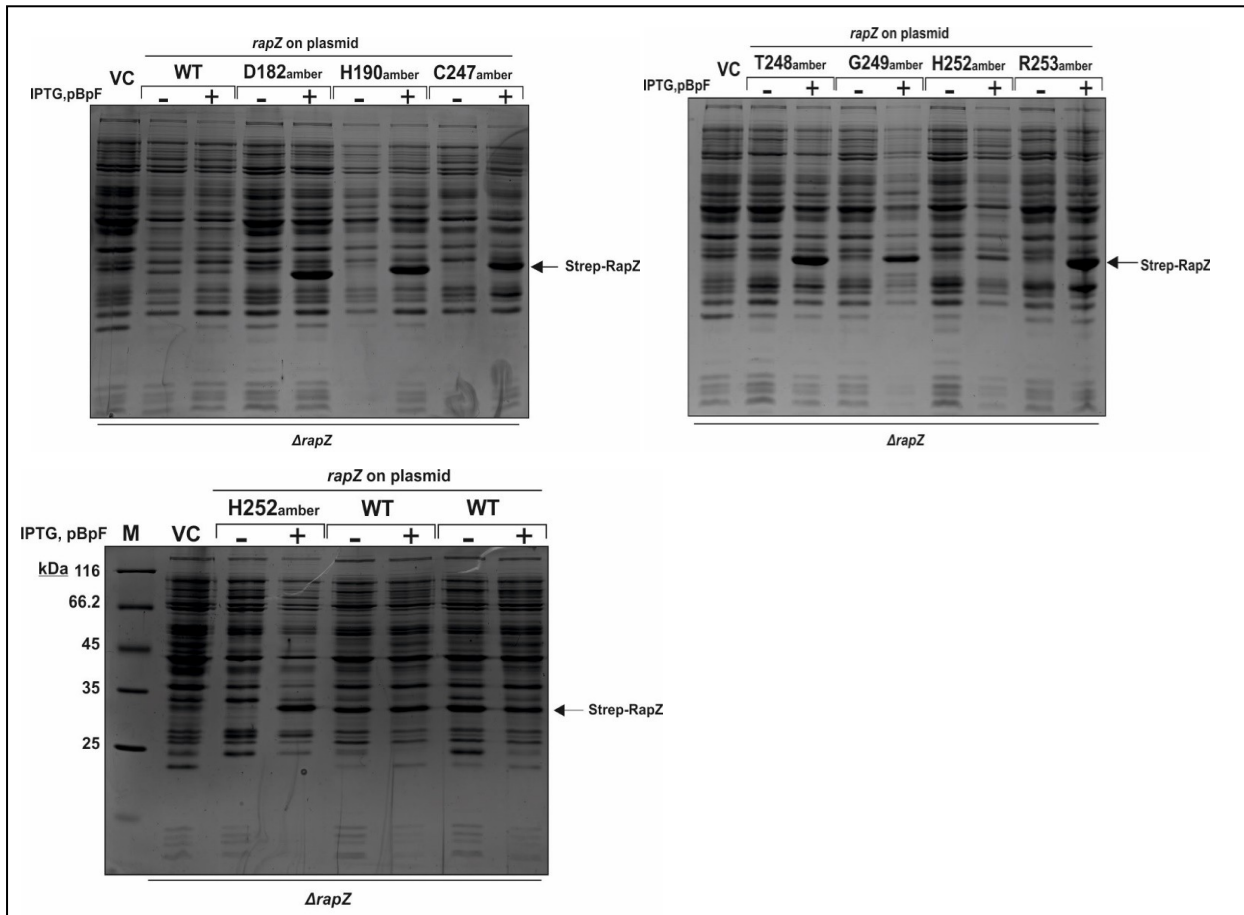


Figure 14. **pBpF incorporation into RapZ at the place of the stop codon.** Cell lysates of strain Z37 double-transformed with one of the plasmids pMK55-61 and pEVOL-pBpF, separated on 12,5% polyacrylamide SDS-PAGE gels. The O/N cultures were inoculated in 250 mL TM/amp/cm/L-ara to  $OD_{600}=0,1$  and grew at 37°C until the exponential growth phase ( $OD_{600}=0,5-0,8$ ). The cultures were induced with 1 mM IPTG and 200  $\mu$ M pBpF and they grew for another 3h at 28°C. For comparison, Z37 double-transformed with pEVOL-pBpF and pMK31 that encodes WT-RapZ (marked as WT on the picture), and pEVOL-pBpF and empty vector pBGG237 were tested. The arrows indicate the band for the full length and truncated RapZ proteins.

Next, lysates of the cells grown in presence of IPTG and pBpF were prepared and the pBpF-labelled Strep-RapZ proteins were purified via StrepTactin affinity chromatography as described in chapter 4.2.22. To follow success of the procedure, samples corresponding to the cleared lysates, column flow-through, the washing steps and the three elution fractions were collected and separated on a 12,5% polyacrylamide gel (Fig. 15). This analysis showed that purification was successful for all Strep-RapZ variants, except for those incorporating pBpF at codon positions D182 and C247 (i.e. the *strep-rapZ*-D182amber and -C247amber variants). Therefore these latter two variants could not be included in subsequent experiments. Since both of the proteins could be overproduced successfully, a possible

explanation for the unsuccessful purification could be that the proteins are insoluble. In case of the Strep-RapZ-H190pBpF and Strep-RapZ-H182pBpF variants, protein signals were missing in the lanes analyzing the cleared lysate or the column flow-through, respectively. This is probably due to a mistake by the experimenter when loading the gel.

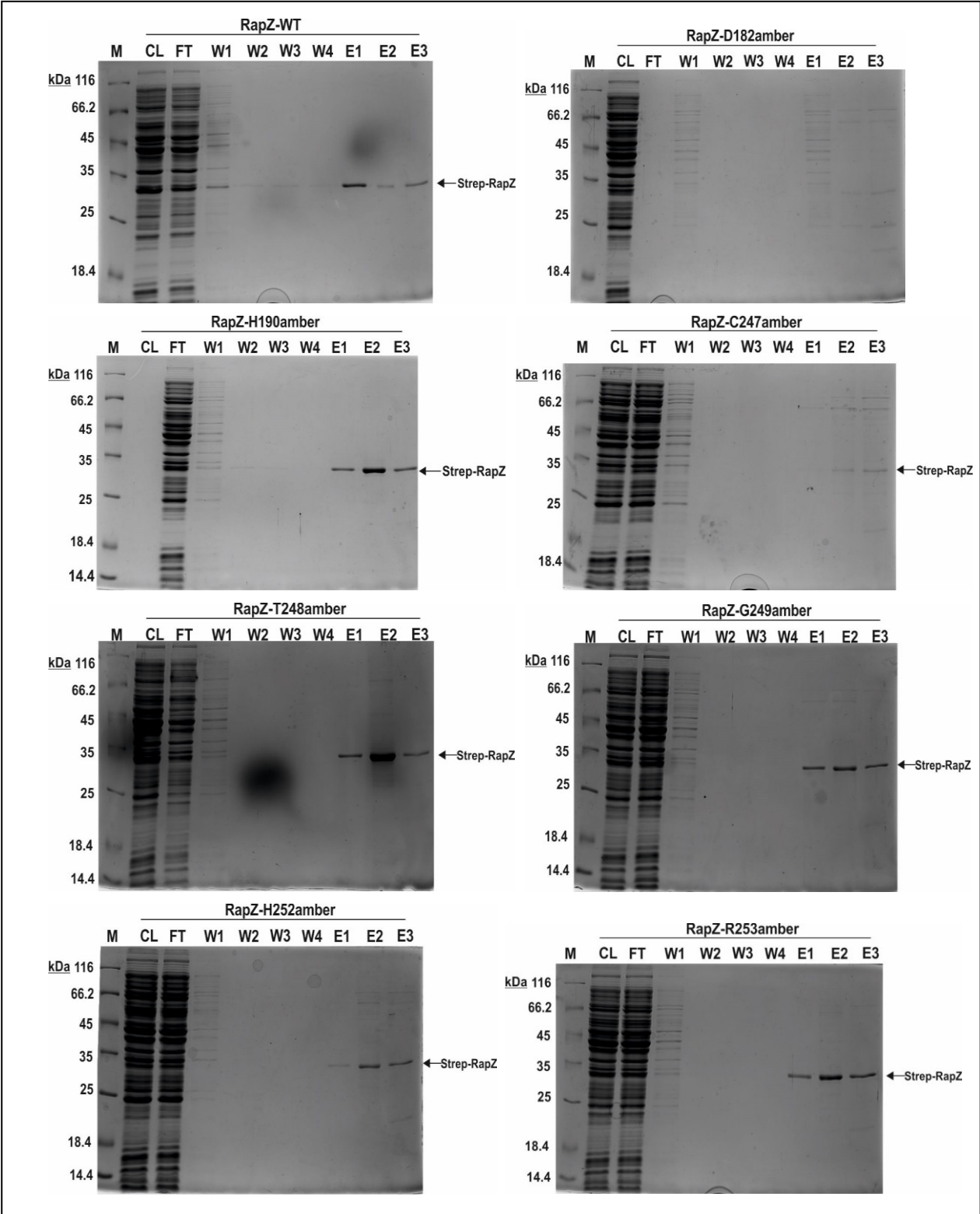


Figure 15. **Purification of Strep tagged RapZ proteins with incorporated pBpF.** Clear lysate, flow through, washes 1-4 and elutions 1-3, separated on 12,5% polyacrylamide SDS-PAGE gels. For CL and FT 3  $\mu$ L were loaded, for the wash steps 10  $\mu$ L and for the elutions 4  $\mu$ L. Above each gel, it is indicated the codon of which amino acid was mutated to an amber stop codon and therefore replaced with pBpF in the RapZ protein. Purification of variant D182amber and C247amber was unsuccessful.

Next, cultures for overproduction of His<sub>10</sub>-QseE and His<sub>10</sub>-QseF were grown to allow for their subsequent purification via Ni<sup>2+</sup>-NTA affinity chromatography. In case of kinase QseE, only the cytoplasmic soluble part of the protein (aa XX-YY) was overproduced as this allows for purification. Corresponding cultures carrying the required overproduction plasmids (pBGG219, pBGG220) were grown in 250 mL LB/amp at 37°C under 165 rpm agitation to the exponential growth phase (OD<sub>600</sub>=0,5-0,8). The cultures were then induced with 1 mM IPTG to elicit overexpression of *his<sub>10</sub>-qseE* and *his<sub>10</sub>-qseF* and growth was continued for 1 h. Analytic samples were harvested before and after induction, and the proteins were separated on a 12,5% SDS-polyacrylamide gel. Overexpression of His<sub>10</sub>-QseF could not be observed and therefore the protein could not be purified. Consequently, following experiments were performed only with His<sub>10</sub>-QseE (Fig. 16A). The latter protein was eluted from the Ni<sup>2+</sup>-NTA resin using increasing concentrations of imidazole. Samples of the cleared lysate, the column flow-through and of the imidazole fractions were collected and separated on a 12,5% SDS-polyacrylamide gel. His<sub>10</sub>-QseE eluted predominantly with the 250 mM fraction, indicating its successful purification (Fig. 16B).

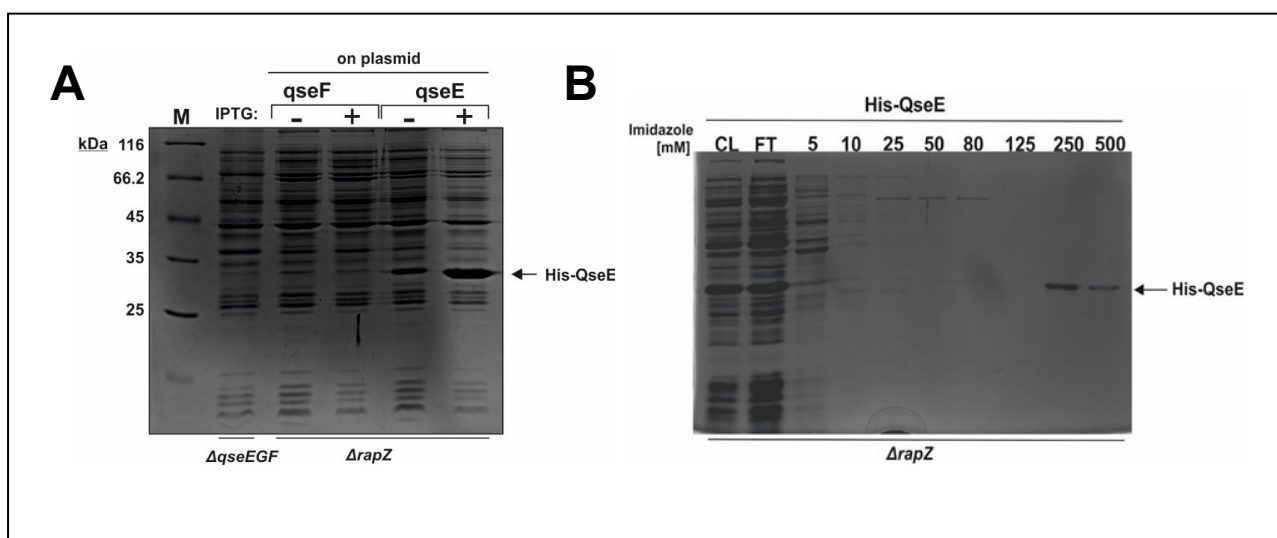


Figure 16. **Expression test and Purification control of His tagged QseE.** **A** Cell lysates of strain BL21 transformed with either pBGG219 or pBGG220, separated on 12,5% polyacrylamide SDS-PAGE gels. The cultures grew at 37°C in LB/amp until the exponential growth phase ( $OD_{600}=0,5-0,8$ ), when they were induced with 1 mM IPTG and continued growing for 1 more hour. **B** 12,5% polyacrylamide SDS-PAGE gel of the clear lysate, flow through and washes with increasing imidazole concentration. For CL and FT 3  $\mu$ L were loaded, for the wash steps 10  $\mu$ L.

### 5.1.5.3. Testing crosslinking of the Strep-RapZ variants with His<sub>10</sub>-QseE

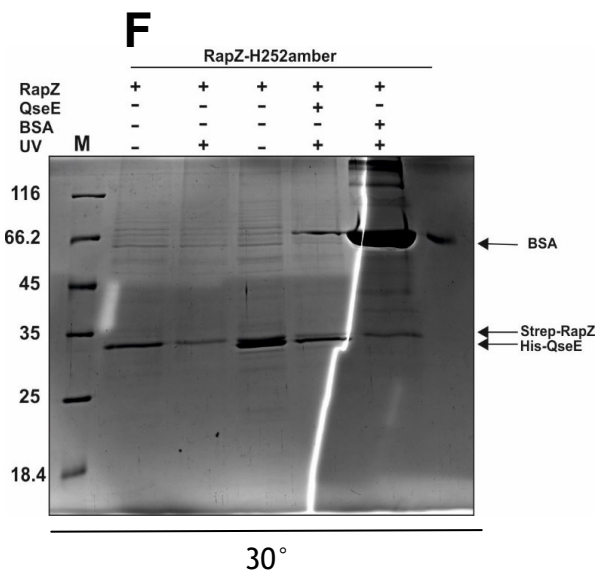
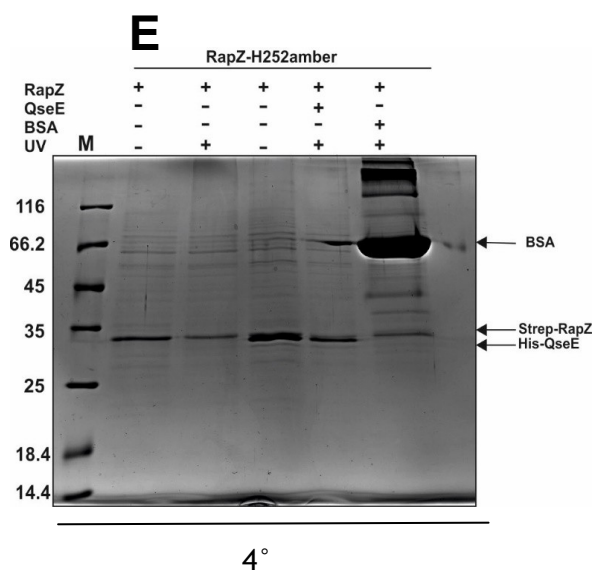
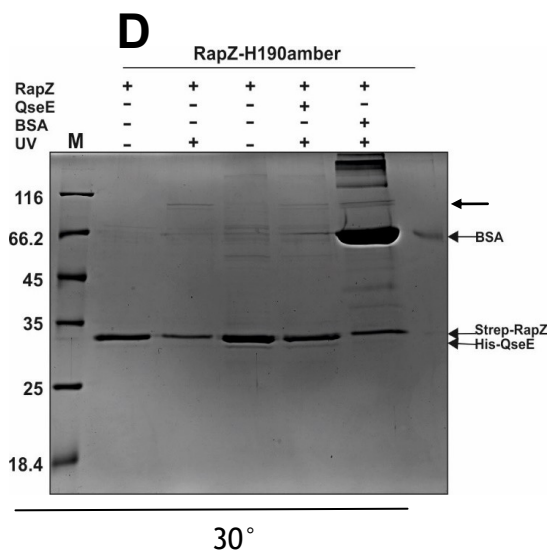
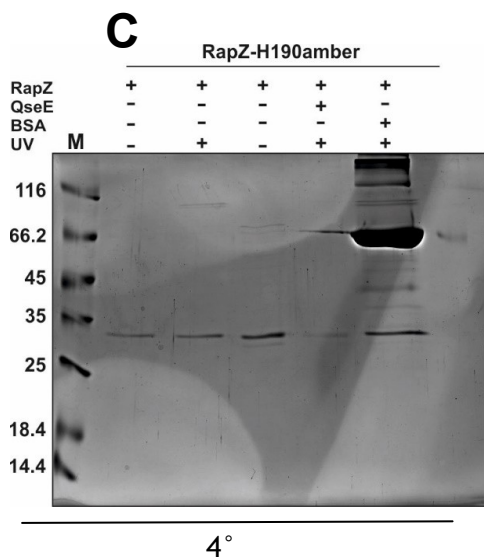
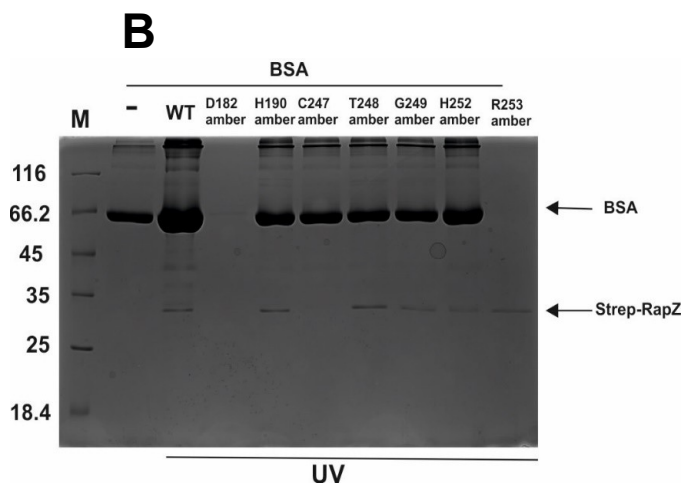
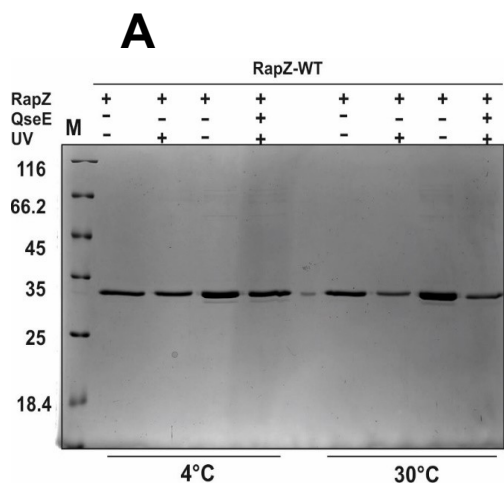
In order to crosslink the Strep-RapZ variants with His<sub>10</sub>-QseE, 1  $\mu$ g of each protein was mixed in 96-well plates in a final volume of 50  $\mu$ L. In order to find optimal conditions for the experiment, different conditions were tested including variation of buffer composition, i.e. either crosslinking (CL) buffer I, II or III were used. CL buffer I is composed of 50 mM Tris-HCL, 200 mM KCl, 10 mM MgCl<sub>2</sub> and 5 mM MnCl<sub>2</sub>, buffer II of 50 mM Tris-HCL, 200 mM KCl, 10 mM MgCl<sub>2</sub>, 5 mM MnCl<sub>2</sub> and 100  $\mu$ M ATP and buffer III of 50 mM Tris-HCL, 50 mM KCl and 1 mM MgCl<sub>2</sub>. In addition, the incubation temperature prior to crosslinking varied. The proteins were crosslinked on ice, by being exposed to 365 nm UV light for 30 min. The following experiments were performed with the kinase part of QseE (aa196-475), which will from now on be referred to as QseE'.

In a first set of crosslinking experiments, the proteins were incubated for 30 min at either 4°C or 30°C prior to crosslinking. BSA was used as a negative control. To allow for specific detection of cross-linked proteins, each reaction was carried out twice. One set of these samples was kept on ice, while the other samples were subjected to UV irradiation for 30 min. The samples were mixed according to the scheme shown in Table 29 and reactions were performed in CL buffer I. Following UV irradiation, the samples were transferred to reaction tubes and 12,5  $\mu$ L of 5x Laemmli buffer was added, respectively. Finally, the samples were denatured for 5 min at 65°C and separated on a 12,5% SDS-polyacrylamide gel.

Table 29 Reactions and controls for the crosslinking experiments

	Reaction 1	Reaction 2	Reaction 3	Reaction 4	Reaction 5	Reaction 6
RapZ	+	+	+	+	+	-
QseE	-	-	+	+	-	+
BSA	-	-	-	-	+	-
UV	-	+	-	+	+	+

Due to errors of the Bradford assay for determination of protein concentrations, much more BSA as compared to the other proteins was loaded (Fig. 17C-F, lane 6). This resulted in a very strong BSA band on the gel, as well as in BSA overflow to neighboring wells (Fig. 17C-F, lane 5). To prevent overflow in other gels, the BSA control was loaded on a separate gel (Fig. 17B). No higher complexes were observed in the gel when the RapZ variants with the incorporated crosslinkable amino acid were mixed with BSA and UV-irradiated (Fig. 17B, lanes 4-10), as compared to BSA alone or a UV-irradiated mixture of BSA and WT-RapZ (Fig. 17B, lanes 2 and 3). In the gel where WT-RapZ was mixed with QseE' and UV-irradiated, no slower migrating bands occurred (Fig. 17A). This was expected, since WT-RapZ does not carry the crosslinkable amino acid pBpF. In the gels addressing the RapZ-H190pBpF variant (Figs. 17C and D), an additional slower migrating band appeared in the gel whenever RapZ was UV-irradiated, either alone or with QseE' (lanes 3,5 and 6; the position on the gel is marked with an arrow). In the case of variant RapZ-T248pBpF, two additional bands showed up when RapZ was UV-irradiated (Fig. 17G, lanes 3,5,7 and 9; the position on the gel is marked with an arrow). Thus, amino acids H190 and T248 could be in close vicinity to another monomer in the RapZ tetramer, resulting in their crosslinking. Interestingly, the additional RapZ bands formed upon UV irradiation appeared regardless of the incubation temperature. In the gel with RapZ-R253amber, a strong band at ~66 kDa appeared when RapZ and QseE were mixed, but not UV irradiated (Fig. 17I, lane 4). It is possible that samples were interchanged and that this band corresponds to the crosslinked RapZ and QseE monomers. Altogether, it can be concluded that amino acids H190 and T248 are perhaps part of or in the vicinity of the interaction surfaces involved in multimerization of RapZ. However, specific RapZ/QseE' complexes could not be detected regardless of the incubation temperature prior to crosslinking.



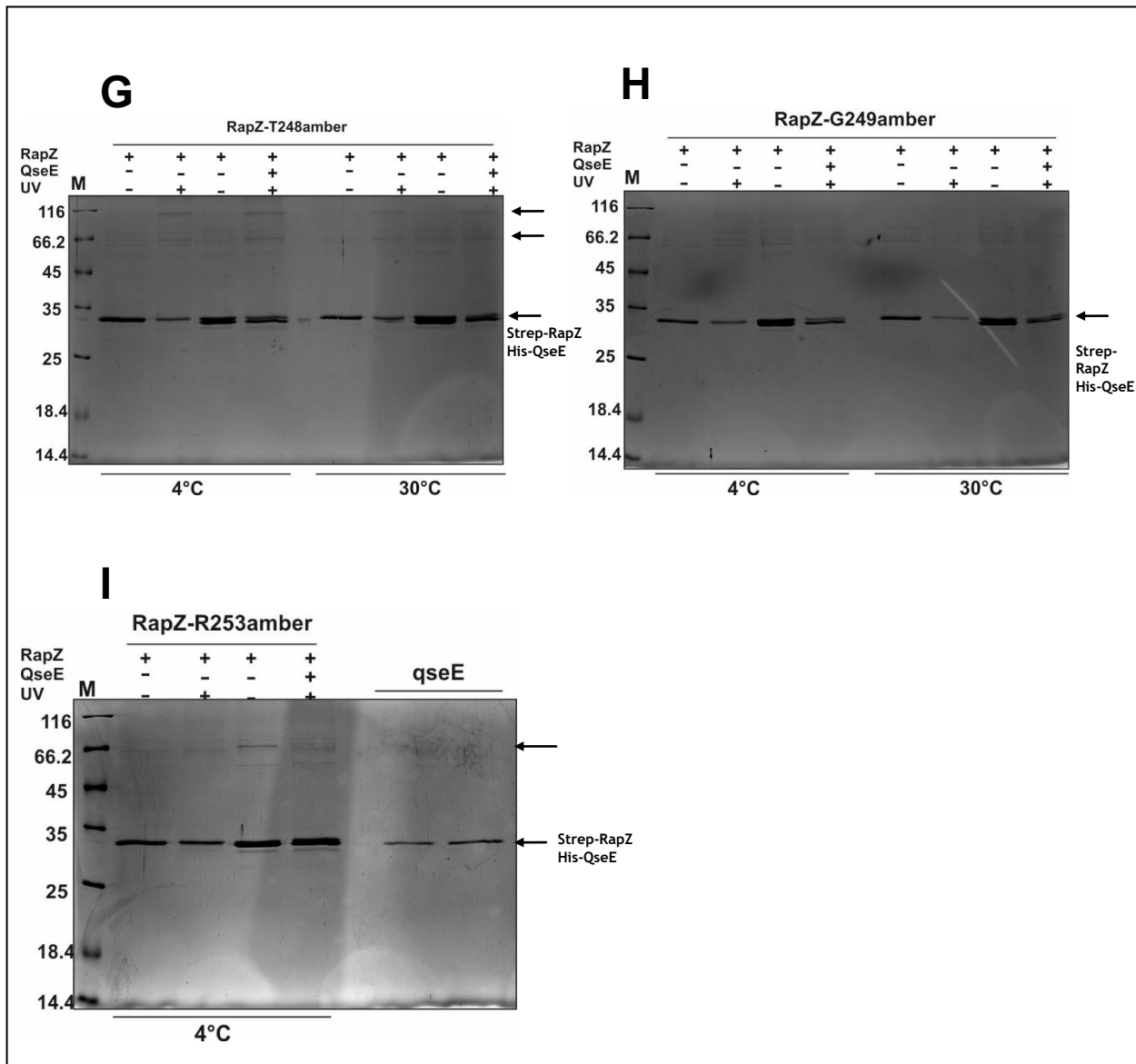


Figure 17. **Impact of different incubation temperatures on potential photocrosslinking of QseE and RapZ.** Mixed and crosslinked proteins, separated on 12,5% polyacrylamide SDS-PAGE gels. 1  $\mu$ g of each protein was mixed in a 96-well plate in CL buffer I to a volume of 50  $\mu$ L. The proteins were incubated for 30 min at either 4°C or 30°C prior to crosslinking. Crosslinking was performed for 30 min on ice, by exposing the samples to 365 nm UV light. The samples were mixed with 12,5  $\mu$ L 5xLaemmli buffer and denatured for 5 min at 65 °C. 20  $\mu$ L were loaded on the gel. Arrows, which don't imply differently, indicate the position of the bands corresponding to potential crosslinked complexes on the gel.

In the second round of crosslinking experiments, two additional buffers, namely CL buffer II and III were tested. CL buffer II contains ATP (Khan et al., 2020), but is otherwise identical with CL buffer I. Kinase QseE' binds and autophosphorylates with ATP, raising the possibility that ATP binding is a prerequisite for interaction with RapZ. In addition, CL buffer III containing a lower salt concentration was tested.

which could be favorable for maintaining weak protein-protein interactions. Since there was no difference between samples incubated at 4 and 30°C, this step was omitted and the samples were crosslinked immediately after mixing. The samples were mixed and crosslinked according to the scheme given in Table 30. 12,5 µL 5x Laemmli buffer was added and the samples were denatured for 5 min at 65°C and separated on a 10% SDS-polyacrylamide gel.

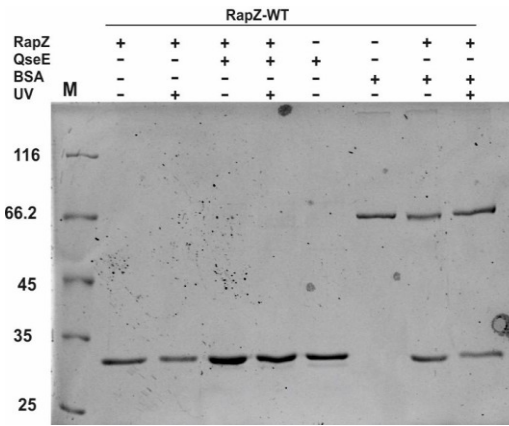
Table 30 Reactions and controls for the crosslinking experiments using buffer II and III.

	Reaction 1	Reaction 2	Reaction 3	Reaction 4	Reaction 5	Reaction 6	Reaction 7	Reaction 8
RapZ	+	+	+	+	-	-	+	+
QseE	-	-	+	+	+	-	-	
BSA	-	-	-	-	-	+	+	+
UV	-	+	-	+	-	-	-	+

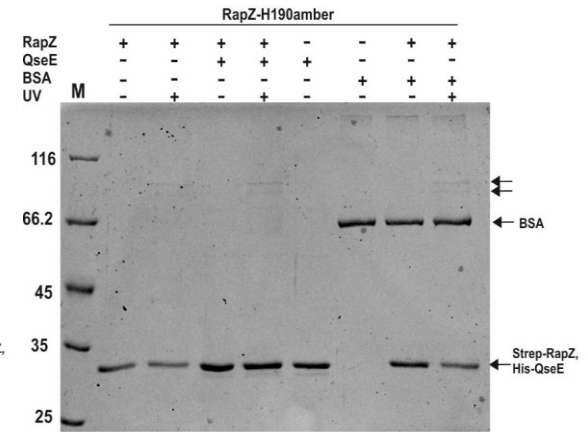
As expected, no higher complexes appeared for the WT protein upon UV irradiation (Figs. 18A and B, gel i), since it did not contain any crosslinkable amino acid. As observed before, higher molecular weight complexes became visible in the gels addressing the RapZ-H190 pBpF and RapZ-T248pBpF variants that were exposed to UV light (Figs. 18A and B, gels ii and iii, lanes 3, 5 and 9). In case of RapZ-R253pBpF a faint band of ~60 kDa appeared when exposed together with QseE' to UV light (Fig. 18A and B, gel vi, lane 5). The theoretical molecular weight of a complex between Strep-RapZ and His<sub>10</sub>-QseE' would refer to ~66 kDa. this band could indicate a crosslink between a RapZ monomer and a QseE' monomer. Consequently, residue R253 could be part or in the vicinity of the surface used by RapZ to contact QseE'. The higher bands that appeared upon crosslinking were more prominent when using the low salt buffer (CL buffer III) (Fig. 18B gels ii and iii, lanes 3, 5 and 9 and gel vi, lane 5) as compared to CL buffer II (Fig. 18A gels ii and iii, lanes 3, 5 and 9 and gel vi, lane 5). Therefore, samples referring to each RapZ variant were separated by SDS-PAGE (10% PAA) and subsequently transferred to a PVDF membrane for western blotting. One membrane was incubated with an anti-His antiserum to detect QseE' whereas the other blot was treated with anti-strep antiserum to detect Strep-RapZ.

**A**

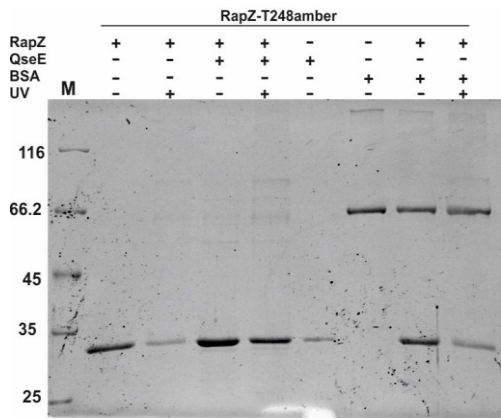
**i**



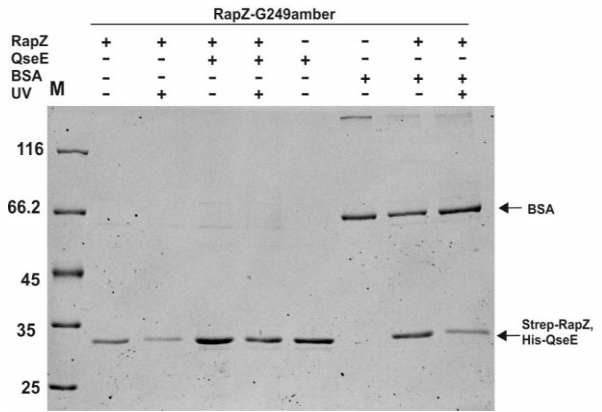
**ii**



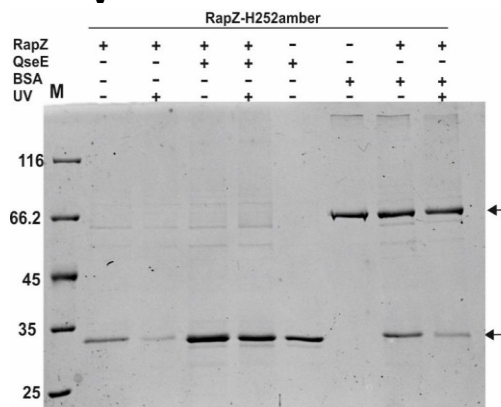
**iii**



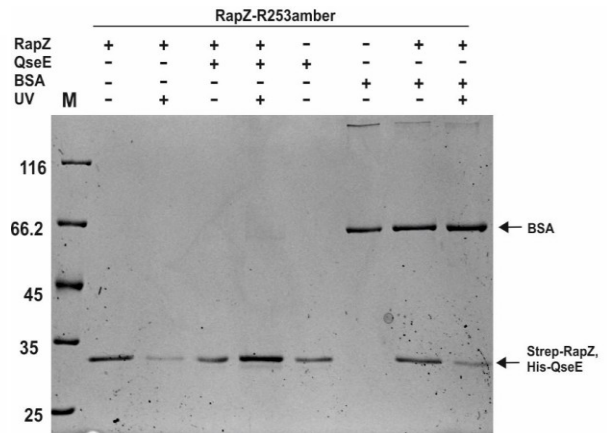
**iv**



**v**



**vi**



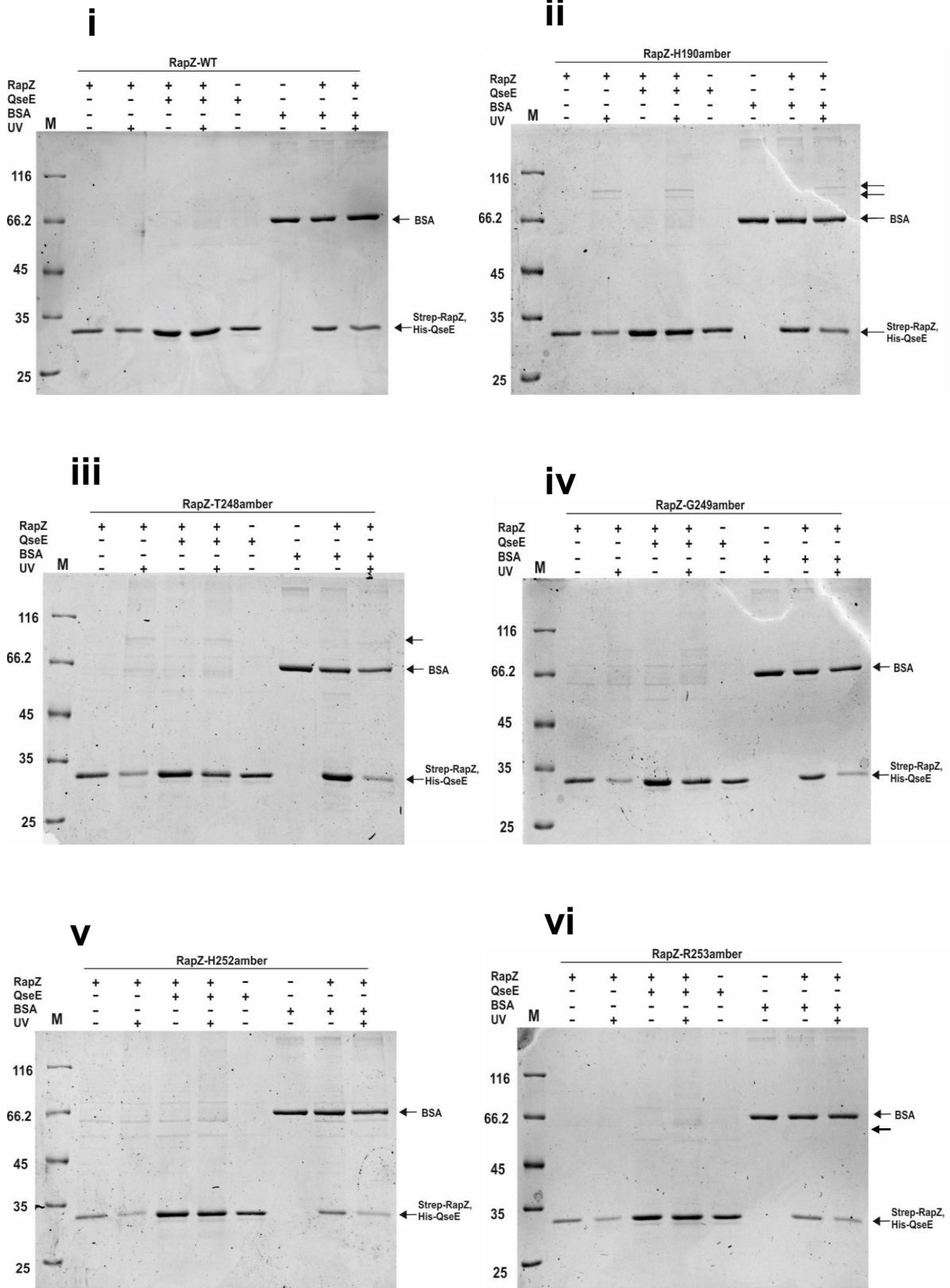
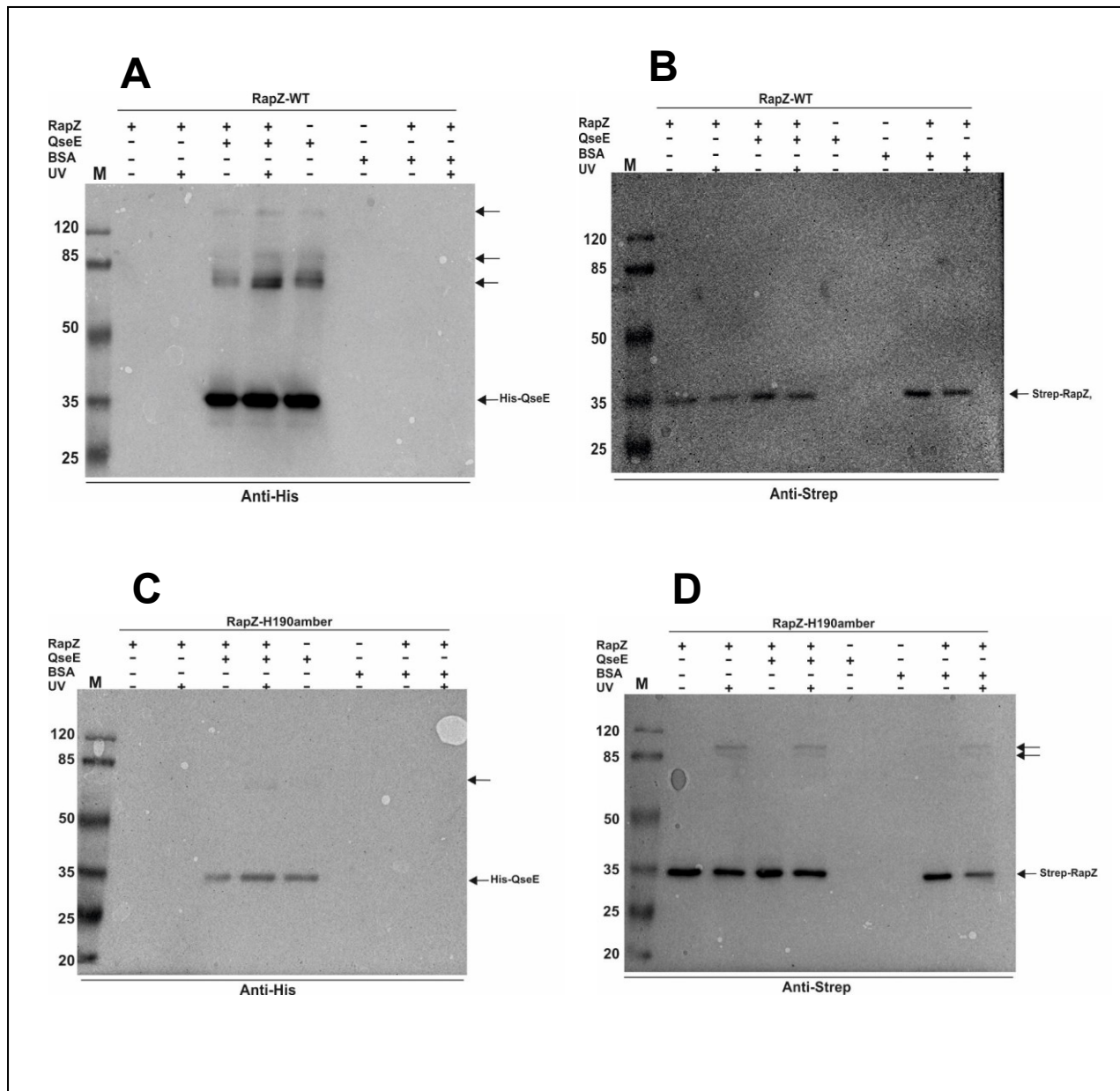
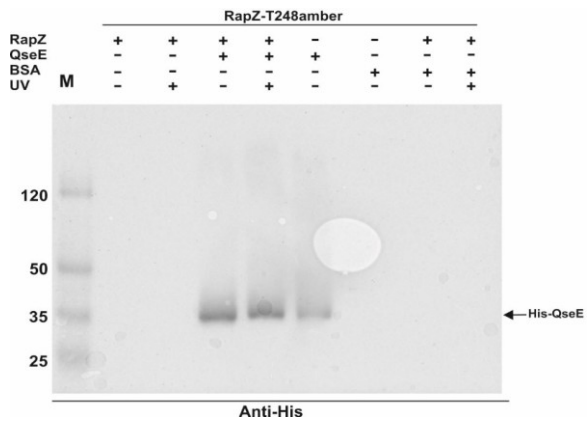
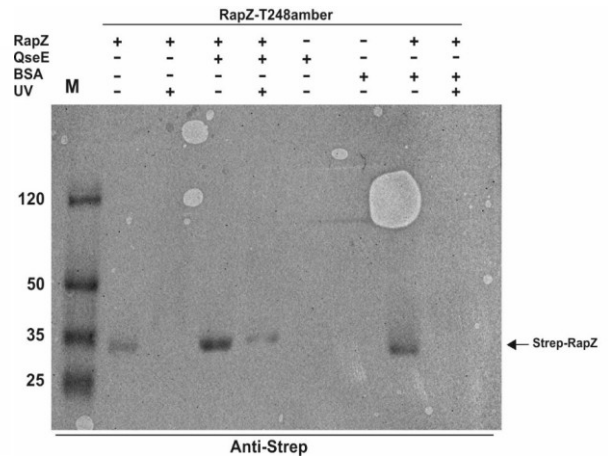
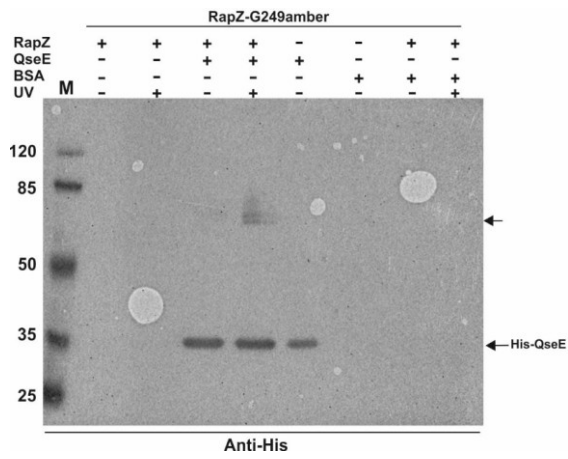
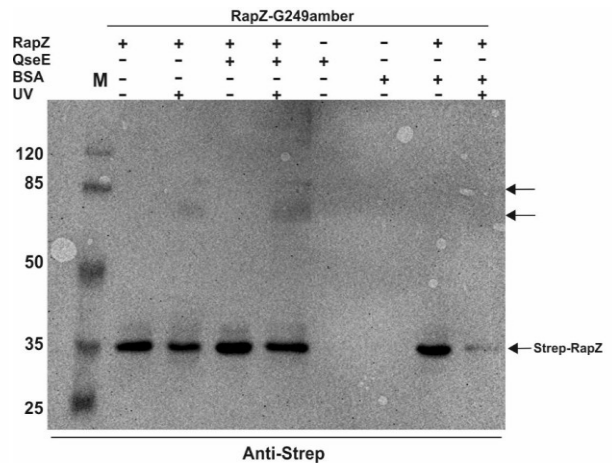
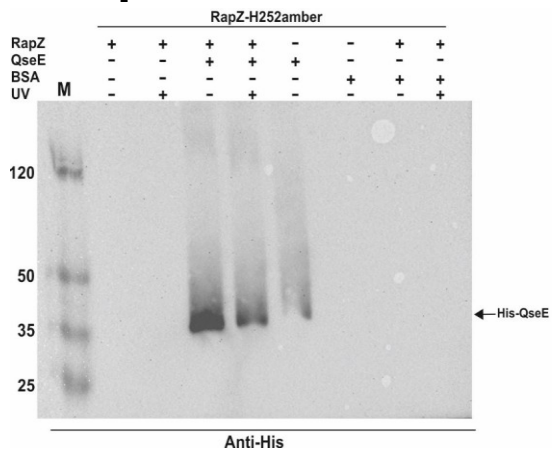
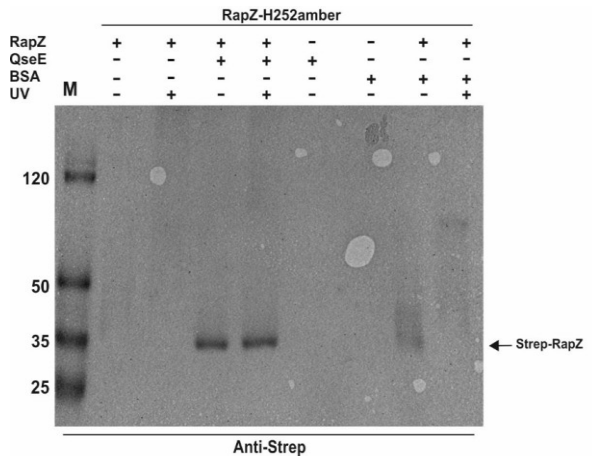
**B**

Figure 18. **SDS-PAGE of samples obtained by photocrosslinking QseE and RapZ in a low salt buffer and a buffer supplemented with ATP.** Mixed and crosslinked proteins, separated on 10% polyacrylamide SDS-PAGE gels. 1  $\mu$ g of each protein was mixed in a 96-well plate in either CL buffer II (**A**) or CL-buffer III (**B**), to a volume of 50  $\mu$ L. Crosslinking was performed for 30 min on ice, by exposing the samples to 365 nm UV light. The samples were mixed with 12,5  $\mu$ L 5xLaemmli buffer and denatured for 5 min at 65  $^{\circ}$ C. 20  $\mu$ L were loaded on the gel. Arrows, which don't imply differently, indicate the position of the bands corresponding to potential crosslinked complexes on the gel.

The Western blotting successfully detected both, the Strep-tagged RapZ variants when using the Strep antiserum as well as His<sub>10</sub>-QseE' when the His antiserum was used. Surprisingly, an additional band of ~70 kDa appeared in some of the samples containing QseE' when analyzed with the anti-his antiserum (Fig. 19 A,C,G and K). In most cases, this band was absent in the blots obtained with the Strep-antiserum (Fig. 19 B,D and H), so one may conclude that it represents a dimer of kinase QseE' (theoretical MW = 65 kDa). In the case of RapZ-R253pBpF variant, a protein complex of ~60-70 kDa became detectable by both antisera (Fig 19 K and L, lane 5). This complex became exclusively visible when both, His<sub>10</sub>-tagged QseE' and Strep-tagged RapZ were mixed and exposed to UV. This observation is a strong indication that a crosslink between the two proteins had formed. The higher molecular weight complex previously observed in the Coomassie-stained SDS gel for the RapZ-H190pBpF became also detectable when using the Strep antiserum (Fig. 19D, lanes 3,5 and 9), but not with the His antiserum (Fig. 19C). Moreover, this complex formed regardless of the additional presence of His<sub>10</sub>-QseE' in the cross-linked sample (Fig. 19D, lane 5). This observation is in favor of the hypothesis that these complexes represent crosslinks between two or more RapZ monomers. In other words, the result indicates that residue H190 is in part of or close to the interaction surfaces involved in RapZ multimerization. A similar band indicating RapZ multimers was also observable for the RapZ-T248pBpF variant on the Coomassie-stained SDS gels. Unfortunately, it could not be confirmed by western blotting, due to an error in loading (Fig. 19F). In case of the RapZ-G249pBpF variant, even two higher molecular weight complexes formed upon UV irradiation in the samples containing this variant. These bands might refer to dimers and trimers (or tetramers) of RapZ (Fig. 19H, lanes 3 and 5). Altogether, these results support the hypothesis that amino acid H190 is in the vicinity to the surfaces involved in RapZ multimerization and that residue R253 is part of the interaction surface of RapZ used to bind QseE. Additionally, the blots indicate

that QseE' may form a dimer, which was not disrupted and sometimes survived the denaturing electrophoresis conditions.



**E****F****G****H****I****J**

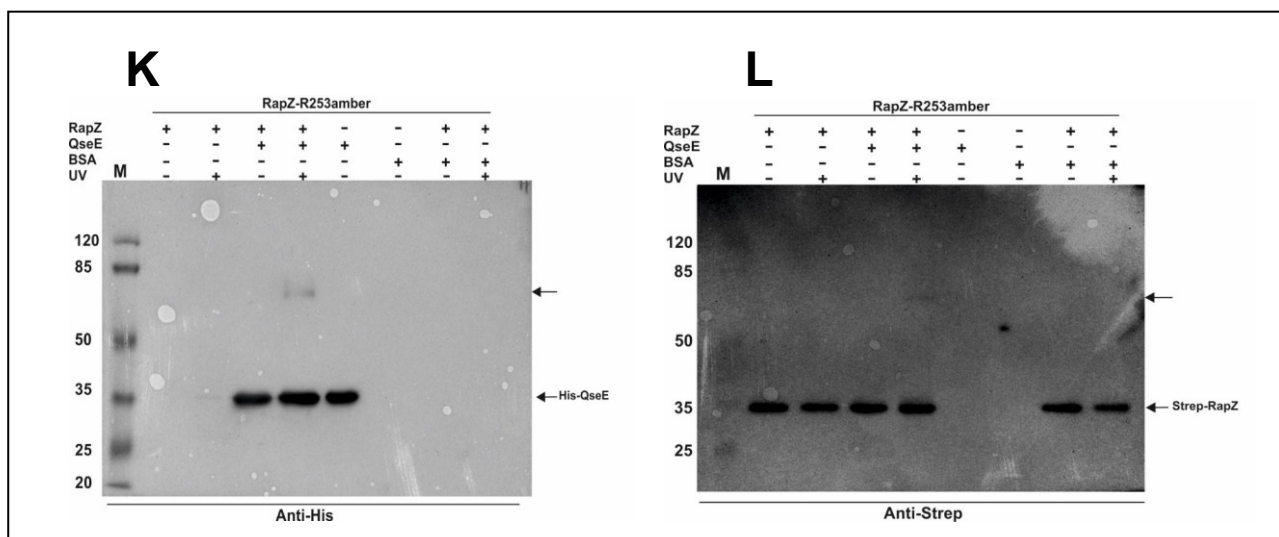


Figure 19. **Western blot analysis of samples obtained by photocrosslinking of QseE' and RapZ in a low salt buffer.** 2x15  $\mu$ L of the sample prepared in CL-buffer III (Fig. 20B), were separated on two 10% polyacrylamide gels and transferred to PVDF membranes via Western blotting. One membrane was incubated with the Anti-His and the other with the Anti-Strep antibody. Arrows, which don't imply differently, indicate the position of the bands corresponding to potential crosslinked complexes on the gel.

Lastly, the crosslinking experiment with variant RapZ-R253pBpF was repeated in order to see if the complexes that were previously observed with blotting (Fig 19K and L) are stable. Since there was a lack of dialyzed QseE protein, an undialyzed sample was thawed and dialyzed in buffer III. All samples were mixed in CL buffer III. As expected a ~60 kDa band appeared in the coomassie-stained gel, in the lane where RapZ and QseE were mixed and irradiated (Fig 20A, lane 5), as well as in the gel detected via Western blotting (Fig 20 B and C, lane 5). An additional band at around 95 kDa appeared in the coomassie-stained gel, whenever RapZ was irradiated, similarly to the band showing up in the blot with RapZ-H190pBpF (Fig 20A, lanes 3, 5 and 9). However, in the gel detected via blotting, the band only showed up when QseE and RapZ were mixed and irradiated (Fig 20C, lane 5).

Since RapZ in it's tetrameric form also interacts with RnaseE (Durica-Mitic et al., 2020), in this round of crosslinking experiments, BSA was omitted and interaction with His<sub>10</sub>-tagged RNase E (aa 1-529; Durica-Mitic et al., 2020) was tested instead. In this case, no higher molecular weight complexes were observed when Strep-RapZ was co-incubated with His<sub>10</sub>-RNase E and UV-irradiated (Figs. 20A,B and C, lane 9). However, as the His<sub>10</sub>-RNase E preparation was stored for some time at -80°C, it is possible that the protein had lost activity and the ability to bind RapZ over time.

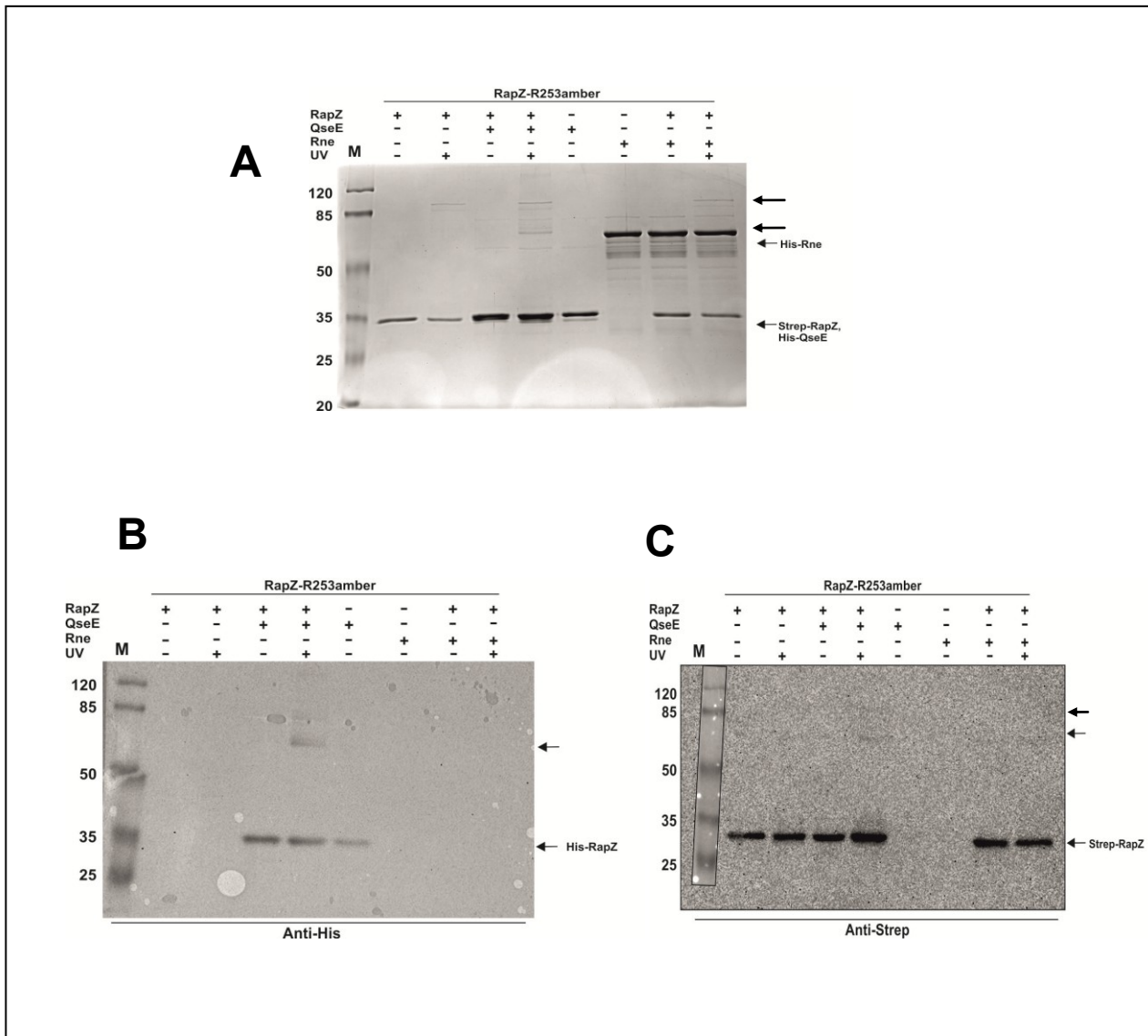


Figure 20. **SDS-PAGE gels of samples obtained by photocrosslinking QseE and RapZ – R253pBpF.** The proteins were mixed together, exposed to UV light and then separated on 10% polyacrylamide SDS-PAGE gels. The gels were analyzed by Coomassie staining (A) and Western blotting (B and C). 1  $\mu$ g of each protein was mixed in a 96-well plate in CL-buffer III to a volume of 50  $\mu$ L. UV-irradiation was performed for 30 min on ice, by exposing the samples to 365 nm UV light. The samples were mixed with 12,5  $\mu$ L 5xLaemmli buffer and denatured for 5 min at 65°C. 20  $\mu$ L were loaded on the polyacrylamide gels for SDS-PAGE and 15  $\mu$ L for Western blotting. Arrows, which don't imply differently, indicate the position of the bands corresponding to potential crosslinked complexes on the gel.

## 5.2 Part II

As mentioned in the introduction, preliminary data suggested that there might be an interaction between RapZ and PtsP and that the interaction is stronger when the autophosphorylation site (His356) was substituted with an Ala residue (Khan, 2019). This interaction could either impact on activity of RapZ or PtsP or both.

### 5.2.1 Interaction of RapZ with PtsP, the first enzyme in the PTS<sup>Ntr</sup> phosphorylation cascade.

To investigate a potential interaction between PtsP and RapZ in more detail, BACTH experiments were performed. In addition to wild type PtsP, interaction with RapZ was also assessed for the phospho-ablative (H356A) and two phospho-mimetic variants of PtsP, as well as PtsN and NPr. Previous studies have shown that Asp can be used to mimic phosphohistidine in some proteins of the sugar PTS (Deutscher et al., 1994), but it was not able to mimic phosphorylation of His73 in PtsN (Lüttmann et al., 2009). To this end, two phospho-mimetic variants of PtsP were tested: H356D and H356E.  $\Delta$ *cyaA* strain RH785 was doubly transformed via PEG transformation with the plasmids encoding the various T18- and T25 fusion proteins. The transformants were selected on MacConkey plates supplemented with Amp, Kan and IPTG. Following an incubation for 48 h at 28°C, the plates were used to inoculate single colonies in 10 mL LB supplemented with Amp, Kan and IPTG. The cultures grew for 16.5 - 20.5 h at 28°C and were then harvested for  $\beta$ -galactosidase activity assays. The interactions were assessed in both orientations, i.e. each protein was tested as fusion with the T18-domain as well as fusion to the T25-domain. The empty pKT25 and pUT18C plasmids were used as a negative control, while pKT25-ZIP and pUT18C-ZIP served as a positive control. The latter two plasmids encode for the leucine zipper of yeast transcription factor Gcn4 fused to the T25- and T18-domains, respectively.

When compared to the positive control, which generated very high  $\beta$ -galactosidase activities, no additional interaction of similar strength was detectable (Fig. 21, top panel). However, when omitting the strong positive control from the graph, weak interactions between T18-RapZ and T25-PtsP-H356A as well as T25-PtsP-H356D became detectable. In these cases,  $\beta$ -galactosidase activities were 2-3 fold higher as compared to the negative control (Fig. 21, bottom panel). However, the deviations observed between individual measurements for these interactions were high, albeit the activities exceeded background levels in each individual experiment. Finally,

these interactions were not detectable when the T18- and T25- domains were swapped between interaction partners. Altogether, these results indicate that there might be an interaction between RapZ and PtsP-H356A(D), even though it is weak and also not robust.

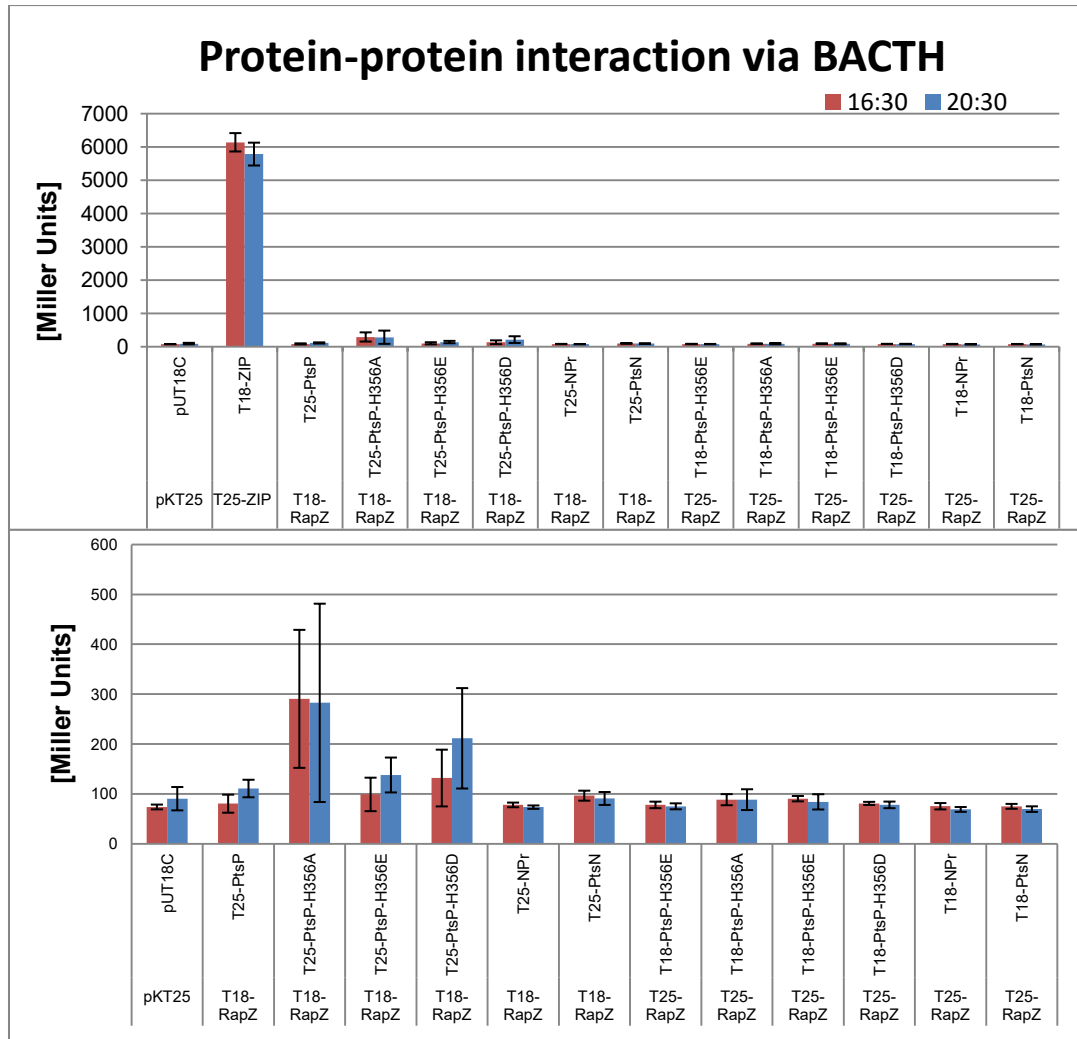


Figure 21. **Interaction of RapZ with proteins from the nitrogen PTS.**  $\beta$ -galactosidase activity of the BACTH system where RapZ was fused to either the T18 or the T25 domain of CyaA and components of the Nitrogen PTS to the other one. The experiment was performed in the RH785 strain. The shown values are the means, calculated from 3 independent measurements. The error bars indicate the standard deviation between different measurements. The lower graph is the same as the upper, but without the positive control.

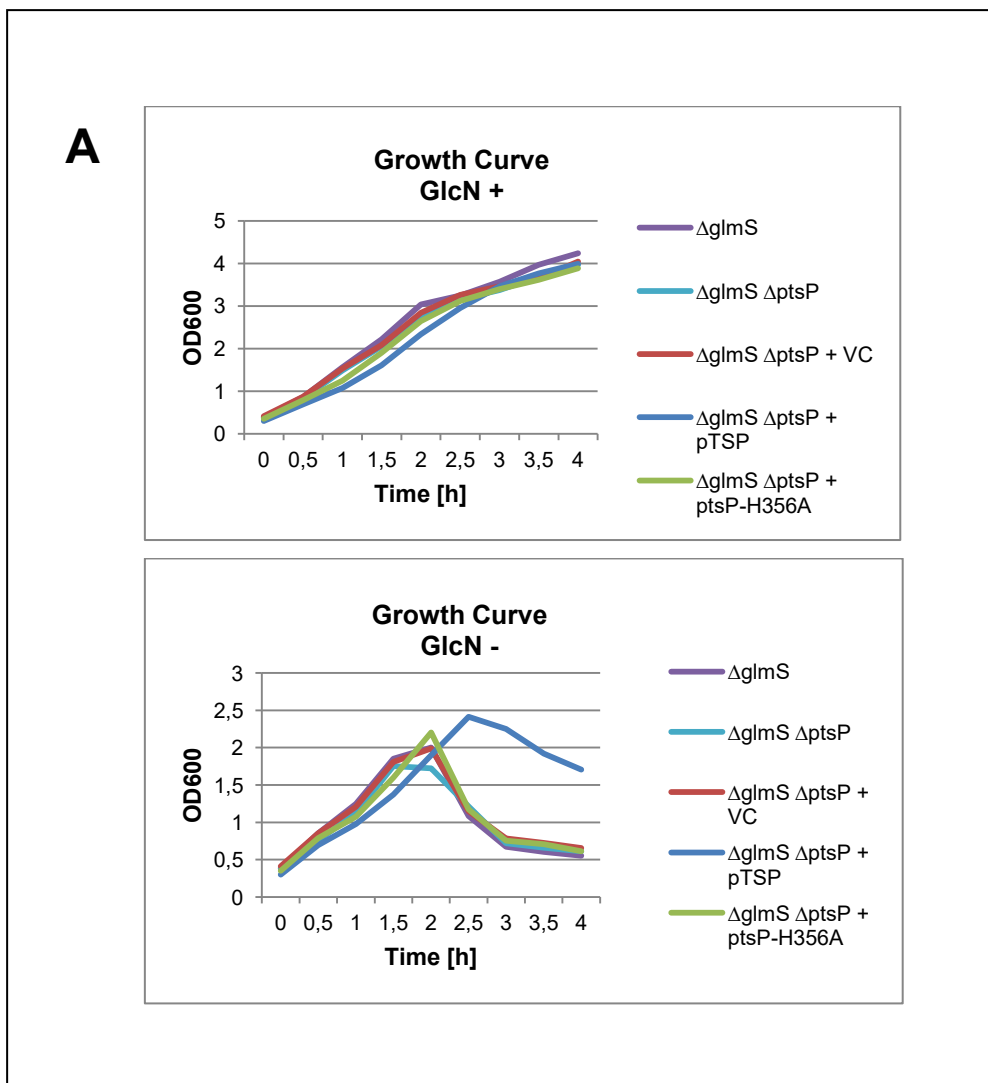
### 5.2.2 Involvement of PtsP in *glmS* transcript regulation

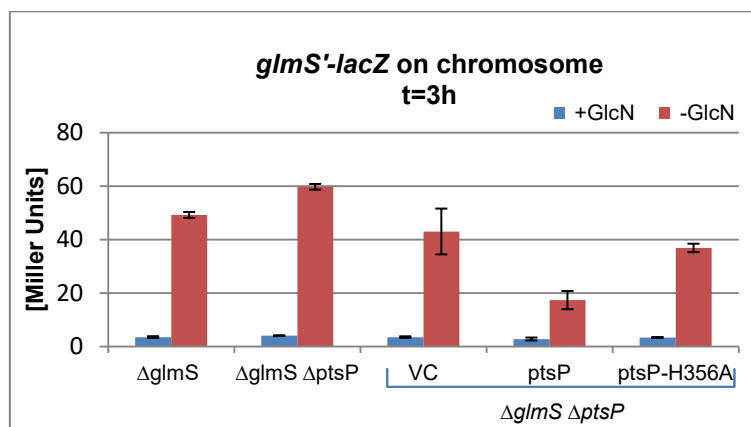
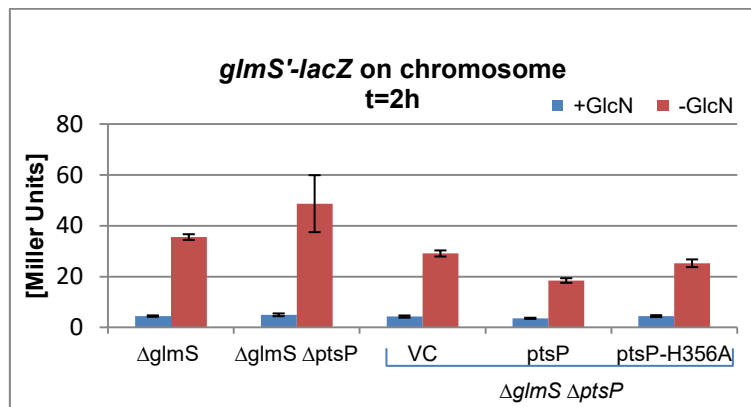
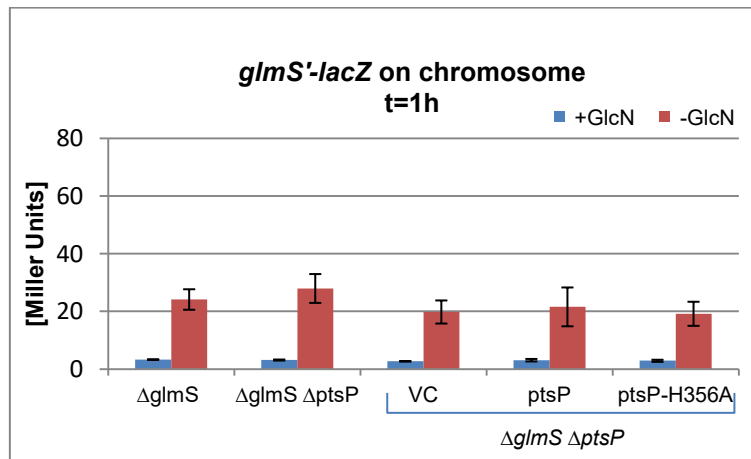
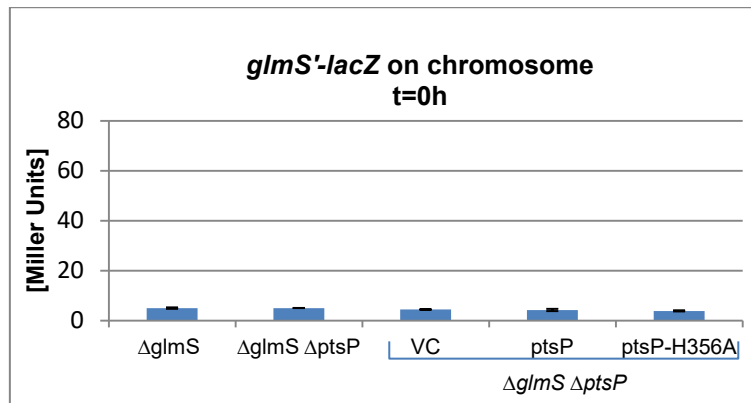
The BACTH experiment indicated a weak interaction between PtsP-H356A and RapZ (Fig. 21). This interaction could affect activity of RapZ. To investigate this possibility, I tested whether PtsP could affect *glmS* expression under conditions of GlcN6P sufficiency as well as depletion. To this end a complementation experiment using strains carrying a chromosomal *glmS'-lacZ* reporter fusion was performed. In addition, the chromosomal *ptsP* copy was deleted. Next, plasmids encoding wild-type PtsP or the phospho-ablative PtsP-H356A variant were used to complement the  $\Delta glmS \Delta ptsP glmS'-lacZ$  strain. Cultivation of the latter strain in absence of an exogenous amino sugar such (e.g. GlcN) results in intracellular depletion of GlcN6P and finally in lysis of the cells due to the inability to synthesize the envelope (Fig. 22A). O/N cultures were inoculated from single colonies in LB/kan supplemented with GlcN. On the next day, the pre-cultures were used to inoculate novel cultures to an  $OD_{600}=0,1$  in 50 mL of the same medium. Following growth until  $OD_{600}=0,3$ , the cultures were washed and split into two sub-cultures, respectively. For washing, the cells were pelleted (3900 rpm, 15 min, temp?), re-suspended in 3 mL LB, pelleted again and finally re-suspended in 25 mL LB/kan. One of the two sub-cultures was supplemented with GlcN, whereas the other culture was treated with H<sub>2</sub>O as mock control. The cultures were grown for additional 4 h (37°C, 165 rpm) and samples were harvested at regular time intervals for determination of  $OD_{600}$  (Fig. 22A) and for  $\beta$ -galactosidase activity assays to determine *glmS* expression (Fig. 22B). The experiment was performed two times using independent transformations.

The cultures supplemented with GlcN grew very similar, reaching a final  $OD_{600}\sim 4$ . In the absence of GlcN, the cultures reached only  $OD_{600}\sim 2$  and started subsequently to lyse, reflecting intracellular depletion of GlcN6P. As exception, the strain carrying *wt-ptsP* on a plasmid, grew differently (Fig. 22A). Namely, this culture grew initially somewhat slower, but reached a higher cell density ( $OD_{600}\sim 2.5$ ) before lysis started. In addition, the lysis was delayed and occurred slower as compared to the other cultures. This observation suggest that PtsP helps the cells to overcome cell envelope stress caused by amino sugar depletion. Interestingly, this positive effect on growth was not observable for the phospho-ablative PtsP-H356A mutant, suggesting that phosphorylation of PtsP is crucial (Fig. 22A).

As expected, *glmS* expression was very low in presence of GlcN6P. Under these conditions, RapZ targets GlmZ to processing, resulting in only low *glmS* expression

levels (Khan et al., 2020). In the absence of exogenous GlcN, GlmZ processing is prevented (through up-regulation of GlmY) and consequently *glmS-lacZ* expression levels were much higher (Fig. 22B; Khan et al., 2020). Interestingly, somewhat higher  $\beta$ -galactosidase activities were measured for the  $\Delta glmS \Delta ptsP$  double mutant as compared to the  $\Delta glmS$  single mutant. Complementation of the  $\Delta glmS \Delta ptsP$  mutant with *wild-type ptsP* on plasmid reduced activities below the  $\beta$ -galactosidase activities measured in the  $\Delta glmS$  single mutant. This effect was not observed when the empty plasmid (VC) or the plasmid encoding PtsP-H356A were used for complementation (Fig. 22B).



**B**

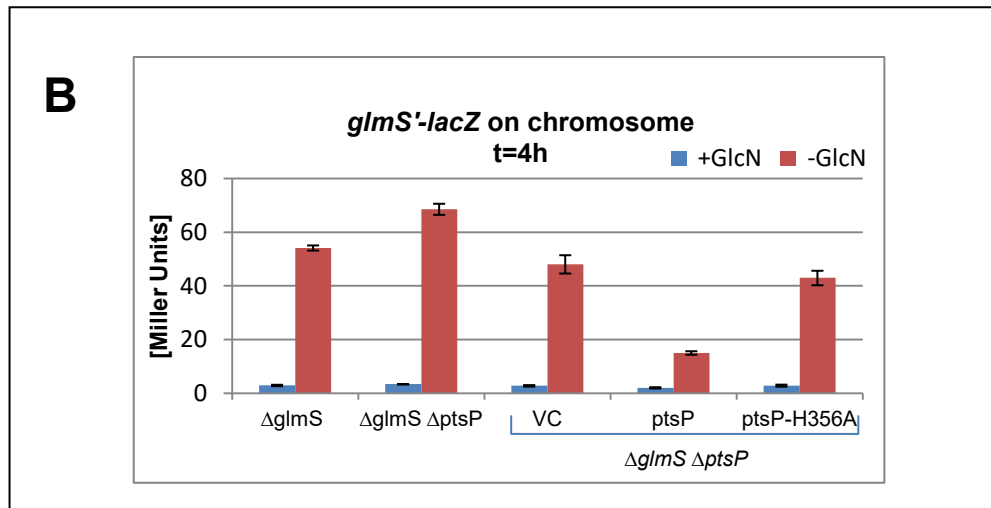


Figure 22. **growth and *glmS* expression upon overexpression of *ptsP***. The experiments were performed in a  $\Delta glmS \Delta ptsP$  strain (Z1228), which was transformed with plasmids carrying WT and phospho-ablative *ptsP* (pMK38 and 39). Cultures were split into two sets of cultures after reaching  $OD_{600}=0,3$ . One set was supplemented with GlcN, the other not. The cultures grew for 4 hours,  $OD_{600}$  was measured every 30 min and a sample was taken every hour. For comparison, a wt strain was tested (Z1126), as well as Z1228 transformed with an empty vector (pKESK23). Figure **A** shows growth curves of the cultures. Figure **B** shows  $\beta$ -Galactosidase activity where the enzyme was expressed from a *glmS'-lacZ* fusion, under a constitutive promoter. The shown values are the means, calculated from 2 independent measurements. The error bars indicate the standard deviation between different measurements

Overexpression of *ptsP* from a plasmid apparently inhibited *glmS'-lacZ* expression. To learn, whether PtsP acts on *glmS* expression through employment of RapZ and GlmZ, a Northern blotting experiment addressing GlmZ levels was performed. To this end, total RNAs were extracted from the 3 h cultures analyzed before in the  $\beta$ -galactosidase activity assays. The total RNAs (2,4  $\mu$ g each) were separated on a denaturing urea gel, transferred to a Nylon membrane and finally hybridized with an RNA probe suitable for detection of GlmZ. After detection, the blot was stripped and re-probed with a 5S-specific probe to provide loading controls. As expected, cleavage of GlmZ was inhibited in the cultures depleted of GlcN6P, leading to accumulation of full-length GlmZ (Fig. 23). However, there were no significant differences between the cultures grown in the absence of GlcN (Fig. 23). This result suggests that PtsP does not act via RapZ and GlmZ on *glmS* expression.

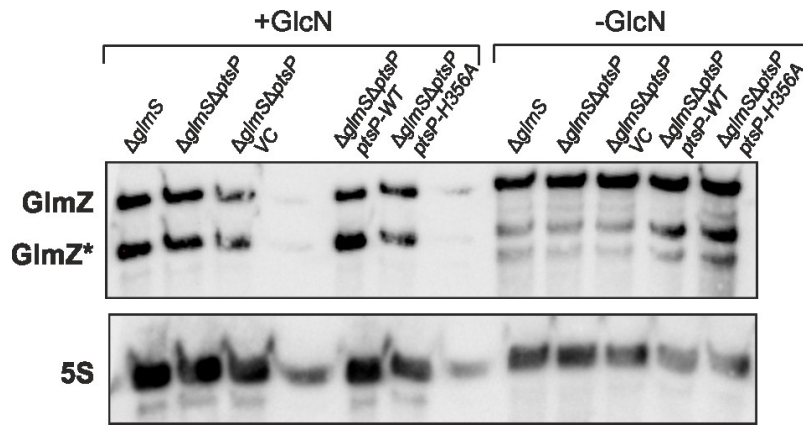


Figure 23. **Impact of *ptsP* on GlmZ cleavage.** Northern blots of total RNAs isolated from strains Z1126 and Z1228, respectively. Strain Z1228 contained either no plasmid, the empty vector control or the plasmids expressing *ptsP* or *ptsP*-H356A. Cultures were split into two sets of cultures after reaching  $OD_{600}=0,3$ . One set was supplemented with GlcN, the other not. Samples were harvested after 4 hours and 2.4  $\mu\text{g}$  of RNA were separated on a 8% urea gel. The blot was hybridized with a probe directed against GlmZ, the membrane was stripped and re-probed for 5S as an internal control.

## **6. Discussion**

### **6.1 Features of the potential ligand binding pocket of RapZ and its involvement in GlcN6P sensing**

GlmS plays an important role in bacterial cell envelope synthesis and homeostasis. Namely, it synthesizes GlcN6P, the source of all amino sugar containing components of the cell wall. Thus, it is crucial for the cell to tightly regulate this enzyme. Besides being regulated at the transcription level, the enzyme is also regulated post-transcriptionally. Regulation of GlmS usually includes some sort of feedback control, reacting to amino sugar availability (Milewski, 2002). In *Escherichia coli*, this feedback regulation is complex and involves the RNA binding protein RapZ, two small RNAs and the TCS QseE/QseF (Khan et al., 2020, Göpel et al., 2013).

The interplay of RapZ with sRNAs GlmY and GlmZ in regulation of *glmS* has been well studied (Göpel et al., 2014; Khan and Görke, 2020). It has been shown that RapZ binds GlmZ and recruits RNase E to achieve cleavage of the sRNA when GlcN6P levels are high (Durica-Mitic et al., 2020; Göpel et al., 2013). In contrast, under GlcN6P starvation conditions, RapZ activates the TCS QseE/QseF to upregulate expression of the decoy sRNA GlmY. GlmY subsequently sequesters RapZ, thereby counteracting its interaction with RNase E and cleavage of GlmZ. These activities are controlled by the metabolite GlcN6P, which according to recent results is directly sensed by RapZ (Khan et al., 2020). However, the mechanism by which RapZ senses this metabolite has not yet been revealed. Recent results have shown that the CTD of RapZ is sufficient for GlcN6P binding (Khan et al., 2020) and a structural study addressing the crystal structure of RapZ revealed a pocket in the CTD that is able to bind a non-water ligand (Gonzalez et al., 2017). Sulfate or malonate molecules were observed to bind to this pocket in the crystal structures, respectively. Consequently, this pocket represents a promising candidate for the GlcN6P-binding site in RapZ. A major aim of the current thesis was to investigate this latter possibility.

Consequently, the properties of the ligand binding pocket have been studied to some detail in this work. For this purpose, the six amino acids composing or surrounding the latter pocket were substituted individually and the properties of the resulting RapZ variants were examined in various experiments. In this context, it was also planned to test the ability of the various respective RapZ variants to bind GlcN6P by using surface plasmon resonance spectroscopy (SPR) experiments. It was planned to perform these latter experiments at the institute of our collaboration partner R. Heermann at the University of Mainz. However, due to the current pandemic, it was impossible to travel and to conduct these experiments.

Tetramerization of RapZ is a pre-requisite for some of its functions, while other functions, like binding of RNA and GlcN6P, can be performed by the CTD alone (Gonzalez et al., 2017). Therefore, both self-interaction of the full-length RapZ, as well as dimerization of its CTD were assessed in the different RapZ variants in order to verify that the loss of self-interaction alone is not a source of changes in protein function. All of the tested variants were able to self interact, however, in RapZ-H252A the CTD dimerization seemed to be somewhat weaker than in WT-RapZ (Fig. 7). In addition to changes in self-interaction, protein function could also be affected by changes in interaction of the RapZ variants with the TCS and RNase E, as compared to the wild type protein. Experiments performed by Dr. Muna Khan and Dr. Svetlana Đurica Mitić, showed that all RapZ variants are able to interact with QseE and QseF and interaction with RNase E is obtained in all RapZ variants, but possibly weakened when substitutions H190A, C247A or R253A were introduced (Table 31, column 5).

Table 31 Summary of the results obtained for amino acids comprising the ligand binding pocket of RapZ

RapZ	1 <i>lacZ</i> assays (This work; Fig. 5 and 6)		2 EMSA (Khan Görke, unpublished)		3 Northern blot experiments (This work; Fig. 10)		4 Self Interaction (This work; Fig. 7)		5 RNase E interactio n (Durica- Mitic and Görke, unpublis hed)	6 <i>In vitro</i> GlmZ Cleavage assays (Durica-Mitic and Görke, unpublished)	7 Crosslinking with QseE (This work, Fig. 17-20) → amino acids exchanged with pBpF
	1.1 <i>glmY</i> - <i>lacZ</i>	1.2 <i>glmS</i> '- <i>lacZ</i> (exponential growth phase)	2.1 GlmY	2.2 GlmZ	3.1 GlmY	3.2 GlmZ	4.1 Full length (both carry mutatio n, RH785)	4.2 CTD (both carry mutatio n, RH785)			
H190A/ amber	Partial complem entation after 4h and 6h	No complementa tion	Binding with reduced affinity	Binding with reduced affinity	Weaker signals than in WT	No cleavage	YES	YES	YES, but weaker than WT	GlmZ not cleaved	Within interaction surface of RapZ monomers
C247A/ amber	No complem entation	No complementa tion	Non- binding	Non- binding	Weaker signals than in WT	No cleavage	YES	YES	YES, but weaker than WT	N/A	N/A
T248A/ amber	Partial complem entation after 4h and 6h	Fully complements	Binding	Binding	Weaker signals than in WT; full length signal stronger that in empty vector	GlmZ cleaved, no cleaved form detected	YES	YES	YES	GlmZ cleaved	Unclear
G249W/ aber	No complem entation	No complementa tion	Non- binding	Non- binding	Weaker signals than in WT	No cleavage	YES	YES	YES	GlmZ not cleaved	Unclear
H252A/ amber	No complem entation	Fully complements	Binding	Binding	Weaker signals than in WT; full length signal stronger that in empty vector	GlmZ cleaved, no cleaved form detected	YES	YES but weaker than WT CTD	YES	N/A	Unclear
R253A/ amber	No complem entation	No complementa tion	Non- binding	Non- binding	Weaker signals than in WT	No cleavage	YES	YES	YES, but weaker than WT	GlmZ not cleaved	Within interaction surface of RapZ and QseE

When looking at *glmS* expression, only variants T248A and H252A were able to regulate *glmS* translation like the wild type protein (Fig. 5). All the other amino acids of the pocket lost this ability, which indicates that they play an important role in the function of the protein. This role becomes clearer, when looking at the RNA binding properties of the variants. Namely, experiments assessing GlmZ accumulation in bacteria encoding different RapZ variants, show that only RapZ-T248A and RapZ-H252A are able to cleave GlmZ. Variants RapZ-H190A, -C247A, -G249W and -R253A lost this ability (Fig. 10). These findings are supported by EMSA and *in vitro* cleavage assay experiments that were performed by co-workers in the lab. Namely, according to that data, only variants RapZ-T248A and -H252A are able to bind RNA in EMSA experiments and in the *in vitro* cleavage experiments, variant RapZ-T248A was able to cleave GlmZ, while the other tested variants were not (Table 31.) Together, those results indicate that all amino acids of the presumptive GlcN6P binding pocket, with the exception of T248 and H252, play an important role in RNA binding. This does not come to a surprise, since the metabolite binding pocket is located in the protein's C terminus, which is known to bind RNA (Gonzalez et al., 2017).

More surprising, however, is the fact that none of the tested RapZ variants were able to activate the QseE/QseF TCS like WT-RapZ (Fig. 6). Only RapZ-H190A and -T248A were able to complement partially and only in stationary growth phase. Since, it has been speculated that the ligand binding pocket binds GlcN6P, it was expected that the tested RapZ variants will activate the QseE/QseF TCS even stronger than WT-RapZ, because QseE/QseF TCS activation occurs in particular under GlcN6P depletion conditions (Khan et al., 2020). Namely, if the ability of RapZ to sense GlcN6P would be abolished, it would most probably act similar as in depletion conditions and upregulate QseE/QseF TCS activation. One possible explanation for the low activation of *glmY* expression is that the pocket is in direct contact with QseE or QseF. It is possible that even though a single amino acid exchange doesn't prevent the interaction between the two proteins, the activation of the system is abolished.

To test this latter hypothesis, a photo-crosslinking approach was used. To this end, residues from the pocket were replaced with the photo-crosslinkable amino acid

pBpF, respectively. RapZ variants containing pBpF at corresponding positions were overproduced and purified via StrepTactin affinity chromatography. Subsequently, it was tested whether the RapZ-pBpF variants can be crosslinked *in vitro* with the cytoplasmic kinase domain of QseE. Putative complexes resulting from the crosslinking were visualized via SDS-PAGE followed by Coomassie blue staining or Western blotting. These complexes could either represent RapZ multimers (when RapZ monomers became crosslinked) or RapZ-QseE complexes. As RapZ and QseE were tagged with different epitopes (His<sub>10</sub>/Strep), these complexes can be discriminated when using corresponding antisera for Western analysis. In any case, crosslinks can only form if the incorporated pBpF residue is in the vicinity or even part of the interaction surfaces used by RapZ to contact itself or QseE. It has been suggested previously that the reactive radius for photoalkylation by benzophenone, the photoreactive moiety of pBpF, is 3.1 Å (Dormán and Prestwich, 1994.). This means that an amino acid needs to be within 3.1 Å distance of pBpF in order for a crosslink to form. Once a crosslink is formed, complexes of higher molecular masses should be observable in the gels.

In order to establish the cross-linking approach for RapZ/QseE, two experimental parameters were tested. Firstly, it was shown that incubation of the proteins at different temperatures (4 or 30°C) prior to UV exposure, did not impact the results. Secondly, three different buffers were tested, of which the buffer with low concentration of salts showed to be most promising. Finally, from all of the performed experiments, it can be concluded that amino acids R253 and H190 are most likely located within or close to the interaction surface of two RapZ monomers. In addition, upon UV exposure of a mixture of QseE and RapZ containing pBpF instead of R253, a higher molecular complex appears on the gel, indicating that amino acid R253 is within or close to the interaction surface of RapZ and QseE (Fig. 17-20).

It is not to be excluded that other amino acids of the pocket are in close proximity to the interaction surface of RapZ and QseE, since the method showed to have some limitations when it comes to testing RapZ-QseE interaction. One limitation is that RapZ interacts with QseE as a tetramer. If the tetramer isn't completely denatured, the complex might be too big to be separated on a small polyacrylamide gel. Next, the purified RapZ variants might not be as active as the wild type; therefore the chances of observing a complex are lowered. In addition to this, the experiments were performed using 1 µg of each protein, which might be too low to detect

crosslinked complexes. Even though, this amount seems to be sufficient to detect all purified proteins, it is possible that the amount of formed crosslinks is too little to be detected on a gel. In future experiments, higher amounts of protein could be used in each reaction, which would increase the amount of formed crosslinks and therefore result in a complex that is easier to detect on a gel.

Since three of the amino acids comprising the putative GlcN6P binding pocket carry a positive charge (H190, H252 and R253), the importance of positive charge in the activation of *glmY* expression was assessed. When R253 is replaced with a neutrally charged alanine, RapZ is not able to activate *glmY* expression (Fig. 6). To test whether this activation was abolished due to the loss of a positive charge, amino acid R253 was substituted with the positively charged lysine. However, RapZ variant R253K was also unable to activate *glmY* expression (Fig. 9). This indicates the importance of an arginine at position 253 for the activation of *glmY* expression and suggests that a positive charge at position 253 is not enough for the activation. RapZ variant H190A is able to partially complement in respect to the activation of *glmY* expression (Fig. 6), however this activation was reduced when the positively charged histidine was replaced with a negatively charged aspartate (Fig. 9). These results imply that the positive charge at position 190 is important for activation of the QseE/QseF TCS and thereby *glmY* expression. When a negative charge is introduced at this position, it is possible that interaction of RapZ with the TCS is abolished due to electrostatic repulsion. As a next step, to further confirm the role of charge at position 190, it could be tested whether RapZ would be able to fully complement when H190 is substituted with a positively charged lysine.

All together, amino acids T248 and H252, of the RapZ protein, do not play an important role in GlmZ binding and *glmS* regulation under GlcN6P sufficiency (Figs. 5 and 10; Table 31, columns 1,2,3 and 6). In contrast, amino acids H190, C247, G249 and R253 are essential for RNA binding and/or cleavage of GlmZ (Fig. 10; Table 31, columns 1,2,3 and 6) and therefore their ability to regulate *glmS* is lost when substituted with other amino acids (Figs. 5). From this it can be concluded that the pocket, comprised of those amino acids, lies within the RNA binding domain of RapZ and it is possible that binding of RNA and GlcN6P is mutually exclusive.

In regard to *glmY* expression, none of the tested RapZ variants were able to fully

complement (Fig. 6), which indicates that all of the amino acids comprising the putative metabolite binding pocket of RapZ play an important role in the activation of *glmY* expression. However, in the case that the pocket is involved in GlcN6P sensing, it would be expected that the activation of *glmY* expression increases when substitutions are introduced. Instead, the RapZ variants abolished activation. There are two possible hypotheses, which could explain this. Firstly, since the activation of the QseE/QseF TCS is controlled by GlcN6P availability, it could be possible that the putative GlcN6P binding pocket is involved in both GlcN6P sensing, as well as TCS activation. Therefore, the inability of the RapZ variants to fully activate *glmY* expression, could be due to their inability to contact and/or activate the TCS. This theory is supported by the importance of the positive charge at position 190 of RapZ for the activation of *glmY* expression (Fig. 9). In addition, amino acid R253 lies within or close to the interaction surface of RapZ and QseE (Figs. 17-20), which further supports this theory and implies that RapZ contacts the TCS through the putative metabolite binding pocket.

Another possibility for the abolished activation of *glmY* expression, when substitutions are introduced to the presumptive metabolite binding pocket of RapZ, is that the corresponding RapZ variants bind GlcN6P, but are not able to release it. RapZ is known to activate the QseE/QseF TCS and therefore *glmY* expression in depletion conditions (Khan et al., 2020) and it is thus possible that the inability of RapZ to release GlcN6P could prevent this activation. It is so far not known how RapZ releases GlcN6P, but it is tempting to speculate that it does so by phosphorylation. Namely, it was shown that an orthologue of RapZ, HpaP from *Xanthomonas campestris pv. Campestris* (*Xcc*) has phosphatase, as well as ATPase activity (Cui et al., 2018). Another study has shown that both RapZ, as well as YvcJ, the RapZ homolog in *Bacillus subtilis* have ATPase and GTPase activity (Luciano et al., 2009). RapZ, as well as HpaP and YvcJ possess a Walker A and B motif (Fig. 24), which are involved in binding of ATP and GTP, as well as a PTP loop (Fig. 24) that is characteristic for Cys-dependent protein tyrosine phosphatases (PTPases) (Walker et al, 1982, Via et al., 2000, Agarwal et al., 2008, Cui et al., 2018). According to previous studies, a cysteine residue in the PTP loop acts as a nucleophile (Xie et al., 2002, Denu et al., 1996, Camps et al., 2000) and an arginine residue is essential for binding of the substrate and stabilization of the transition state (Xie et al., 2002, Zhang et al., 1994). Substitution of amino acids C256 and R262, which are found in

the PTP loop of HpaP, with alanine, abolishes the phosphatase activity of HpaP (Cui et al., 2018). Those two residues are homologous to the RapZ amino acids C247 and R253 (Fig. 24), both of which were investigated in this thesis. Other amino acids (T248, G249, H252) from the potential GlcN6P binding pocket are also part of the PTP loop of RapZ (Fig. 24). It might be possible that the pocket in question contains phosphatase activity and that it releases GlcN6P by phosphorylating it. This could explain the inability of the tested RapZ variants to activate *glmY* expression. Namely, if the phosphatase activity of RapZ is abolished in the different RapZ variants, it could mean that RapZ can still bind GlcN6P, but cannot release it.

			Walker A	
HpaP	(1)	---MSIAASTLMIVSGLSGSGKSVALKTFEDLDYYCSDNLPVELLPDFVRSRLRGNPLGD		
RapZ	(1)	-----MVLMIIVSGRSGSGKSVLRALRLEDMGFYCVNLPVLLPDLAR-TLADR---E		
YvcJ	(1)	MSVSESHDIQLVITITGMSGAGKTVAIQSFEDLGYFCVDNLPSSLKPKFLELMKESNS-KM		
			Walker B	
HpaP	(58)	QRLAVGIDVRSRSDLTQLAQWRQAAQEQY-GIEARLLFFEASDEALLKRYADTRRRHPLSQ		
RapZ	(49)	ISAAVSI DVNMPESPEIFEQAMSNLPD-AFSPQLLFLDADRNTLIRRYSDTRRLHPLSS		
YvcJ	(60)	SKVALVMDLRGREFFDRLIEALDEMAENPWITPRILFLDAKDSILVTRYKETRRSHPLAA		
HpaP	(117)	LGLALPEAITRERELTAPLRAQADAIIDTSALNVHQLRRRVVTEFALGNSDRLSLLFESF		
RapZ	(108)	KNLSLESAIDKESDLEPLRSRADLIVDTSEMSVHELAEMLRTRLLGKRERELTMVFESF		
YvcJ	(120)	TGLPLEG-IALERELLEELKGRSQIITYDTS DMKPRDLREKIVKHFATNQGETFTVNVMSF		
HpaP	(177)	AYKRGVPAEADFVFDARVLPNPHWDPELRLPRTGRDAGVRDYLDKEPDVIRYSAQIVDLLD		
RapZ	(168)	GFKHGIPIADADYVFDVRFNPNHWDPKLRPMTGLDKPVA AFLDRHTEVHNFIYQTRSYLE		
YvcJ	(179)	GFKYGIPIADADLVFDVRFNPNYYIESMRELTGKDKEVSSYVMKWN ETQKFNEKLIDLLS		
			PTP loop	
HpaP	(237)	TWLPRLRNDTRS YVTIAFGCTGGKHSVYLAERMARHAREQGWPEVATFHREQD----		
RapZ	(228)	LWLPMLETNNRSYLTVAIGCTGGKHSVYIAEQ LADYFRSRG-KNVQSRHRTLEKRKP		
YvcJ	(239)	FMLPSYKREGK SQVVIAIGCTGGQHRSVTLAENLADYFKKDYYTHVTHRDI EKRSRK-		

Figure 24. Sequence alignment of RapZ with similar proteins in *Xanthomonas campestris pv. Campestris* (HpaP) and *Bacillus subtilis* (YvcJ). Identical amino acids are marked in dark or light grey; X represents any amino acid. (Cui et al., 2018).

In conclusion, the potential metabolite binding pocket of RapZ seems to be involved in several different functions of the protein. The amino acids surrounding the pocket are binding RNA and some seem to be close to or within the interaction surface of RapZ and QseE or two RapZ monomers. Because of that, amino acid substitutions introduced in this pocket, affect various functions of the protein and it is difficult to assess solely its role in GlcN6P binding. Since RapZ activates *glmY* expression in GlcN6P depletion conditions (Khan et al., 2020), it was expected that *glmY* expression would increase upon the introduction of substitutions in the potential

metabolite binding pocket of RapZ. However, this is not the case and the RapZ variants that carry substitutions in the potential GlcN6P binding pocket lost their ability to activate *glmY* expression. This could mean that either the ability to activate the QseE/QseF TCS was lost when substitutions were introduced in the pocket or that the corresponding RapZ variants lost the ability to release GlcN6P. It is also possible that the RapZ variants lose both abilities, or that depending on the amino acid that is substituted, some variants lose the ability to release GlcN6P and others the ability to activate the TCS. Variants RapZ-H190A and -T248A were still able to partially complement, when it comes to *glmY* expression, while the other variants abolished activation completely. It is possible that the reason for the decreased activation of *glmY* expression is different for those two RapZ variants, as compared to the other ones.

As a next step, GlcN6P binding of the RapZ variants could be assessed with Surface Plasmon Resonance (SPR). In this way, not only binding of the metabolite could be assessed, but also its dissociation constant. This would give new insights about the ability of the variants to release GlcN6P. In addition, phosphatase assays could be performed using the different RapZ variants, in order to tackle the potential phosphatase activity of the pocket. Lastly, in order to gain more knowledge about the role of the presumptive metabolite binding pocket of RapZ in the activation of the QseE/QseF TCS, the photo-crosslinking method that was used in this work, could be improved and further adjusted.

## 6.2 The interaction of RapZ with the PTS<sup>Ntr</sup>

In the second part of this work, the relationship between RapZ and the nitrogen PTS was investigated. Two proteins of the PTS<sup>Ntr</sup>, PtsN and NPr are expressed from genes that are located within the same operon as *rapZ* (Pflüger-Grau and Görke, 2010, Jones et al., 1994). In addition, previous studies have shown that this PTS might play a role in the regulation of the activity of the GlnS protein (Yoo et al., 2016). Preliminary results indicate that there is interaction between RapZ and PtsP and that this interaction is stronger when the autophosphorylation site (His356) was substituted with alanine (Khan, 2019).

In order to investigate the interaction observed in the preliminary experiments in more detail, interaction of RapZ with the different components of the Nitrogen PTS was assessed. From the obtained results it can be concluded that RapZ does not interact with PtsO or PtsN (Fig 21.). When it comes to the interaction of RapZ and PtsP, the results indicate that there might be an interaction between RapZ and PtsP-H356A(D), even though it is weak and not robust (Fig. 21). One explanation for this could be that the two proteins need specific conditions for stable interaction. Another possibility is that the two proteins don't interact directly, but through another protein.

The interaction between RapZ and PtsP could either have an impact on the activity of RapZ or PtsP or both. In this work, experiments were performed to see whether PtsP impacts the activity of RapZ. For this purpose, a complementation assay was performed to test whether *ptsP* deletion or overexpression of wild type *ptsP* or *ptsP-H356A* could affect *glmS* expression under conditions of GlcN6P sufficiency or depletion. In addition, growth of the cells in this experiment was monitored. It was observed that when *wt-ptsP* was overexpressed under depletion conditions, the cells died slower (Fig. 22A). However, this was only observed for the wild type protein and not for the phospho-ablative form (*ptsP-H356A*). These results indicate that PtsP plays a role in resistance to cell wall stress in the form of GlcN6P depletion. In addition, phosphorylation of the protein seems to be important for this role. Previous studies have already linked the nitrogen PTS to cell wall stress. For example, PTS<sup>Ntr</sup> has been reported to activate two component systems like KdpD/KdpE and PhoR/PhoB and it was suggested that PTS<sup>Ntr</sup> might regulate the activity of those systems in response to cell envelope stress (Lüttmann et al., 2009, Lüttmann et al., 2012). However, both two component systems can be activated by phospho-ablative PtsN. The change in growth, observed in this study, only appeared when wild type *ptsP* was overexpressed, but not the phospho-ablative form. Therefore, the mechanism by which *ptsP* overexpression causes better resistance to cell wall stress, remains a mystery. Surprisingly, according to the measured  $\beta$ -galactosidase activities, overexpression of *ptsP* from a plasmid seems to be inhibiting *glmS'-lacZ* expression (Fig. 22B). This effect was not observed when the empty plasmid (VC) or the plasmid encoding PtsP-H356A were used. Since the *glmS'-lacZ* fusion is expressed from a constitutional promoter, the only possible mode of regulation is

through transcript stabilization or translation initiation. In that case, PtsP would most likely regulate *glmS* translation through stimulation of RapZ.

To test whether PtsP modulates *glmS* expression through RapZ, GlmZ levels were assessed. In the case that PtsP stimulates RapZ, cleavage of GlmZ would be increased in the cultures that overexpress *ptsP* from plasmid, which would lead to the accumulation of the full length variant of GlmZ. However, no difference was observed in the levels of the full length and cleaved GlmZ variants between the cultures where *ptsP* was overexpressed as compared to the cultures where it was not (Fig. 22B). This indicates that RapZ is not affected by the overexpression of PtsP. These results are also in agreement with a previous study, which shows that other members of the Pts<sup>Ntr</sup>, PtsN and Npr, have no impact on *glmS* expression (Kalamorz et al., 2007). However, a possibility remains that GlmZ cleavage is increased at an earlier time point in the cell. Since the  $\beta$ -Galactosidase enzyme accumulates in the cell, it records the “history” of events that occurred in the cell. Namely, if an event occurred at an earlier time point, it is still possible to detect the effects later on. To determine if this is the case, GlmZ levels could be assessed at an earlier stage of depletion. In addition, the experiment could be repeated in a  $\Delta rapZ$  strain, to see if *glmS* expression would be affected in the same way.

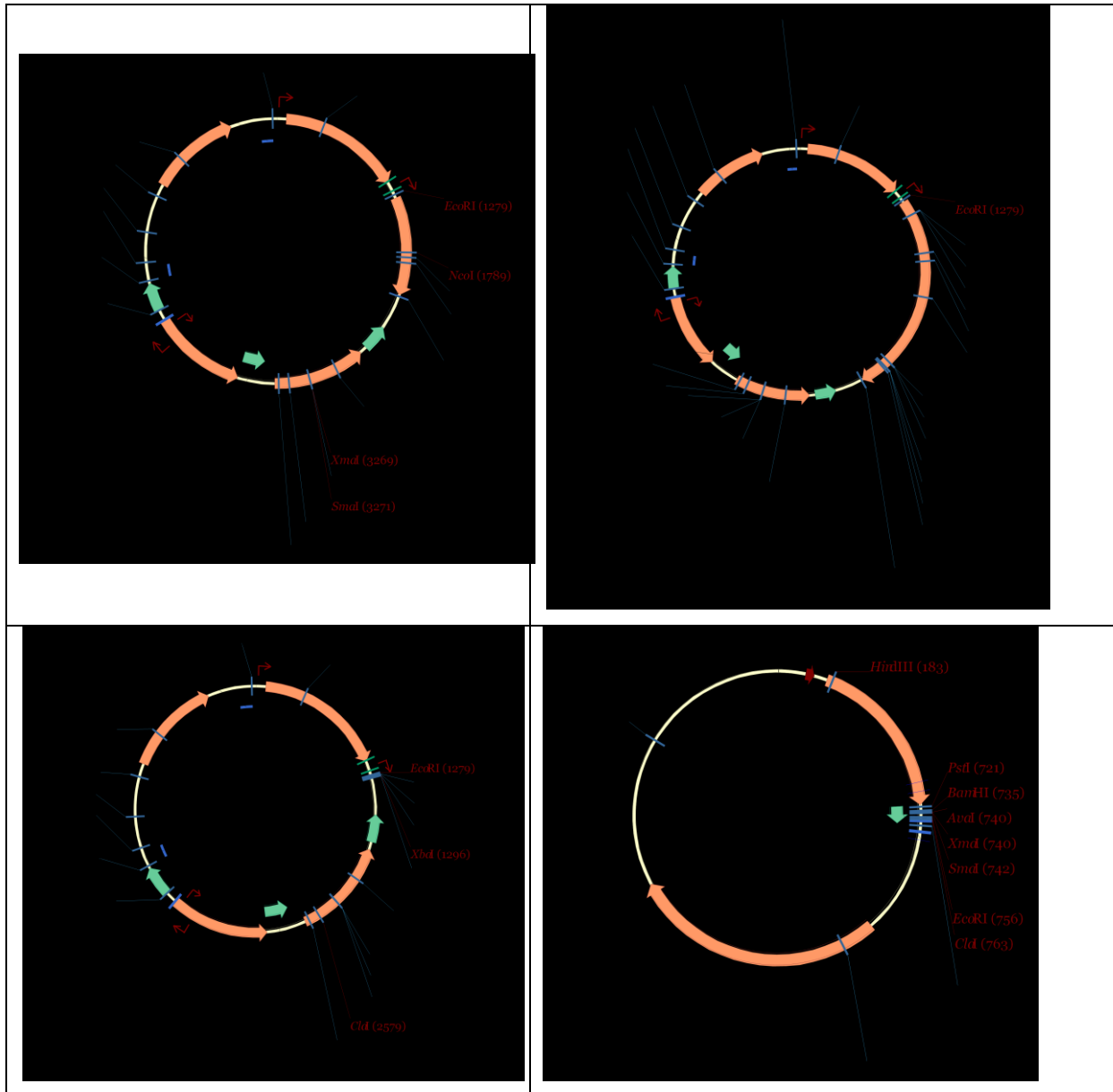
The obtained results indicate that overexpression of *ptsP* affects *glmS* expression post-transcriptionally (Fig. 22B), however this regulation seems to be independent of RapZ (Fig. 23). A possibility remains that PtsP regulates *glmS* expression through another mechanism; however, it is also possible that the results obtained in the complementation experiment (Fig. 22B) are a product of the different growth pattern of the cells that overexpress *ptsP* (Fig. 22A). It has to be taken into account that the experiment is performed under conditions where cells are dying. Therefore, the measured OD<sub>600</sub> might not correspond to the measured activity. For example  $\beta$ -Galactosidase might still be active in dead cells and therefore the amount of enzyme per living cell could be overestimated. To minimize this error, the cells were pelleted before the assays were performed. This allowed for removal of any free enzyme from the culture; however it might not have eliminated the error completely. As mentioned before, the culture where *ptsP* was overexpressed had a different growth curve than the rest of the cultures (Fig. 22A). Since the endogenous *glmS* gene is deleted in the

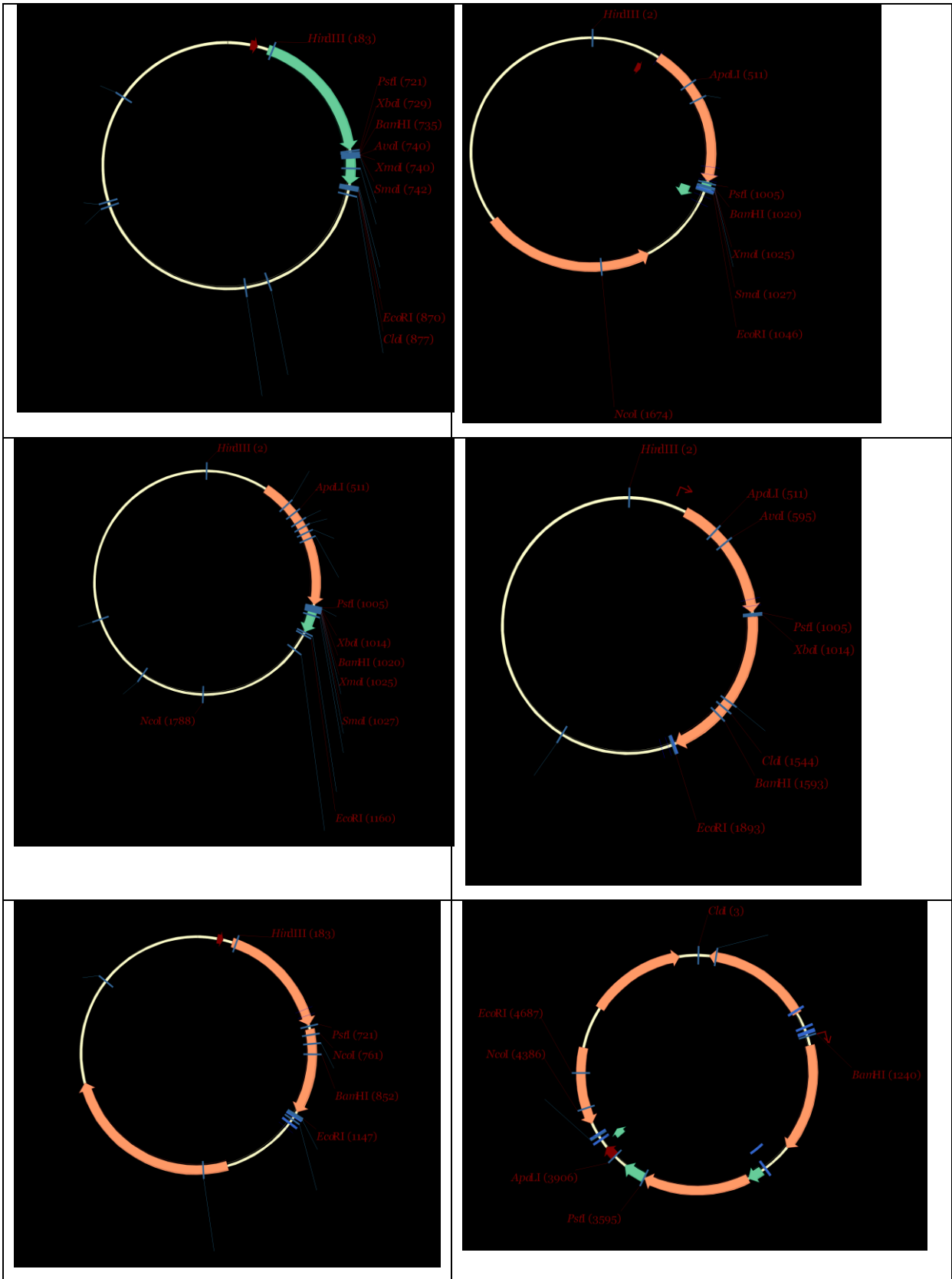
used strain, it can be excluded that the observed differences are due to changes in *glmS* expression. On the other hand, it is possible that the growth pattern affected the measured  $\beta$ -Galactosidase activity. Namely, the differences in *glmS* expression between the culture where *ptsP* was overexpressed and the empty vector, were the highest at time points t=3h and t=4h. At those exact time points the differences in growth between the two cultures were the highest. Perhaps, the error, overestimating enzyme activity per living cell, is higher in the cultures with lower OD<sub>600</sub>, thus creating a false impression about *glmS* expression.

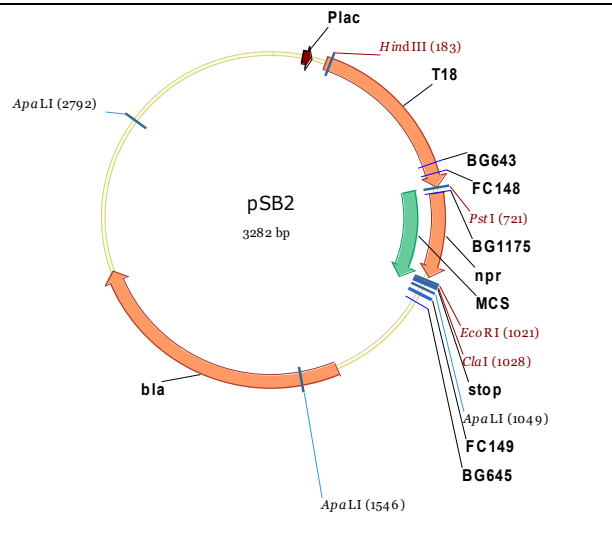
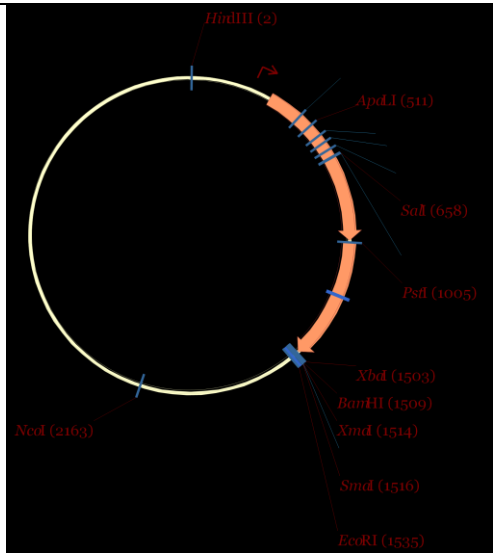
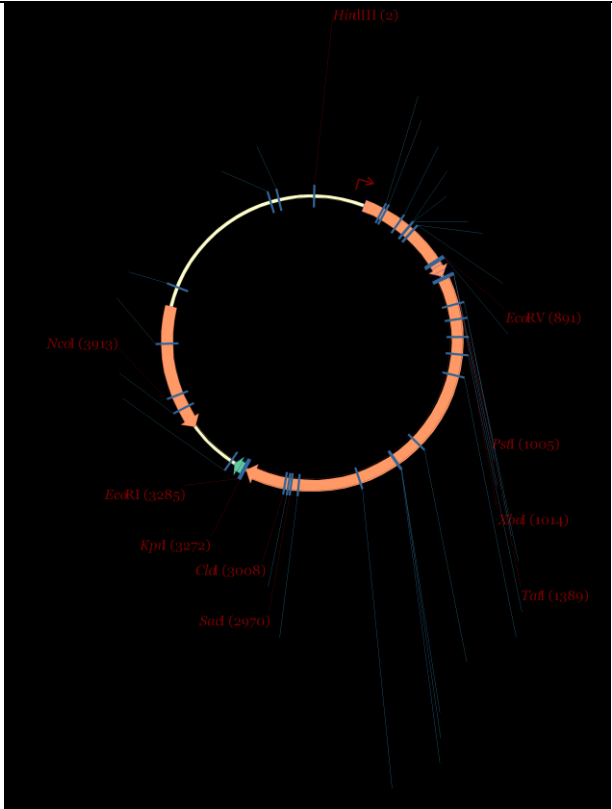
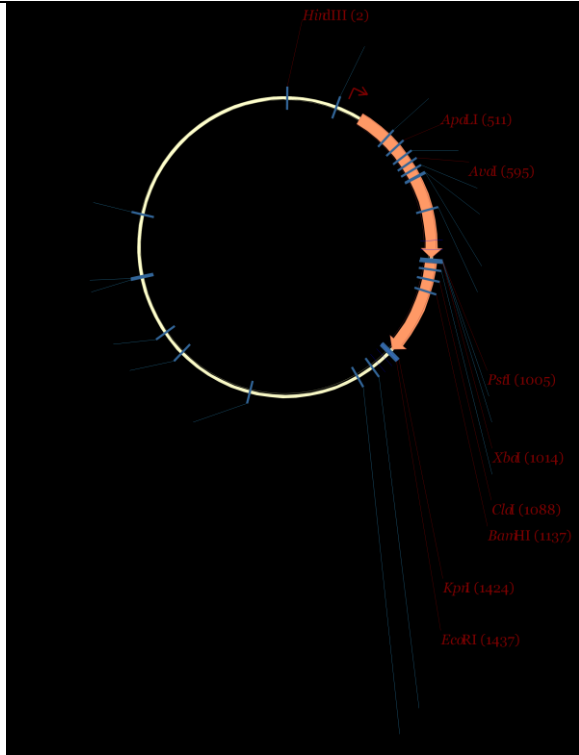
All in all, from the performed experiments it is difficult to conclude whether or not PtsP and RapZ interact directly. In addition, PtsP does not regulate the expression of *glmS* through RapZ, however, it might do so independently of RapZ. However, further experiments are needed to draw conclusions about the relationship of PtsP and the nitrogen PTS, as well as *glmS* regulation by PtsP.

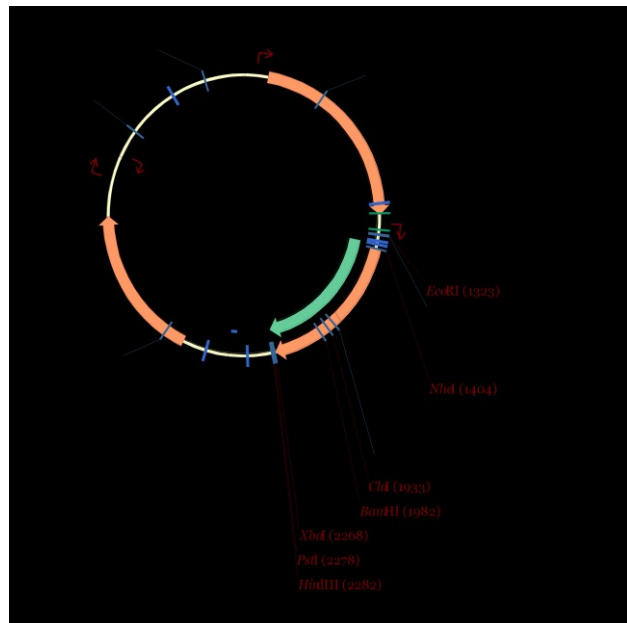
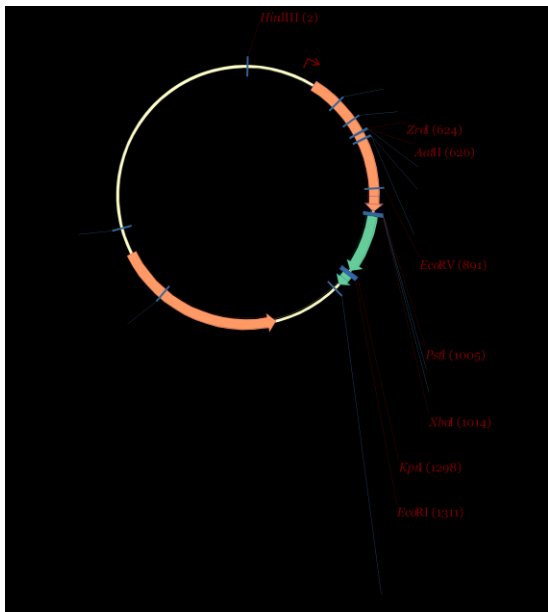
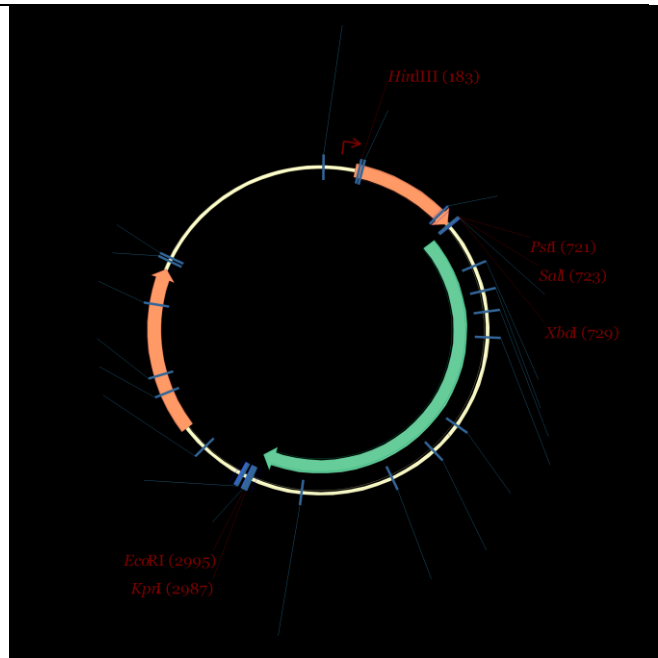
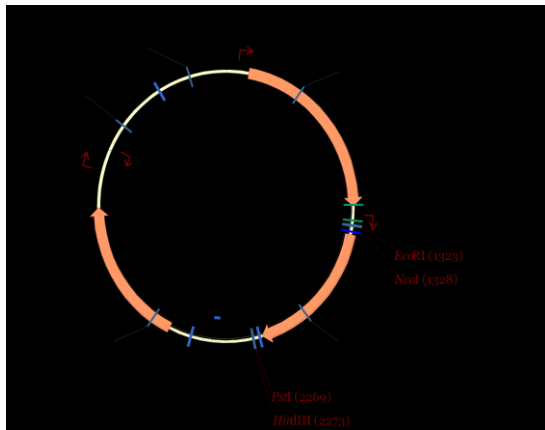
# 7. Supplementary Data

Supplementary table 1 Plasmid maps for plasmids used in this work









## **8. Abstract**

Amino sugars are important building blocks of the bacterial cell envelope. GlcN6P, the first amino sugar in the synthesis pathway, is synthesized by the enzyme GlcN6P synthase (GlmS). GlmS is tightly controlled on different levels. In *Escherichia coli*, the translation of *glmS* transcript is regulated by a complex feedback circuit, which involves two small RNAs, GlmY and GlmZ and the RNA binding protein RapZ. GlmZ base pairs with *glmS* mRNA to enable the translation of *glmS*. RapZ regulates this, by recruiting GlmZ for cleavage, while GlmY counters this. The entire circuit is dependent on GlcN6P availability, which is sensed by RapZ. The RapZ structure has revealed a ligand binding pocket, which could be responsible for GlcN6P binding and sensing. In the first part of this work, the potential metabolite binding pocket was investigated. To this end, six amino acids surrounding the pocket were substituted and the corresponding RapZ variants were tested for various features. In addition, a crosslinking method was used to determine direct interaction of the 6 amino acids with other proteins. The results showed that the pocket is involved in several different functions of the protein: from RNA binding, to activation of the QseE/QseF two component system.

In the second part of this work, the relationship between RapZ and the PTS<sup>Ntr</sup> was investigated. PTS<sup>Ntr</sup> is a phosphotransferase system, which regulates various pathways in gram negative bacteria. Among many other roles, it is involved in cell envelope stress regulation and two of its proteins are encoded within the same operon as RapZ. Previous experiments have shown that RapZ might interact with PtsP, an enzyme of this system. Therefore, the interaction between RapZ and PtsP was tested more thoroughly and it showed to be unstable. In addition, it was found that that PtsP might influence *glmS* translation, however independently of RapZ.

## 9. Zusammenfassung

Aminozucker sind integrale Bausteine der bakteriellen Zellhülle. Der Aminozucker Syntheseweg beginnt mit der Katalyse von Glucosamine-6-phosphat (GlcN6P), durch das Enzym GlcN6P-Synthase (GlmS). GlmS wird auf verschiedenen Ebenen streng kontrolliert. In *Escherichia coli*, beteiligen sich zwei kleine RNAs (sRNAs), GlmY und GlmZ, und das RNA-Bindungsprotein RapZ an der translationalen Regulation von GlmS. GlmZ bindet die *glmS*-mRNA und ermöglicht die Translation des Proteins. RapZ reguliert dies, indem es GlmZ zum Abbau durch RNase E rekrutiert, während GlmY RapZ daran hindert. Das regulatorische Netzwerk wird von der Verfügbarkeit von GlcN6P beeinflusst, welche durch RapZ wahrgenommen wird. Die Struktur von RapZ zeigt eine mögliche Bindetasche für Liganden, die für die Bindung und Wahrnehmung von GlcN6P verantwortlich sein könnte. Im ersten Teil dieser Arbeit wurde diese potenzielle Metaboliten-Bindetasche untersucht. Zu diesem Zweck wurden sechs Aminosäurereste in der Tasche mutiert und die Mutanten auf verschiedene Funktionen hin getestet. Zusätzlich wurde eine Methode zum „Photo-Crosslinking“ etabliert und angewendet, um die direkte Interaktion dieser 6 Aminosäuren mit relevanten anderen Proteinen zu bestimmen. Die Ergebnisse zeigen, dass die Tasche an verschiedenen Funktionen des Proteins beteiligt ist: von der RNA-Bindung bis zur Aktivierung des QseE/QseF Zwei-Komponentensystems.

Im zweiten Teil dieser Arbeit wurde die Beziehung zwischen RapZ und PTS<sup>Ntr</sup> untersucht. PTS<sup>Ntr</sup> ist ein Phosphotransferase-System, das verschiedene Stoffwechselwege in Gram-negativen Bakterien beeinflusst. Unter anderem ist es an der Regulation des Zellhüllstress beteiligt, und zwei der involvierten Proteine sind im selben Operon wie RapZ kodiert. Frühere Experimente haben gezeigt, dass RapZ mit PtsP, einem Enzym dieses Systems, interagieren könnte. Daher wurde die Interaktion zwischen RapZ und PtsP eingehender erforscht, wobei sich die Bindung der beiden Proteine als instabil erwies. Zusätzlich, ergab es sich dass PtsP die *glmS*-Translation beeinflussen könnte, jedoch unabhängig von RapZ.

## **10. References**

Abel S, Chien P, Wassmann P, Schirmer T, Kaever V, Laub MT, Baker TA, Jenal U. Regulatory cohesion of cell cycle and cell differentiation through interlinked phosphorylation and second messenger networks. *Mol Cell*. 2011 Aug 19;43(4):550-60. doi: 10.1016/j.molcel.2011.07.018. PMID: 21855795; PMCID: PMC3298681.

Agarwal R, Burley SK, Swaminathan S. Structure of human dual specificity protein phosphatase 23, VHZ, enzyme-substrate/product complex. *J Biol Chem*. 2008 Apr 4;283(14):8946-53. doi: 10.1074/jbc.M708945200. Epub 2008 Feb 1. PMID: 18245086.

Álvarez-Añorve LI, Gaugué I, Link H, Marcos-Viquez J, Díaz-Jiménez DM, Zonszein S, Bustos-Jaimes I, Schmitz-Afonso I, Calcagno ML, Plumbridge J. Allosteric Activation of *Escherichia coli* Glucosamine-6-Phosphate Deaminase (NagB) In Vivo Justified by Intracellular Amino Sugar Metabolite Concentrations. *J Bacteriol*. 2016 May 13;198(11):1610-1620. doi: 10.1128/JB.00870-15. PMID: 27002132; PMCID: PMC4959280.

Baba T, Ara T, Hasegawa M, Takai Y, Okumura Y, Baba M, Datsenko KA, Tomita M, Wanner BL, Mori H. Construction of *Escherichia coli* K-12 in-frame, single-gene knockout mutants: the Keio collection. *Mol Syst Biol*. 2006;2:2006.0008. doi: 10.1038/msb4100050. Epub 2006 Feb 21. PMID: 16738554; PMCID: PMC1681482.

Bandyra KJ, Luisi BF. RNase E and the High-Fidelity Orchestration of RNA Metabolism. *Microbiol Spectr*. 2018 Apr;6(2). doi: 10.1128/microbiolspec.RWR-0008-2017. PMID: 29676248.

Bi W, Stambrook PJ. Site-directed mutagenesis by combined chain reaction. *Anal Biochem*. 1998 Feb 1;256(1):137-40. doi: 10.1006/abio.1997.2516. PMID: 9466810.

Bullock WO, Fernandez JM and Short JM. XI1-Blue: a high efficiency plasmid transforming *recA* *Escherichia coli* strain with beta-galactosidase selection.

Biotechniques. 1987; 5, 376–379.

Camps M, Nichols A, Arkinstall S. Dual specificity phosphatases: a gene family for control of MAP kinase function. *FASEB J*. 2000 Jan;14(1):6-16. PMID: 10627275.

Chin JW. Expanding and reprogramming the genetic code. *Nature*. 2017 Oct 4;550(7674):53-60. doi: 10.1038/nature24031. PMID: 28980641.

Chin JW, Martin AB, King DS, Wang L, Schultz PG. Addition of a photocrosslinking amino acid to the genetic code of *Escherichia coli*. *Proc Natl Acad Sci U S A*. 2002 Aug 20;99(17):11020-4. doi: 10.1073/pnas.172226299. Epub 2002 Aug 1. PMID: 12154230; PMCID: PMC123203.

Chung CT, Niemela SL, Miller RH. One-step preparation of competent *Escherichia coli*: transformation and storage of bacterial cells in the same solution. *Proc Natl Acad Sci U S A*. 1989 Apr;86(7):2172-5. doi: 10.1073/pnas.86.7.2172. PMID: 2648393; PMCID: PMC286873.

Cleveland DW, Fischer SG, Kirschner MW, Laemmli UK. Peptide mapping by limited proteolysis in sodium dodecyl sulfate and analysis by gel electrophoresis. *J Biol Chem*. 1977 Feb 10;252(3):1102-6. PMID: 320200.

Cui P, Li RF, Zhang DP, Tang JL, Lu GT. HpaP, a novel regulatory protein with ATPase and phosphatase activity, contributes to full virulence in *Xanthomonas campestris* pv. *campestris*. *Environ Microbiol*. 2018 Apr;20(4):1389-1404. doi: 10.1111/1462-2920.14046. Epub 2018 Feb 28. PMID: 29345052.

Datsenko KA, Wanner BL. One-step inactivation of chromosomal genes in *Escherichia coli* K-12 using PCR products. *Proc Natl Acad Sci U S A*. 2000 Jun 6;97(12):6640-5. doi: 10.1073/pnas.120163297. PMID: 10829079; PMCID: PMC18686.

Denu JM, Lohse DL, Vijayalakshmi J, Saper MA, Dixon JE. Visualization of intermediate and transition-state structures in protein-tyrosine phosphatase catalysis.

Proc Natl Acad Sci U S A. 1996 Mar 19;93(6):2493-8. doi: 10.1073/pnas.93.6.2493. PMID: 8637902; PMCID: PMC39825.

Deutscher J, Aké FM, Derkaoui M, Zébré AC, Cao TN, Bouraoui H, Kentache T, Mokhtari A, Milohanic E, Joyet P. The bacterial phosphoenolpyruvate:carbohydrate phosphotransferase system: regulation by protein phosphorylation and phosphorylation-dependent protein-protein interactions. *Microbiol Mol Biol Rev.* 2014 Jun;78(2):231-56. doi: 10.1128/MMBR.00001-14. PMID: 24847021; PMCID: PMC4054256.

Deutscher J, Reizer J, Fischer C, Galinier A, Saier MH Jr, Steinmetz M. Loss of protein kinase-catalyzed phosphorylation of HPr, a phosphocarrier protein of the phosphotransferase system, by mutation of the ptsH gene confers catabolite repression resistance to several catabolic genes of *Bacillus subtilis*. *J Bacteriol.* 1994 Jun;176(11):3336-44. doi: 10.1128/jb.176.11.3336-3344.1994. PMID: 8195089; PMCID: PMC205505.

Dormán G, Prestwich GD. Benzophenone photophores in biochemistry. *Biochemistry.* 1994 May 17;33(19):5661-73. doi: 10.1021/bi00185a001. PMID: 8180191.

Durica-Mitic S, Göpel Y, Amman F, Görke B. Adaptor protein RapZ activates endoribonuclease RNase E by protein-protein interaction to cleave a small regulatory RNA. *RNA.* 2020 Sep;26(9):1198-1215. doi: 10.1261/rna.074047.119. Epub 2020 May 18. PMID: 32424019; PMCID: PMC7430671.

Durica-Mitic S, Görke B. Feedback regulation of small RNA processing by the cleavage product. *RNA Biol.* 2019 Aug;16(8):1055-1065. doi: 10.1080/15476286.2019.1612693. Epub 2019 May 22. PMID: 31116083; PMCID: PMC6602413.

Edelstein PH, Edelstein MA, Higa F, Falkow S. Discovery of virulence genes of *Legionella pneumophila* by using signature tagged mutagenesis in a guinea pig pneumonia model. *Proc Natl Acad Sci U S A.* 1999 Jul 6;96(14):8190-5. doi:

10.1073/pnas.96.14.8190. PMID: 10393970; PMCID: PMC22210.

Gonzalez GM, Durica-Mitic S, Hardwick SW, Moncrieffe MC, Resch M, Neumann P, Ficner R, Görke B, Luisi BF. Structural insights into RapZ-mediated regulation of bacterial amino-sugar metabolism. *Nucleic Acids Res.* 2017 Oct 13;45(18):10845-10860. doi: 10.1093/nar/gkx732. PMID: 28977623; PMCID: PMC5737377.

Goodwin RA, Gage DJ. Biochemical characterization of a nitrogen-type phosphotransferase system reveals that enzyme EI(Ntr) integrates carbon and nitrogen signaling in *Sinorhizobium meliloti*. *J Bacteriol.* 2014 May;196(10):1901-7. doi: 10.1128/JB.01489-14. Epub 2014 Mar 14. PMID: 24633875; PMCID: PMC4011000.

Göpel Y, Görke B. Interaction of lipoprotein QseG with sensor kinase QseE in the periplasm controls the phosphorylation state of the two-component system QseE/QseF in *Escherichia coli*. *PLoS Genet.* 2018 Jul 24;14(7):e1007547. doi: 10.1371/journal.pgen.1007547. PMID: 30040820; PMCID: PMC6075780.

Göpel Y, Khan MA, Görke B. Domain swapping between homologous bacterial small RNAs dissects processing and Hfq binding determinants and uncovers an aptamer for conditional RNase E cleavage. *Nucleic Acids Res.* 2016 Jan 29;44(2):824-37. doi: 10.1093/nar/gkv1161. Epub 2015 Nov 3. PMID: 26531825; PMCID: PMC4737144.

Göpel Y, Khan MA, Görke B. Ménage à trois: post-transcriptional control of the key enzyme for cell envelope synthesis by a base-pairing small RNA, an RNase adaptor protein, and a small RNA mimic. *RNA Biol.* 2014;11(5):433-42. doi: 10.4161/rna.28301. Epub 2014 Feb 27. PMID: 24667238; PMCID: PMC4152352.

Göpel Y, Lüttmann D, Heroven AK, Reichenbach B, Dersch P, Görke B. Common and divergent features in transcriptional control of the homologous small RNAs GlmY and GlmZ in *Enterobacteriaceae*. *Nucleic Acids Res.* 2011 Mar;39(4):1294-309. doi: 10.1093/nar/gkq986. Epub 2010 Oct 21. PMID: 20965974; PMCID: PMC3045617.

Göpel Y, Papenfort K, Reichenbach B, Vogel J, Görke B. Targeted decay of a

regulatory small RNA by an adaptor protein for RNase E and counteraction by an anti-adaptor RNA. *Genes Dev.* 2013 Mar 1;27(5):552-64. doi: 10.1101/gad.210112.112. PMID: 23475961; PMCID: PMC3605468.

Guzman LM, Belin D, Carson MJ, Beckwith J. Tight regulation, modulation, and high-level expression by vectors containing the arabinose PBAD promoter. *J Bacteriol.* 1995 Jul;177(14):4121-30. doi: 10.1128/jb.177.14.4121-4130.1995. PMID: 7608087; PMCID: PMC177145.

Hayden JD, Ades SE. The extracytoplasmic stress factor, sigmaE, is required to maintain cell envelope integrity in *Escherichia coli*. *PLoS One.* 2008 Feb 6;3(2):e1573. doi: 10.1371/journal.pone.0001573. PMID: 18253509; PMCID: PMC2215328.

Higa F, Edelstein PH. Potential virulence role of the *Legionella pneumophila* ptsP ortholog. *Infect Immun.* 2001 Aug;69(8):4782-9. doi: 10.1128/IAI.69.8.4782-4789.2001. PMID: 11447151; PMCID: PMC98565.

Hsieh YJ, Wanner BL. Global regulation by the seven-component Pi signaling system. *Curr Opin Microbiol.* 2010 Apr;13(2):198-203. doi: 10.1016/j.mib.2010.01.014. Epub 2010 Feb 18. PMID: 20171928; PMCID: PMC2847643.

Huang Y, Liu T. Therapeutic applications of genetic code expansion. *Synth Syst Biotechnol.* 2018 Oct 3;3(3):150-158. doi: 10.1016/j.synbio.2018.09.003. Erratum in: *Synth Syst Biotechnol.* 2020 Oct 14;5(4):330-331. PMID: 30345400; PMCID: PMC6190509.

Jones DH, Franklin FC, Thomas CM. Molecular analysis of the operon which encodes the RNA polymerase sigma factor sigma 54 of *Escherichia coli*. *Microbiology (Reading).* 1994 May;140 ( Pt 5):1035-43. doi: 10.1099/13500872-140-5-1035. PMID: 8025669.

Kalamorz F, Reichenbach B, März W, Rak B, Görke B. Feedback control of

glucosamine-6-phosphate synthase GlmS expression depends on the small RNA GlmZ and involves the novel protein YhbJ in *Escherichia coli*. *Mol Microbiol*. 2007 Sep;65(6):1518-33. doi: 10.1111/j.1365-2958.2007.05888.x. PMID: 17824929.

Karimova G, Pidoux J, Ullmann A, Ladant D. A bacterial two-hybrid system based on a reconstituted signal transduction pathway. *Proc Natl Acad Sci U S A*. 1998 May 12;95(10):5752-6. doi: 10.1073/pnas.95.10.5752. PMID: 9576956; PMCID: PMC20451.

Khan MA. Signal perception and transduction within the GlmY/GlmZ small RNA cascade in *Escherichia coli*. 2019. Doctoral thesis, University of Vienna.

Khan MA, Durica-Mitic S, Göpel Y, Heermann R, Görke B. Small RNA-binding protein RapZ mediates cell envelope precursor sensing and signaling in *Escherichia coli*. *EMBO J*. 2020 Mar 16;39(6):e103848. doi: 10.15252/embj.2019103848. Epub 2020 Feb 17. PMID: 32065419; PMCID: PMC7073468.

Khan MA, Görke B. A multifunctional small RNA binding protein for sensing and signaling cell envelope precursor availability in bacteria. *Microb Cell*. 2020 Apr 15;7(5):139-142. doi: 10.15698/mic2020.05.717. PMID: 32391395; PMCID: PMC7199280.

Kim HJ, Lee CR, Kim M, Peterkofsky A, Seok YJ. Dephosphorylated NPr of the nitrogen PTS regulates lipid A biosynthesis by direct interaction with LpxD. *Biochem Biophys Res Commun*. 2011 Jun 10;409(3):556-61. doi: 10.1016/j.bbrc.2011.05.044. Epub 2011 May 14. PMID: 21605551.

Klein G, Stupak A, Biernacka D, Wojtkiewicz P, Lindner B, Raina S. Multiple Transcriptional Factors Regulate Transcription of the *rpoE* Gene in *Escherichia coli* under Different Growth Conditions and When the Lipopolysaccharide Biosynthesis Is Defective. *J Biol Chem*. 2016 Oct 28;291(44):22999-23019. doi: 10.1074/jbc.M116.748954. Epub 2016 Sep 14. PMID: 27629414; PMCID: PMC5087721.

Lederberg EM, Cohen SN. Transformation of *Salmonella typhimurium* by plasmid

deoxyribonucleic acid. *J Bacteriol.* 1974 Sep;119(3):1072-4. doi: 10.1128/JB.119.3.1072-1074.1974. PMID: 4605400; PMCID: PMC245717.

Lee CR, Cho SH, Yoon MJ, Peterkofsky A, Seok YJ. *Escherichia coli* enzyme IANtr regulates the K<sup>+</sup> transporter TrkA. *Proc Natl Acad Sci U S A.* 2007 Mar 6;104(10):4124-9. doi: 10.1073/pnas.0609897104. Epub 2007 Feb 8. PMID: 17289841; PMCID: PMC1794712.

Lee CR, Park YH, Kim M, Kim YR, Park S, Peterkofsky A, Seok YJ. Reciprocal regulation of the autophosphorylation of enzyme INtr by glutamine and  $\alpha$ -ketoglutarate in *Escherichia coli*. *Mol Microbiol.* 2013 May;88(3):473-85. doi: 10.1111/mmi.12196. Epub 2013 Mar 21. PMID: 23517463; PMCID: PMC3633653.

Leroy A, Vanzo NF, Sousa S, Dreyfus M, Carpousis AJ. Function in *Escherichia coli* of the non-catalytic part of RNase E: role in the degradation of ribosome-free mRNA. *Mol Microbiol.* 2002 Sep;45(5):1231-43. doi: 10.1046/j.1365-2958.2002.03104.x. PMID: 12207692.

Luciano J, Foulquier E, Fantino JR, Galinier A, Pompeo F. Characterization of YvcJ, a conserved P-loop-containing protein, and its implication in competence in *Bacillus subtilis*. *J Bacteriol.* 2009 Mar;191(5):1556-64. doi: 10.1128/JB.01493-08. Epub 2008 Dec 12. PMID: 19074378; PMCID: PMC2648190.

Lüttmann D, Göpel Y, Görke B. Cross-Talk between the Canonical and the Nitrogen-Related Phosphotransferase Systems Modulates Synthesis of the KdpFABC Potassium Transporter in *Escherichia coli*. *J Mol Microbiol Biotechnol.* 2015;25(2-3):168-77. doi: 10.1159/000375497. Epub 2015 Jul 9. PMID: 26159077.

Lüttmann D, Göpel Y, Görke B. The phosphotransferase protein EIIA(Ntr) modulates the phosphate starvation response through interaction with histidine kinase PhoR in *Escherichia coli*. *Mol Microbiol.* 2012 Oct;86(1):96-110. doi: 10.1111/j.1365-2958.2012.08176.x. Epub 2012 Aug 3. PMID: 22812494.

Lüttmann D, Heermann R, Zimmer B, Hillmann A, Rampp IS, Jung K, Görke B.

Stimulation of the potassium sensor KdpD kinase activity by interaction with the phosphotransferase protein IIA(Ntr) in *Escherichia coli*. *Mol Microbiol.* 2009 May;72(4):978-94. doi: 10.1111/j.1365-2958.2009.06704.x. Epub 2009 Apr 28. PMID: 19400808.

Miczak A, Kaberdin VR, Wei CL, Lin-Chao S. Proteins associated with RNase E in a multicomponent ribonucleolytic complex. *Proc Natl Acad Sci U S A.* 1996 Apr 30;93(9):3865-9. doi: 10.1073/pnas.93.9.3865. PMID: 8632981; PMCID: PMC39450.

Milewski S. Glucosamine-6-phosphate synthase--the multi-facets enzyme. *Biochim Biophys Acta.* 2002 Jun 3;1597(2):173-92. doi: 10.1016/s0167-4838(02)00318-7. PMID: 12044898.

Miller JH. *Experiments in molecular genetics.* 1972

Mörk-Mörkenstein M, Heermann R, Göpel Y, Jung K, Görke B. Non-canonical activation of histidine kinase KdpD by phosphotransferase protein PtsN through interaction with the transmitter domain. *Mol Microbiol.* 2017 Oct;106(1):54-73. doi: 10.1111/mmi.13751. Epub 2017 Jul 31. PMID: 28714556.

Noguez R, Segura D, Moreno S, Hernandez A, Juarez K, Espín G. Enzyme I NPr, NPr and IIA Ntr are involved in regulation of the poly-beta-hydroxybutyrate biosynthetic genes in *Azotobacter vinelandii*. *J Mol Microbiol Biotechnol.* 2008;15(4):244-54. doi: 10.1159/000108658. Epub 2007 Sep 20. PMID: 17878711.

Pflüger-Grau K, Görke B. Regulatory roles of the bacterial nitrogen-related phosphotransferase system. *Trends Microbiol.* 2010 May;18(5):205-14. doi: 10.1016/j.tim.2010.02.003. Epub 2010 Mar 2. PMID: 20202847.

Plumbridge JA, Cochet O, Souza JM, Altamirano MM, Calcagno ML, Badet B. Coordinated regulation of amino sugar-synthesizing and -degrading enzymes in *Escherichia coli* K-12. *J Bacteriol.* 1993 Aug;175(16):4951-6. doi: 10.1128/jb.175.16.4951-4956.1993. PMID: 8349539; PMCID: PMC204958.

Plumbridge J, Vimr E. Convergent pathways for utilization of the amino sugars N-acetylglucosamine, N-acetylmannosamine, and N-acetylneuraminic acid by *Escherichia coli*. *J Bacteriol.* 1999 Jan;181(1):47-54. doi: 10.1128/JB.181.1.47-54.1999. PMID: 9864311; PMCID: PMC103530.

Pompeo F, Luciano J, Brochier-Armanet C, Galinier A. The GTPase function of YvcJ and its subcellular relocalization are dependent on growth conditions in *Bacillus subtilis*. *J Mol Microbiol Biotechnol.* 2011;20(3):156-67. doi: 10.1159/000329298. Epub 2011 Jun 28. PMID: 21709426.

Postma PW, Lengeler JW, Jacobson GR. Phosphoenolpyruvate:carbohydrate phosphotransferase systems of bacteria. *Microbiol Rev.* 1993 Sep;57(3):543-94. PMID: 8246840; PMCID: PMC372926.

Powell BS, Court DL, Inada T, Nakamura Y, Michotey V, Cui X, Reizer A, Saier MH Jr, Reizer J. Novel proteins of the phosphotransferase system encoded within the *rpoN* operon of *Escherichia coli*. Enzyme IANtr affects growth on organic nitrogen and the conditional lethality of an *erats* mutant. *J Biol Chem.* 1995 Mar 3;270(9):4822-39. doi: 10.1074/jbc.270.9.4822. PMID: 7876255.

Rabus R, Reizer J, Paulsen I, Saier MH Jr. Enzyme I(Ntr) from *Escherichia coli*. A novel enzyme of the phosphoenolpyruvate-dependent phosphotransferase system exhibiting strict specificity for its phosphoryl acceptor, NPr. *J Biol Chem.* 1999 Sep 10;274(37):26185-91. doi: 10.1074/jbc.274.37.26185. PMID: 10473571.

Ramos-Aires J, Plésiat P, Kocjancic-Curty L, Köhler T. Selection of an antibiotic-hypersusceptible mutant of *Pseudomonas aeruginosa*: identification of the GImR transcriptional regulator. *Antimicrob Agents Chemother.* 2004 Mar;48(3):843-51. doi: 10.1128/aac.48.3.843-851.2004. PMID: 14982774; PMCID: PMC353099.

Reaves ML, Rabinowitz JD. Characteristic phenotypes associated with *ptsN*-null mutants in *Escherichia coli* K-12 are absent in strains with functional *ilvG*. *J Bacteriol.* 2011 Sep;193(18):4576-81. doi: 10.1128/JB.00325-11. Epub 2011 Apr 29. PMID: 21531803; PMCID: PMC3165713.

Reichenbach B, Göpel Y, Görke B. Dual control by perfectly overlapping sigma 54- and sigma 70- promoters adjusts small RNA GlmY expression to different environmental signals. *Mol Microbiol.* 2009 Dec;74(5):1054-70. doi: 10.1111/j.1365-2958.2009.06918.x. Epub 2009 Oct 27. PMID: 19843219.

Reichenbach B, Maes A, Kalamorz F, Hajnsdorf E, Görke B. The small RNA GlmY acts upstream of the sRNA GlmZ in the activation of glmS expression and is subject to regulation by polyadenylation in *Escherichia coli*. *Nucleic Acids Res.* 2008 May;36(8):2570-80. doi: 10.1093/nar/gkn091. Epub 2008 Mar 11. PMID: 18334534; PMCID: PMC2377431.

Reizer J, Reizer A, Merrick MJ, Plunkett G 3rd, Rose DJ, Saier MH Jr. Novel phosphotransferase-encoding genes revealed by analysis of the *Escherichia coli* genome: a chimeric gene encoding an Enzyme I homologue that possesses a putative sensory transduction domain. *Gene.* 1996 Nov 28;181(1-2):103-8. doi: 10.1016/S0378-1119(96)00481-7. PMID: 8973315.

Rezuchova B, Miticka H, Homerova D, Roberts M, Kormanec J. New members of the *Escherichia coli* sigmaE regulon identified by a two-plasmid system. *FEMS Microbiol Lett.* 2003 Aug 8;225(1):1-7. doi: 10.1016/S0378-1097(03)00480-4. PMID: 12900013.

Rust HL, Subramanian V, West GM, Young DD, Schultz PG, Thompson PR. Using unnatural amino acid mutagenesis to probe the regulation of PRMT1. *ACS Chem Biol.* 2014 Mar 21;9(3):649-55. doi: 10.1021/cb400859z. Epub 2014 Jan 6. PMID: 24358983; PMCID: PMC4505744.

Schnetzer K, Stülke J, Gertz S, Krüger S, Krieg M, Hecker M, Rak B. LicT, a *Bacillus subtilis* transcriptional antiterminator protein of the BglG family. *J Bacteriol.* 1996 Apr;178(7):1971-9. doi: 10.1128/jb.178.7.1971-1979.1996. PMID: 8606172; PMCID: PMC177893.

Schulte JE, Goulian M. The Phosphohistidine Phosphatase SixA Targets a

Phosphotransferase System. *mBio*. 2018 Nov 27;9(6):e01666-18. doi: 10.1128/mBio.01666-18. PMID: 30482831; PMCID: PMC6282199.

Schulte JE, Roggiani M, Shi H, Zhu J, Goulian M. The phosphohistidine phosphatase SixA dephosphorylates the phosphocarrier NPr. *J Biol Chem*. 2020 Nov 16;296:100090. doi: 10.1074/jbc.RA120.015121. Epub ahead of print. PMID: 33199374; PMCID: PMC7948535.

Segura D, Espín G. Mutational inactivation of a gene homologous to *Escherichia coli* ptsP affects poly-beta-hydroxybutyrate accumulation and nitrogen fixation in *Azotobacter vinelandii*. *J Bacteriol*. 1998 Sep;180(18):4790-8. doi: 10.1128/JB.180.18.4790-4798.1998. PMID: 9733679; PMCID: PMC107501.

Sharma R, Shimada T, Mishra VK, Upreti S, Sardesai AA. Growth Inhibition by External Potassium of *Escherichia coli* Lacking PtsN (EIIANtr) Is Caused by Potassium Limitation Mediated by YcgO. *J Bacteriol*. 2016 Jun 13;198(13):1868-1882. doi: 10.1128/JB.01029-15. PMID: 27137496; PMCID: PMC4907114.

Studholme DJ, Buck M. The biology of enhancer-dependent transcriptional regulation in bacteria: insights from genome sequences. *FEMS Microbiol Lett*. 2000 May 1;186(1):1-9. doi: 10.1111/j.1574-6968.2000.tb09074.x. PMID: 10779705.

Szurmant H, White RA, Hoch JA. Sensor complexes regulating two-component signal transduction. *Curr Opin Struct Biol*. 2007 Dec;17(6):706-15. doi: 10.1016/j.sbi.2007.08.019. Epub 2007 Oct 29. PMID: 17913492; PMCID: PMC2175030.

Tan MW, Mahajan-Miklos S, Ausubel FM. Killing of *Caenorhabditis elegans* by *Pseudomonas aeruginosa* used to model mammalian bacterial pathogenesis. *Proc Natl Acad Sci U S A*. 1999 Jan 19;96(2):715-20. doi: 10.1073/pnas.96.2.715. PMID: 9892699; PMCID: PMC15202.

Tan MW, Rahme LG, Sternberg JA, Tompkins RG, Ausubel FM. *Pseudomonas aeruginosa* killing of *Caenorhabditis elegans* used to identify *P. aeruginosa* virulence

factors. *Proc Natl Acad Sci U S A*. 1999 Mar 2;96(5):2408-13. doi: 10.1073/pnas.96.5.2408. PMID: 10051655; PMCID: PMC26797.

Updegrove TB, Shabalina SA, Storz G. How do base-pairing small RNAs evolve? *FEMS Microbiol Rev*. 2015 May;39(3):379-91. doi: 10.1093/femsre/fuv014. Epub 2015 Apr 30. PMID: 25934120; PMCID: PMC4542690.

Urban JH, Vogel J. Two seemingly homologous noncoding RNAs act hierarchically to activate *glmS* mRNA translation. *PLoS Biol*. 2008 Mar 18;6(3):e64. doi: 10.1371/journal.pbio.0060064. PMID: 18351803; PMCID: PMC2267818.

Velázquez F, Pflüger K, Cases I, De Eugenio LI, de Lorenzo V. The phosphotransferase system formed by PtsP, PtsO, and PtsN proteins controls production of polyhydroxyalkanoates in *Pseudomonas putida*. *J Bacteriol*. 2007 Jun;189(12):4529-33. doi: 10.1128/JB.00033-07. Epub 2007 Apr 6. PMID: 17416664; PMCID: PMC1913348.

Via A, Ferrè F, Brannetti B, Valencia A, Helmer-Citterich M. Three-dimensional view of the surface motif associated with the P-loop structure: cis and trans cases of convergent evolution. *J Mol Biol*. 2000 Nov 3;303(4):455-65. doi: 10.1006/jmbi.2000.4151. PMID: 11054283.

Vogel J, Luisi BF. Hfq and its constellation of RNA. *Nat Rev Microbiol*. 2011 Aug 15;9(8):578-89. doi: 10.1038/nrmicro2615. PMID: 21760622; PMCID: PMC4615618.

Walker JE, Saraste M, Runswick MJ, Gay NJ. Distantly related sequences in the alpha- and beta-subunits of ATP synthase, myosin, kinases and other ATP-requiring enzymes and a common nucleotide binding fold. *EMBO J*. 1982;1(8):945-51. PMID: 6329717; PMCID: PMC553140.

Xie L, Zhang YL, Zhang ZY. Design and characterization of an improved protein tyrosine phosphatase substrate-trapping mutant. *Biochemistry*. 2002 Mar 26;41(12):4032-9. doi: 10.1021/bi015904r. PMID: 11900546.

Yoo W, Yoon H, Seok YJ, Lee CR, Lee HH, Ryu S. Fine-tuning of amino sugar homeostasis by EIIA(Ntr) in *Salmonella Typhimurium*. *Sci Rep*. 2016 Sep 15;6:33055. doi: 10.1038/srep33055. PMID: 27628932; PMCID: PMC5024086.

Zhang ZY, Malachowski WP, Van Etten RL, Dixon JE. Nature of the rate-determining steps of the reaction catalyzed by the *Yersinia* protein-tyrosine phosphatase. *J Biol Chem*. 1994 Mar 18;269(11):8140-5. PMID: 8132539.

Zimmer B, Hillmann A, Görke B. Requirements for the phosphorylation of the *Escherichia coli* EIIANtr protein in vivo. *FEMS Microbiol Lett*. 2008 Sep;286(1):96-102. doi: 10.1111/j.1574-6968.2008.01262.x. PMID: 18625021.

Zschiedrich CP, Keidel V, Szurmant H. Molecular Mechanisms of Two-Component Signal Transduction. *J Mol Biol*. 2016 Sep 25;428(19):3752-75. doi: 10.1016/j.jmb.2016.08.003. Epub 2016 Aug 9. PMID: 27519796; PMCID: PMC5023499.